Effects of membrane lipid composition on the organization and signalling properties of bacterial chemoreceptors

Dissertation

zur

Erlangung des Grades eines

Doktor der Naturwissenschaften

(Dr. rer. nat.)

des Fachbereichs Biologie der Philipps-Universität Marburg

vorgelegt von

Nadja Sachs
aus München, Deutschland

Marburg/Lahn, August 2020

Die Untersuchungen zur vorliegenden Arbeit wurden von November 2015 bis August 2020 am Max-Planck-Institut für terrestrische Mikrobiologie in Marburg unter der Leitung von Prof. Dr. Victor Sourjik durchgeführt.

Vom Fachbereich Biologie der Philipps Universität Marburg
(Hochschulkennziffer 1180) als Dissertation angenommen am: 02.11.2020

Erstgutachter: Prof. Dr. Victor Sourjik

Zweitgutachter: Prof. Dr. Martin Thanbichler

Weitere Mitglieder der Prüfungskommission:

Prof. Dr. Simon Ringgaard

Prof. Dr. Hans-Ulrich Mösch

Tag der Disputation: 04.11.2020

Zum Zeitpunkt der Einreichung dieser Dissertation wird die folgende Originalpublikation vorbereitet, um die erzielten Ergebnisse zu veröffentlichen:

“Effect of cardiolipin on mobility and assembly of chemotaxis receptors in *Escherichia coli*”

Meiner Familie

To my family

“*How can a bird that is born for joy*
Sit in a cage and sing?”

William Blake

Acknowledgements

First of all, I want to express my sincere gratitude to my supervisor Prof. Dr. Victor Sourjik for giving me the opportunity to do my PhD thesis in a great working environment and for supporting my project throughout the whole time.

Additionally, I would like to thank the other members of my Thesis Advisory Committee, Prof. Dr. Martin Thanbichler and Dr. Simon Ringgaard, for helpful discussions, valuable advice and comments on my project.

Further I want to thank the TRR174 community and especially the members of the Young-Scientists Committee for a great and interesting time, for amazing events and for all I have learned while being part of the YSC.

I also want to acknowledge Dr. Gabriele Malengo and Silvia Gonzáles Sierra for always finding time to help me with flow cytometry and every kind of microscopy.

I thank Dr. Bartosz Turkowyd and Dr. Paulina Jacek for proofreading my thesis and for their helpful comments.

I would like to gratefully acknowledge all previous and present lab members of the AG Sourjik for helping and supporting me during these years. Further I would like to thank David Kraus for his help with data analysis. Some special thanks go to Melissa Kivoloka, Alexandra Hahn, Manuel Seip, Claudia Einloft, Inka Henseling and Sarah Hoch for their flawless technical assistance and for keeping the lab running.

Danke an alle meine Freunde. Allen voran Vroni, Alexa, Maxi und Melissa. Für die Unterstützung während der letzten Jahre und die vielen großartigen Momente, die diese Zeit unvergesslich gemacht zu haben. Vor allem aber für eure Freundschaft.

Und schließlich gilt, der größte und herzlichste Dank meiner Familie, vor allem meinen Eltern, Peter und Petra. Ohne eure Unterstützung, Ermutigung und Liebe, wäre nichts von dem, was ich bis jetzt erreicht habe, möglich gewesen.

TABLE OF CONTENT

ABBREVIATIONS

bp	base pair
cfu	colony forming units
CL	cardiolipin
CL-	cardiolipin deficient strain
ddH_20	double distilled water
DNA	desoxyribonucleicacid
h	hours
IPTG	isopropyl-β-D-thiogalactopyranoside
L	liter
LPG	lysyl- phosphatidylglycerol
min	minutes
mL	milliliter
PA	phosphatidicacid
PCR	polymerase chain reaction
PE	phosphatidlethanolamin
PG	phosphatidylglycerol
rpm	rounds per minute
sal	salicalate
WT	wildtyp

ZUSAMMENFASSUNG

Die bakterielle Zytoplasmamembran ist eine der dynamischsten Strukturen in der Zelle und fungiert hauptsächlich als selektive Permeabilitätsbarriere. Ziel dieser Arbeit war es, die Auswirkungen der Zusammensetzung dieser Lipid-Doppelschicht auf verschiedene bakterielle Zelleigenschaften wie Wachstum, Chemosensorik und Motilität zu untersuchen. Dabei konzentrierten wir uns hauptsächlich auf den Effekt von Cardiolipin (CL), einer Nebenkomponente der bakteriellen Zytoplasmamembran, die in *Escherichia coli* von drei Enzymen (ClsA, YbhO, YmdC) synthetisiert wird. Während einzelne Deletionen dieser Synthasen das Wachstum und teilweise auch die Zellmorphologie beeinflussten, beeinträchtigte der dreifache Knockout Δ*cl*sA ΔybhO ΔymdC das Wachstum nicht negativ und ist vergleichbar mit dem Ausgangsstamm. Überraschenderweise verursachte der Cardiolipin-Mangel unter verschiedenen osmotischen und antibiotischen Stressbedingungen keine oder nur geringfügige Wachstumsdefekte, was darauf hindeutet, dass Cardiolipin für das Wachstum von *E. coli* entbehrlich ist. Das Überleben beweglicher Mikroorganismen hängt nicht nur vom Wachstum ab, sondern auch von ihrer Fähigkeit, chemische Gradienten zu erfassen und die dadurch bedingte, gerichtete Fortbewegung zu kontrollieren. Dazu verwendet *E. coli* methylakzeptierende Chemotaxis-Proteine, die sich an den Zellpolen und seitlich, entlang des Zellkörpers, gruppieren. Wir konzentrierten uns auf den Einfluss der membranabhängigen Interaktionen zwischen den Rezeptoren und der Phospholipid-Zusammensetzung der Zellmembran. Wir konnten zeigen, dass die Membran nicht nur für die Funktionalität der Chemorezeptoren, sondern auch für die Bildung der chemosensorischen Cluster eine wesentliche Rolle spielt. Ebenso, dass die Clusterbildung des Chemorezeptors Tar durch die Abwesenheit von Cardiolipin um die Hälfte verringert ist, unabhängig von Temperatur und Wachstumsphase. Das Clustering in einem Cardiolipin-defizienten Hintergrund konnte durch Modifikation der Transmembrandomäne von Tar wiederhergestellt werden. Um zu untersuchen, ob die Abnahme der Clusterbildung die Folge einer reduzierten Proteinmobilität sein könnte, oder der Assemblierungsprozess in Kombination mit einer hydrophoben Fehlanpassung von Protein und Membran behindert wird,

verwendeten wir FRAP (Fluoreszenz Recovery After Photobleach) -Mikroskopie, was die Messungen von Proteindiffusionskoeffizienten ermöglicht. Wir führten FRAP-Messungen für die wichtigsten *E. coli*-Rezeptoren, Tar und Tsr, durch. Dabei konnten wir beobachteten, dass die Diffusion von Tar im CL-defizienten Stamm bei einem engen Temperaturbereich um 18°C signifikant verlangsamt ist. Bei höheren und niedrigeren Temperaturen ist der Unterschied in der Tar-Diffusion im *WT* und der CL-defizienten Mutante nicht erkennbar, was auf einen plötzlichen, Cardiolipin bedingten, Abfall der Mobilität von Tar in einem kritischen Temperaturbereich hinweist. Eine Fluidisierung der Membran mit Benzylalkohol konnte den Effekt wiederherstellen. Weiterhin konnte der Cardiolipin bedingte Effekt auch durch eine Erweiterung der Tar-Transmembrandomäne aufgehoben werden. Für Tsr konnten wir keinen membranabhängigen Effekt auf die Rezeptordiffusion nachweisen. Wir nehmen an, dass die CL-abhängige Zunahme der Rezeptormobilität von Tar in einem bestimmten Temperaturbereich auf Protein-Membran-Wechselwirkungen zurückzuführen ist, die unter anderem von der Länge der Transmembrandomänen abhängen. Die Zusammenhänge zwischen der Cardiolipin-vermittelten Erhöhung des Rezeptor-Clusterings und der Cardiolipin-bedingten Erhöhung der Rezeptormobilität müssen noch erforscht werden. Desweiteren konnten wir zeigen, dass CL das Motilitätssystem von *E. coli* beeinflusst. Mit steigenden Temperaturen nimmt die Motilität eines Cardiolipin-defizienten Stammes zu, im Gegensatz zum Ausgangsstamm mit unveränderter Membranzusammensetzung. Dies konnte durch Untersuchung der Expression der Motilitätsgene *fliC* und *fliA* bestätigt werden. Darüber hinaus untersuchten wir den Effekt von Membranveränderungen auf *E. coli* durch Überexpression verschiedener Phospholipidsynthasen, sowie den Effekt veränderter Membranzusammensetzungen in *B. subtilis*.

SUMMARY

The bacterial cytoplasmic membrane is one of the most dynamic cellular structures, functioning mainly as selective permeability barrier. The aim of this thesis was to investigate effects of lipid bilayer composition on several bacterial cell properties like growth, chemosensing and motility. I mainly focused on the effect of cardiolipin (CL), a minor component of the bacterial cytoplasmic membrane, synthesised by three enzymes (ClsA, YbhO, YmdC) in *Escherichia coli*. While individual deletions of these synthase genes affected growth and partly cell morphology, the triple knockout *ΔclsA ΔybhO ΔymdC* grew comparably to the parental strain. Surprisingly, cardiolipin deficiency caused no or only minor growth defects under various osmotic and antibiotic stress conditions, which indicates that cardiolipin is expendable for growth of *E. coli*. Survival of motile microorganisms does not only depend on growth but also on their ability to sense and control their directed motility in chemical gradients. Therefore, *E. coli* utilizes methyl-accepting chemotaxis proteins, which are clustering at the cell poles and laterally along the cell body. We focused on the influence of membrane-dependent interactions between the receptors and the phospholipids. With this we could show that the membrane plays not only a considerable role in chemoreceptor functionality but also in clustering. We showed the reduced assembly of Tar clusters in a strain with cardiolipin deficiency, independent of temperature and growth phase. Clustering in a cardiolipin-deficient background could be restored by modification of the transmembrane domain of Tar. To investigate whether the decrease in clustering could be the consequence of reduced protein mobility, hindering the assembly process in combination with hydrophobic mismatch, we utilized FRAP microscopy that allows measurements of fluorescent protein recovery after photobleaching. We performed FRAP measurements for the major *E. coli* receptors, Tar and Tsr. We observed that the diffusion of Tar is significantly decelerated in the cardiolipin-deficient strain at a narrow temperature range around 18°C. At higher and lower temperature, the difference in Tar recovery in the *WT* and cardiolipin-deficient strain is negligible, indicating a sudden drop of Tar mobility in a critical temperature range in the cardiolipin-deficient strain. Solubilizing the membrane using benzyl alcohol could

restore the effect. Additionally, the effect could also be abolished by extension of the Tar transmembrane domain. For Tsr we could not detect any membrane-dependent effect on receptor diffusion. We assume that the cardiolipin-dependent increase of Tar receptor mobility in a certain temperature range is due to protein-membrane interactions depending inter alia on the length of transmembrane domains. The connections between the cardiolipin mediated enhancement in receptor clustering and the cardiolipin-dependent increase of receptor mobility remains to be explored. Additionally, we could show, that cardiolipin is influencing the motility system of *E. coli*. With raising temperatures, the motility of a cardiolipin-deficient Tar-only strain increases, in contrast to the parental strain. This could be confirmed by examining the expression of the motility genes *fliC* and *fliA*. Furthermore, we examined the effect of membrane alterations on *E. coli*, by overexpressing various phospholipid synthases, as well as the effect of changing membrane composition in *B. subtilis*.

1 INTRODUCTION

1.1. Bacterial cell envelope

Bacteria can be found in many different habitats, where they have to oppose continuously changing and unpredictable conditions like temperature or pH changes. To face these constant environmental changes, they use highly complex multilayer structures, such as the cell envelope. Bacteria can be generally classified into two major groups, gram-positive and gram-negative based on the structure of their cell envelope. The nomenclature comes from an early but still used method (gram-staining) for classifying bacterial species into the two major groups (*1*). The gram staining method for fixed cells is based on the stainability of gram-positive cells with crystal-violet turning the cells purple and a counterstain of the gram-negative cells with safranin colouring the cells pinkish-red.

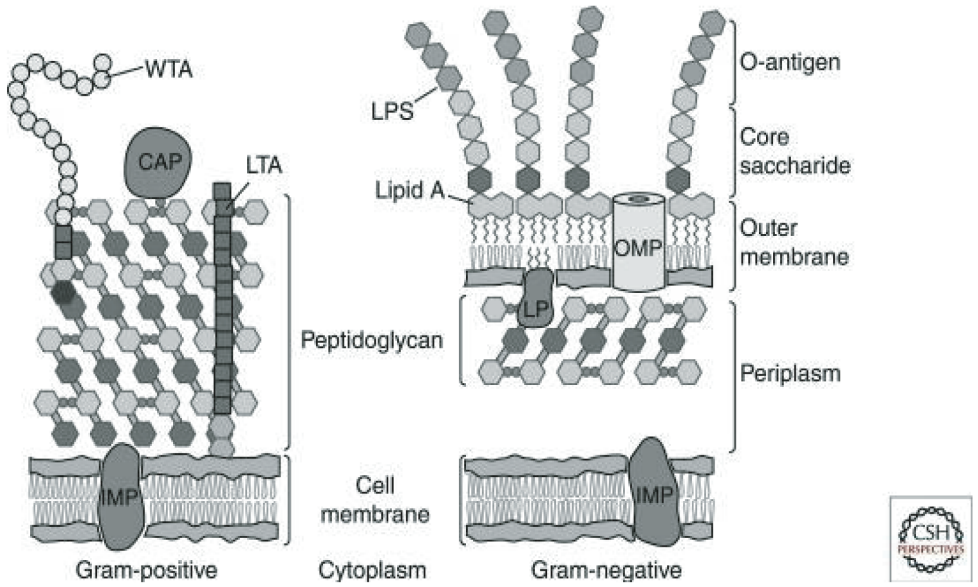

Figure 1. The bacterial cell envelope. Illustration of a gram-positive and a gram-negative cell envelope. CAP: covalently attached protein, IMP: integral membrane protein, LP: lipoprotein, LPS: lipoteichoic acid, OMP: outer membrane protein, WTA: wall teichoic acid. Reprinted from Silhavy *et al*., The bacterial cell envelope, 2010 (*2*).

The major difference between gram-positive and gram-negative bacteria (Figure 1) is the lack of the outer membrane for gram-positive cells resulting in a drastically thicker cell wall layer. The gram-positive cell envelope (e.g., *Bacillus subtilis*) consists of several layers of peptidoglycan (30-100nm thick) (*2*), pervaded by long anionic polymers, the so-called teichoic acids. These teichoic acids are mostly composed of glycerol phosphates, glucosyl phosphates or ribitol phosphate repeats. Those are either covalently attached to the peptidoglycan layer (wall teichoic acids) or anchored on the head groups of the cytoplasmic membrane lipids (lipoteichoic acids) (*3*). Additionally, to the teichoic acids, the cell wall of gram-positive bacteria is covered by a wide variety of proteins. They are either attached to the cytoplasmic membrane by membrane-spanning lipid anchors or membrane anchoring helices, tightly association or covalently attachment with the peptidoglycan layer or the teichoic acids (*4*). In gram-negative bacteria, like *Escherichia coli* (*E. coli*), the complex cell envelope consists mainly of three different layers. In contrast to gram-positive cells, *E. coli* is surrounded by a thin layer of peptidoglycan with just a few nm thickness, which is itself enclosed by an outer membrane and an inner membrane (*5*). In addition to a substantial role as stabilizing layer of the outer membrane, it also constitutes a major role by protecting the organism from environmental influences and outer cellular toxins (*2*). The outer membrane (OM) is a lipid bilayer containing lipids confining the inner leaflet and glycolipids (lipopolysaccharide, LPS), shaping the outer leaflet (*6*) and LPSs play a critical role in the function as barrier of the OM (*7*). Proteins pervading this OM can be separated into two classes. On the one hand the functional mostly unknown Lipoproteins that contain lipid moieties attached to an amino-terminal cysteine residue. And, on the other hand, the integral β-barrel proteins (OMPs) representing the transmembrane proteins (*8-10*). OMPs act in diverse roles, like as adhesion factors in processes of virulence, as (passive or active) channels for the uptake of nutrients and small molecules, as siderophore receptors and also as enzymes such as lipases and proteases (*11*). The OM is stapled on the cell wall by the Lipoprotein Lpp, one of *E. coli*'s most abundant proteins (*12*). The aqueous phase enclosed by the IM and OM, called periplasm, is tightly packed with proteins and oligosaccharides(*13*). The bacterial inner membrane (IM) is also called plasma membrane. Bacteria are

lacking organelles comparable to the eukaryotic ones; therefore, the IM is performing all these membrane-associated functions. This membrane accomplishes functions like a selective nutrient transport, lipid biosynthesis functions, protein translocations, and oxidative phosphorylation's (*14*), comparable to the eukaryotic plasma membrane, mitochondrial inner membrane, and the endoplasmic reticulum. The IM lipid bilayer is mainly comprised of phosphatidylethanolamine, phosphatidylglycerol, as well as diphosphatidylglycerol and phosphatidylserine, which are synthesized by enzymes of the Kennedy pathway (*15*). During energy transduction those IM proteins play a key role because they are involved in processes like signal transduction, in the uptake and efflux of substances. (*16*). Adjacent to outer membrane proteins, the membrane-spanning segments of inner membrane proteins (IMPs) are largely α-helical and apolar, which applies to both single-span for anchoring proteins with highly polar domains or for multiple membrane-spanning helices of transport proteins (*14*). The peptidoglycan cell wall functions as rigid exoskeleton, which is supporting the cells turgor pressure. The cell shape is made up of several repeating units of N-acetyl glucosamine-N-acetyl muramic acid, crosslinked by pentapeptide side chains (*17*).

1.1.1 The phospholipid bilayer of *E. coli*

In the phylogenetic bacterial branch exist an abundant diversity of phospholipid structures; most membrane phospholipids are glycerolipids made of glycerides substituted with two fatty acid chains. Phospholipids are amphiphilic, they are soluble in water and oil. This quality arises from their hydrophobic hydrocarbon tail of the fatty acid chains and their additional hydrophilic phosphate head group. Previous studies investigating the bacterial lipid metabolism have already shown the ability of bacteria to adapt their membrane composition as a response to environmental changes like temperature, osmolarity, salinity, and pH (*18*).

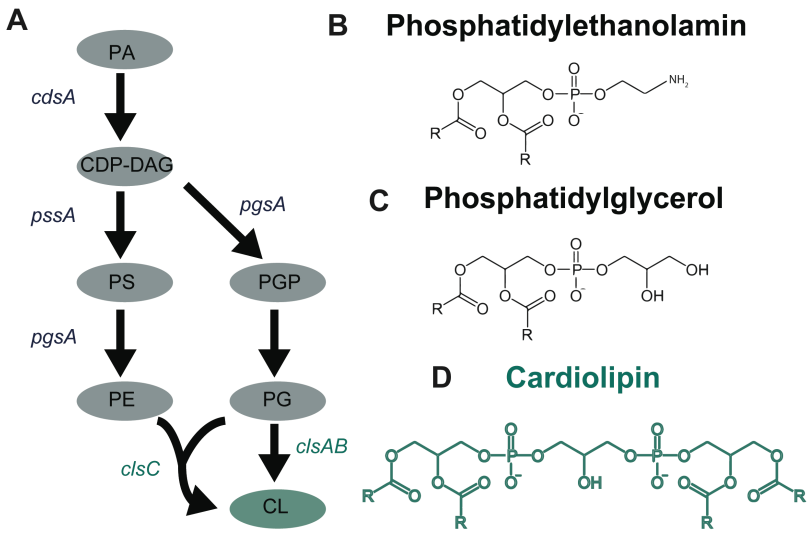

Figure 2. Phospholipids in *E. coli*. Synthesis pathway (A) and structures (B, C, D) of the major phospholipids of *E. coli*. PA: phosphatidic acid, CDP-DAG: cytidine diphosphate – diacylglycerol, PS: phosphatidylserine, PE: phosphatidylethanolamine, PGP: phosphatidylglycerol diphosphate, PG: phosphatidylglycerol, CL: cardiolipin. Genes of the affiliated phospholipid synthases are indicated.

The schematic phospholipid pathway of *E. coli* is shown in Figure 2. The pathway starts with the synthesis of *sn*-glycerol 3-phosphate (G3P) from dihydroxyacetone phosphate, catalysed in GpsA (G3P dehydrogenase [NAD^+]) (*19*). The fastening of the first fatty acid to G3P, thereby forming monoacyl-G3P (lysophosphatidic acid) as the second step in the *E. coli* phospholipid pathway, is performed by PlsB (*sn*-glycerol-3-phosphate 1-O-acyltransferase) (*20, 21*). The next step of the pathway in *E. coli* is catalysed by PlsC (1-acyl-*sn*-glycerol-3-phosphate 2-O-acyltransferase) (*22*). PlsC promotes the formation of the key intermediate: phosphatic acid (PA), by catalysing the attachment of the second fatty acid to the G3P backbone. CdsA (Phosphatydate cytidylyltransferase) catalyses the conversion of PA into the activated intermediate CDP-diacylglycerol (CDP-DG) in *E. coli*. On the contrary of the enzymes being part of the phosphatidic acid pathway, most so far sequenced bacterial genomes encode a protein exhibiting strong homology to this CDP-diglyceride synthase (phosphatidate cytidylyltransferase) (*23*). CDP-DG is utilized as a precursor building block for synthesising the major IM phospholipids of *E. coli* phosphatidylethanolamine (PE) or phosphatidylglycerol (PG) and cardiolipin (CL) (*15*). The cytoplasmic membrane of *E. coli* consists of approximately 75% PE,

20% PG and 5% CL during the logarithmic growth phase (*24*). Upon reaching the stationary phase during bacterial growth, the relative amount of CL in the cytoplasmic membrane of *E. coli* increases up to 10%, whereas the level of PG decreases almost stoichiometrically. The same effect can be discerned if the energy metabolism gets affected by pharmacological active substance such as dinitrophenol, penicillin, cyanide (*25-27*) or the bacteriophage T4 (*28*) which both lead to a decreased phosphorylation ability (*29*).

1.1.1.1. Phosphatodylethanolamin

PE is an essential, zwitterionic phospholipid (Figure 2) synthesized in *E. coli* by two enzymes. In the first step, the amphotrophic phosphatidylserine synthase PssA (*30*) is adding L-serine to CDP-diaglycerol while releasing CMP, and with this phosphatidylserine is generated (*31*). Subsequently, the phosphatidylserine decarboxylase (Psd) can synthesize PE by removing the carboxyl group (*32, 33*). PE has a comparably small head group, which can comply with the insertion of proteins within the membrane while still maintaining its integrity (*34*). PE is needed for the proper folding of the lactose permease, LacY. Without PE, the membrane insertion of LacY is inverting, meaning the normally cytosolic N-terminal half of the protein is deferred to the periplasm (*35, 36*). PE acts in this case, as analogous to a protein chaperon, like SecB. PE shows particular specificity in sustaining the correct protein folding (*37-39*). Temperature-sensitive *E. coli* mutants lacking PE do lyse at a nonpermissive temperature, most likely due to the accumulation of the intermediate PS (*40*). It has been reported that PE is reducing the secretion efficiency of the *E. coli* alkaline phosphatase (PhoA), raising the accumulation of prePhoA (*41*). Nevertheless, the regulatory two-component system Cpx is activated in PE deficient cells (*42*). PE deficiency leads to suppression of flagellin (*43*). The activity of the Tat transporting system in *E. coli*, which transports folded proteins across the cytoplasmic membrane, is reported to require PE (*44*). Additionally, a PE deficiency in *E. coli* results in an impaired adhesion due to the downregulation of the lipopolysaccharide synthesis pathway (*45*).

1.1.1.2 Phosphatidylglycerol

By dephosphorylation of the PG precursor phosphatidylglycerol-phosphate using the synthase PgsA, *E. coli* can produce the second partially essential anionic phospholipid PG (Figure 2) (*46*). The deletion of the *pgsA* gene blocks the synthesis of PG as well as the following synthesis of CL and results in not viable strains (*47*). This can be reversed by mutations of the gene *lpp* (*48*), which subsequently prevents the cells from accumulating the outer membrane lipoprotein Lpp, as this protein requires PG for its modification and proper localization (*49, 50*). Additionally, studies have argued that the failure in Lpp modification due to lack of PG is lethal to *E. coli*. Additionally, a defective DNA replication might be a reason for growth limitation. It is expected that with a lack of PG, the cells have a reactivation inability of DnaA due to its interactions with acidic phospholipids (*51, 52*). Comparable with the absence of PE, a lack of PG has been accused of having a negative effect in protein translocation. *E. coli* cells deficient in PG synthesis have been reported to be deficient in translocation of the outer membrane porins OmpA and PhoE (*53, 54*). A recent study has proven that PG can also be synthesized *pgsA* independently, by a cardiolipin synthase YbhO using PE and glycerol as substrates (*47*).

1.1.1.3 Cardiolipin

Cardiolipin (CL) is a large redundant anionic phospholipid (Figure 2) mostly found in energy-transducing membranes like the bacterial periplasmic membrane or the eukaryotic mitochondria (*55, 56*). CL is composed of two diacylphosphatodyl moieties bound to a glycerol molecule (*57*). In *E. coli,* there are three known cardiolipin synthases: ClsA, YbhO and YmdC (*58*). Each of these synthases contributes differently to the CL content under different growth conditions and in different growth phases. In *E. coli* the CL levels are increasing with reaching the stationary phase (*59*) or as a response to energy deprivation and osmotic stress (*60*). ClsA catalyses the reaction of two L-1-phosphatidyl-sn-glycerols (PG) to cardiolipin and glycerol (*61, 62*).

Deletion of the phospholipase D ClsA by disruption of the *clsA* gene of *E. coli* resulted in no detectable CL in cells harvested during logarithmic growth in low

salt medium (*63-65*). However, further studies have shown that the ∆*clsA ΔybhO* mutant is still able to generate CL, mostly in the stationary phase, leading to the discovery of an additional third CL synthase, YmdC (*58*). The CL synthesis by YbhO and YmdC is different than the reaction catalysed by ClsA, as they use PE and PG as substrates and forming CL and ethanolamine (*66*). The large hydrophobic side chains of the CL molecules opposing its relatively small hydroxyl head group, assigns to its peculiar physical properties (*67, 68*). These are essential in the formation of membrane domains in mitochondria as well as in bacteria (*69*). This prominent characteristic of a CL molecule is responsible for its large intrinsic curvature. Due to the binding of divalent cations across phosphate groups, the molecule sustains a curvature of ~1.3 nm^{-1} (70, 71). Cardiolipin is expected to raise membrane fluidity and to decrease the force required to pierce the membrane (*72*). This indicates a decrease in the mechanical stability of the lipid bilayer with an increase of CL. Elimination of diphosphatidylglycerol leads to cell size heterogeneity and an altered cell size homeostasis upon nutrition availability (*73*). Studies are suggesting, that CL is preferentially localising at the septa and cell poles of rod-shaped bacteria, irrespective of gram-positive *B. subtilis* (*74*) or gram-negative *E. coli* (*75*), as well as in *E. coli* minicells (*76*). This is supported by the finding that also CL microdomains are localising to negatively curved membrane regions (*77*). However, the limitation of specific assertions regarding CL localisations in membranes based on membrane staining with NAO (nonyl acridine orange) and following its predicted spectroscopic changes due to binding of NAO and CL (*78*) are discussed (*79*). Nevertheless, the mechanism underlying the CL accumulation at the cell poles remains unclear. Polar CL concentration could, for example, result from its biophysical properties or preferential interaction of CL with one or more proteins directed to the cell poles during growth (*60*).

1.1.1.4 Cardiolipin in eukaryotic mitochondria

In eukaryotic cells, cardiolipin is rather found in the mitochondrial membrane than in the plasma membrane (*80*). This fact supports the endosymbiosis theory, according to which the eukaryotic mitochondria goes back to the engulfment of bacteria through phagocytosis (*81*). For the mitochondria, CL is fulfilling a variety

of essential functions due to multiple interactions with a broad range of different proteins. Various signalling pathways are directly dependent on CL. Additionally, CL represents a structural constituent of the respiratory chain, which makes it essential for an effective respiration (*82*).

1.1.2 The cell membrane of *B. subtilis*

The phospholipid pathway of the gram-positive *B. subtilis* resembles to the one of *E. coli*. The lipids synthesis starts with phosphatic acid (PA), as common precursor. For the production of PE, PA in the first step is converted to CDP-diacylglycerol (CDP-DAG), followed by a decarboxylation. These two steps are performed by PssA and Psd. PgsA is responsible for the modification of CDP-DAG with glycerol-3-phosphate and subsequent secession of a phosphate group leading to PG, the only essential lipid of *B. subtilis* (*83, 84*). PG is the precursor for cardiolipin and lysyl-PG (L-PG). CL is formed out of two PG moieties by three paralogous synthases: ClsA, YwiE and YwjE. ClsA, the major CL synthase is expressed during logarithmic growth. YwiE, one of the two minor CL synthases is additionally required for protection against paraquat stress. YwjE is on the other hand involved in sporulation (*74, 85, 86*). MprF is transferring a lysyl group to PG, creating LPG (*87*). UgtP is synthesizing GL, a glycerolipid (*88*). Synthesis and desaturation of fatty acids are controlled by two regulatory systems: FapR and DesRK (*89, 90*) and additionally it is influenced by several stress conditions (*91, 92*). PE and CL rich domains are expected to localize at poles as well as in the septal regions (*74, 84*). The localisation corresponds to the FtsZ-dependent subcellular localization of the phospholipid synthases PssA, ClsA and PgsA (*84*). Recent studies using a phospholipid specific styryl dye from the FM series, propose a localisation of PG in a helical structure along the cell axis (*93, 94*), contrary to the indicated localization in a band or dot vice manner in *E. coli* (*95*). The general membrane composition of *B. subtilis* while logarithmic growth phase is divided in 20% of PE, 40% of PG and 25% of CL as well as roughly 15% percent of LPG. The distribution varies during the life cycle of *B. subtilis* (*96, 97*).

1.1.3 Membrane fluidity

As bacteria encounter a wide range of partly rapid environmental changes, they must immediately adapt to the new circumstances. To survive, the cells remodel their envelope including changes of the protein content of the outer and inner, the LPS structure as well as the phospholipid composition of the membranes (*98, 99*). The plasma membrane (IM) plays a crucial role in terms of cell viability, as it constitutes a barrier between the cells and their surrounding habitat. The intact physical state of the lipid bilayer plays a significant role in the effectiveness of the membrane barrier function (*100*). For a normal cell function, a mostly fluid membrane is required which is the case for most organisms at their physiological temperatures (*101*). *E. coli* responds to an increasing temperature with the synthesis of shorter lipids with more saturated acyl chains. The acyl chains of the lipids of the inner membrane exhibit a higher degree of unsaturation, as well as they get slightly longer (*102*). Contrariwise, with a sudden drop in temperature, the membrane fluidity is drastically reduced, which involves the inhibition of normal membrane functions. Without immediate correction of the composition, and in effect the fluidity, such shifts can cause physiological damage up to cell death (*103*). Several essential cellular activities are depending on proper membrane function, e.g. the cells sensing of pH, temperature, osmotic and atmospheric pressure, as well as the maintenance of the bacterial cell morphology, adaptation and homeostasis. As a result, abrupt environmental changes can cause modifications of membrane structures leading to a loss of physiological functions (*73, 104*).

1.1.4 Membrane proteins and their insertion into the phospholipid bilayer

In general, membrane proteins play a crucial role in every living cell. For processes like cell division, signal transduction, transport systems and energy production, *E. coli,* but also other organisms make use of integrated membrane proteins (IMPs). Roughly 20 to 30% of the genes encode IMPs belonging to the helical bundle class (*105*). However, the IMPs vary enormously in the number of transmembrane regions, as well as in their cytoplasmic and periplasmic domains (*106*). Many IMPs are components of bigger protein complexes and additionally,

some contain cofactors. The biogenesis of IMPs can be split in three different steps: the targeting of the nascent protein by the signal recognition particle SRP, insertion of the emerging protein into the membrane followed by folding and assembly, and quality control of the inserted protein in step three (*107*). The SRP, representing an ubiquitous targeting ribonucloeprotein particle, can be encountered in all kingdoms of life (*108*). *E. coli* SRP consists of the 4.5S RNA and the Ffh protein. This complex recognizes exposed signal anchor sequences and binds to the hydrophobic targeting signal when the nascent protein emerges from the ribosomal exit tunnel (*108-110*). With this the targeting of the ribosomal nascent chain complex (RNC) to the SRP receptor FtsY happens (*111*). Subsequently, the SRP-FtsY (co-translational) pathway targets the RNC to the Sec translocation for integration of the given inner membrane protein (*112*). To ensure that only the specific inner membrane proteins get integrated, the proteins are checked against incorrectness to ensure the fidelity of the system at each step (*113*). This just described integration steps can be named as the first part of inner membrane protein integration. It can be followed, if required, by a second part which consists of the formation of tertiary and even quaternary structures of interacting transmembrane proteins. Due to the integration of membrane proteins into the lipid bilayers, their stability and function can be dependent or at least affected by lipid interactions (*114, 115*). For example, the lactose permease of *E. coli* LacY has a mean membrane helix length of 24+/-4 residues (*116*), whereas the transmembrane helix length of the leader peptidase exhibit only 15 amino acids (*117*).

1.1.5 Hydrophobic mismatch

In case when the hydrophobic thickness of the membrane-spanning region of the integrated protein does not match with the membrane thickness, a so-called hydrophobic mismatch is targeted. This hydrophobic mismatch can occur for smaller peptides but also for transmembrane proteins traversing the membrane with several TM regions. The response of the membrane can vary depending on the type (positive or negative) of emerged mismatch (Figure 3, A and a). A hydrophobic mismatch can lead to conformational alterations and changes in protein folding, as well as to differences in oligomerization. These are followed by

changes in activity due to the mismatch response of lipids and proteins (*118*). The IMP surrounding the lipid bilayer responses to a mismatch either by thinning or by thickening the bilayer (Figure 3, B, b) which results in an increase or decrease of the acyl chain order (*119*). Several types of mismatches can be distinguished: lipids affecting the membrane integrated proteins or vice versa proteins influencing the lipids of the cytoplasmic membranes. A positive hydrophobic mismatch occurs when the TM segments are longer than the surrounding lipids. To overcome this positive length distinction, the TM region can tilt, occurring as a rotation of the TM region depending on the cross-section diameter of the protein. However, this is more likely for proteins with a single span TM region (*120*). Besides the tilting phenomena, a hydrophobic mismatch can also be mitigated by the oligomerization of membrane proteins (Figure 3, D, d). This means the helix-helix self-association is simply promoted by the less favoured helix-lipid interplay, meaning self-organisation of membrane proteins with increasing mismatch in the membrane (*121, 122*). The third possible reaction of a protein to a positive hydrophobic mismatch are conformational changes. Therefore, changes in the conformation of the backbone of the protein occur upon changes in the lipid environments (Figure 3, C, c). However, these backbone alterations are mostly minor changes (*123*) but occur frequently with local distortion (*124*). It is speculated that the length of the TM region can predict where in the membrane the protein will finally localise; however, meaningful evidence is lacking and therefore the theory is remaining vague. Apart from the lipids affecting the reaction of a transmembrane protein, the membrane integrated proteins can also affect the surrounding lipids to overcome a hydrophobic mismatch. Under conditions of a positive mismatch, the lipids can be stretched. As reaction to negative mismatch, the lipid acyl-chains can be disordered, and with this a formation of non-lamellar-structures is implemented (Figure 3, E, e). Additionally, the lipid sorting can be changed with the recruitment of a best matching mixture of lipids in terms of lipid and TM helix length (*125*).

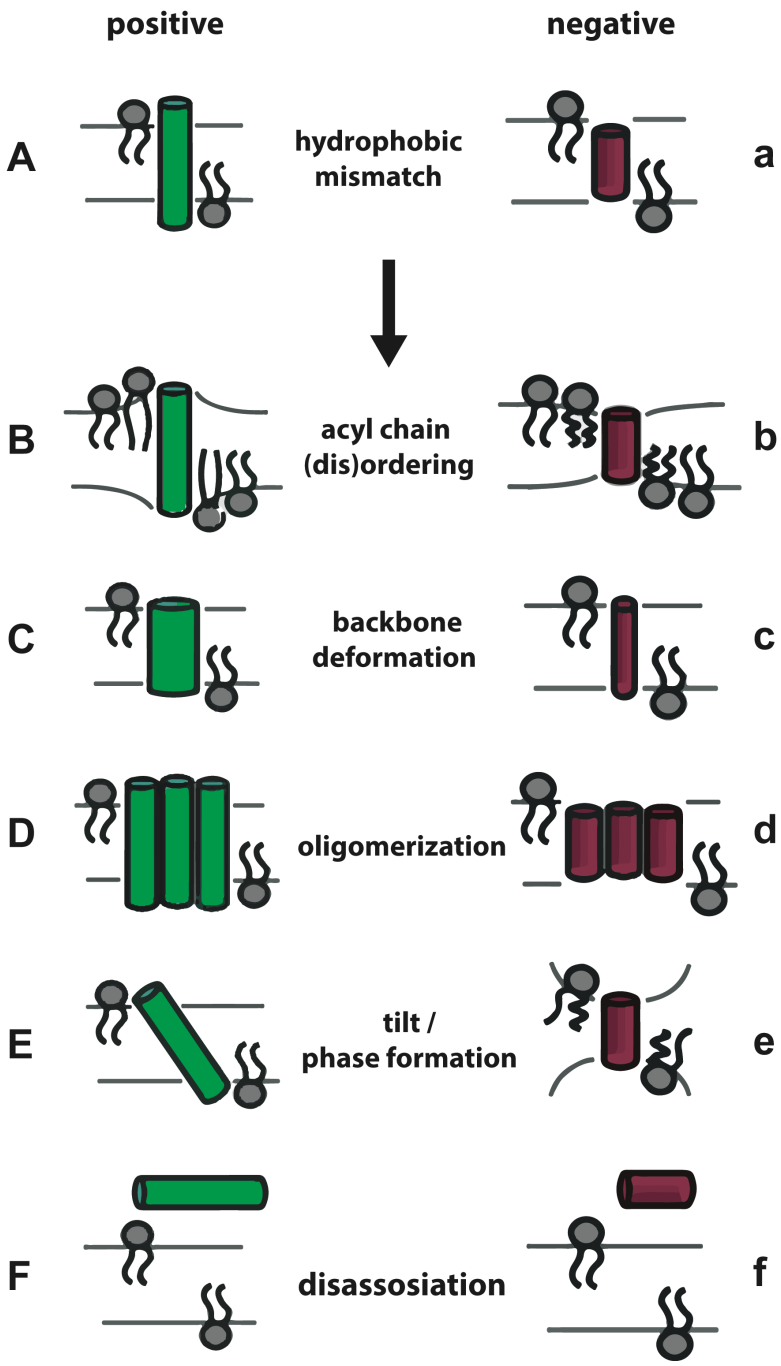

Figure 3. Effect of hydrophobic mismatch. Schematic description of possible adaptations to overcome positive (big letters) and negative (small letters) mismatch between transmembrane proteins and the lipid bilayer. Adapted from Planque *et al.*, 2003, (*119*).

1.2 The *E. coli* motility system

Throughout the prokaryotic world, several types of motility are known: e.g. gliding, swarming, twitching and also flagellar based motility (*126*). For *E. coli*, the

combination of the effective chemotaxis system and flagellar motility helps to reach the most preferred environments. Additionally, it allows the cells to compete with other species in reacting to surrounding stimuli. The flagellum is the filamentous motor organelle driving the cells locomotion. However, these appendages are not only involved in motility but also in host cell invasion and surface attachment. They enable the cells to be motile in liquids (swimming), as well as in static surface conditions (swarming). Flagella are surface-associated at the cells distal end, extending from the cytoplasm towards the outside. The flagellum consists of a basal body, including several rings and the central rod, the hook and a long helical filament (*127*). Flagella assembly and function involve more than 50 gene products (Figure 4).

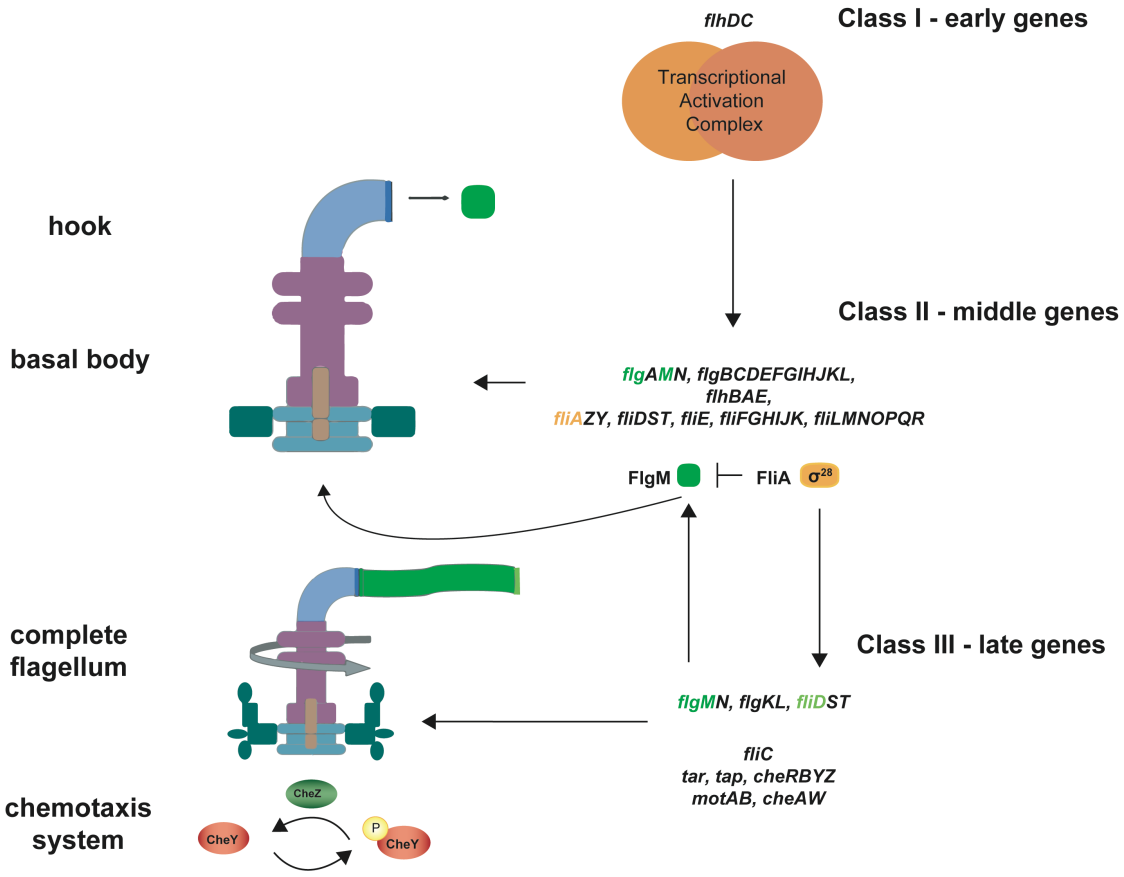

Figure 4. Flagella gene regulation and assembly in *E. coli*. The master regulator FlhDC (class 1) activates class 2 genes, one of which, FliA, regulates class 3 genes. Class 3 genes are not turned on until basal body and hook structures (BBH) are completely assembled. This is regulated by FlgM, by binding and inhibits FliA. When BBH are completed, FlgM gets exported, leaving FliA free for activation of the class 3 genes. *flgM* is transcribed from class 2 and a class 3 promoter.

The flagellums basal body consists of FliF as basic structure building the integral MS ring, a perch traversing the periplasmic space. The periplasmic P ring requires FlgA and FlgI for its assembly. The L or lipopolysaccharide ring is located in the outer membrane and build-up of FlgH. The basal body conceives the torque from the motor and transmits it to the hook and filament (*128*). The rotary motor which is reversible powered by proton or sodium motive force, is embedded in the cells envelope. It consists of two parts: a rotary part, responsible together with the Mot proteins for torque generation and a stator responsible for energy conversion. The stator consists of an integral membrane structure, which is formed by several copies of MotA and MotB and located around the basal body noncovalent attached to the cell walls peptidoglycan layer. The rotor part, consisting of several FliG copies, is attached to the MS ring of the basal body (*129*). The flagella motor operates in two modes as a response to the output of the chemotaxis system: CW (clock-wise) and CCW (counter-clock-wise). Therefore, a switch between the two rotating types is needed. The large switch complex comprises three proteins: FliG, FliM and FliN that form the cytoplasmic cup-like structure named as C ring (*130*). FliG can form a functional fusion with FliF elements of the MS ring (*131*) and is involved in switching as well as in torque generation. FliM is organized in multiple domains and represents the target for sensory transduction output (*132, 133*), whereas the exact role apart from its organization of FliN remains unclear (*134*). The hook, a cylindrical structure, functions as a joint between the long filament and the cell, and is formed by polymerized FlgE (*135*). As *E. coli* has multiple flagella emerging from several parts of the cell body, the hooks are essential for the effective bundle function of the flagella (*136*). The filament has a long, cylindrical structure and functions due to its helical shape as propeller. The filament grows length independently at their distal ends (*137*), that are formed by flagellin (FliC). The flagellin is forced out from the cytoplasm by a pump powered by a proton motive force (*138*). At the tip of the growing filament, a capping structure called the filament cap (FliD) can be found. FliD plays a decisive role in the assembly of FliC monomers while filament growth (*139*). Between filament and hook are two junction proteins located, FlgK and FlgL, acting as structural adapters (*140*).

The production and assembly of the complex flagella is energetic ornate. Therefore, the macromolecular complex is only synthesized if it constitutes beneficial to the cells survival. Regulation ensures efficiency of flagella assembly, meaning that all components are produced in roughly the order they are needed for assembly. This is achieved by a hierarchical transcription network (*141, 142*). Promoters tightly regulate the expression of flagellar genes that can be structured into three groups (Class 1, 2 and 3). The FlhDC master operon builds the top of the regulation hierarchy (*143*); it can be deliberated as an exclusive transcription unit of class 1 genes. FlhDC expression is controlled by multiple, also environmental, signals, e.g. pH, temperature and osmolarity, but also nutrient availability and growth-phase-dependent signals (*144-148*). Vice versa, FlhDC, is either directly or indirectly activating the transcription of the flagella machinery. Promoters of primary σ70-dependent transcription of class 2 genes are directly activated by FlhDC (*149, 150*). The seven FlhDC-dependent operons (flgAMN, flgBCDEFGHIJ, flhBAE, *fliA*ZY, fliE, fliFGHIJK, fliLMNOPQR) are encoding structural components and substantial regulation factors of the flagella's basal body and the belonging secretion apparatus (*135*). *fliA* encodes for the alternative minor sigma factor, σ28 (*151*) and *flgM* encodes the corresponding anti-sigma-factor (*152*). These two regulate the switch from early to late state flagella gene expression. With the presence of both factors in the bacterial cytoplasm, FlgM binds FliA, and with this preventing its interaction with RNAP, thereby the FliA-dependent transcription gets repressed. With completion of the class 2 gene assembly, FlgM gets exported to the outer space, initiating the FliA-dependent transcription of Class 3 genes. FliA activates the transcription of six operons: *flgKL*, *flgMN, fliC, fliDST, tar-tap-cheRBYZ*, and *motAB-cheAW* (*153*), additionally it can also initiate its operon. These Class 3 genes encode for products required in the late flagella assembly e.g. flagellin, the flagella motor as well as for chemotaxis related factors and genes (e.g. Tsr, Trg, Aer) and cyclic-di-GMP regulation of motility (*154-157*). It has been suggested that FliA can also activate transcription of the class 2 operons, e.g. *fliLMNOPQR* (*158, 159*).

1.3 Chemotaxis in *E. coli*

Chemotaxis names the ability of an organism to perform directed motion toward favourable or away from hazardous conditions by making use of a metabolism-independent sensory transduction system (*160*). The chemotaxis sensory system has two main features: the high degree of sensitivity and the high range of background concentrations over which the differences in certain compound concentrations can still be sensed (*161*). The bacterial chemotaxis is one of the most thoroughly studied signal transduction systems. The chemotaxis system is a unique two-component system, which converts an extracellular signal (chemoeffector) into an appropriate intracellular response (motility control).

Different types of bacterial motility can be distinguished, e.g. swimming, twitching and gliding (*162*). Swimming, the most common bacterial way of moving, is dependent on several long flagella anchored in the bacterial cell membrane. The flagellums are controlled by molecular motors which make use of transmembrane proton motive force as an energy source (*163*). The *E. coli* motility is referred to as “zick-zack” movement. This motion arises through switching sequences between the two distinct swimming modes called runs and tumbles. Flagella can rotate either in clockwise (CW) inducing tumbles, or in counter-clockwise (CCW) fashion inducing smooth running. While CCW rotation, several flagella form a large bundle and propel the cells in a forward direction, leading to smooth running. These so-called runs can last several seconds. With changing the rotation direction of at least one flagellum, the bundle gets disrupted, resulting in a short interval (roughly 0.1 seconds) of tumbling for reorientation of the cell. The reorientation angle depends on the number of CW rotating flagella (*161, 164, 165*). Without a gradient, the swimming of *E. coli* is composed of runs and tumbles, resulting in a random walk. This allows the cells to screen their current habitat for possibly better conditions. However, when *E. coli* encounters a favourable or unfavourable gradient, the straight runs get elongated and the frequency of tumble gets suppressed. The interplay of run and tumbles allows the cells to swim smoothly up or down a gradient for locating a better or more favourable environment (*166, 167*). The bacterial chemotaxis system relies on

temporal comparisons of sensed environmental changes of chemo effectors (*168*). Contrary to the bacterial system for eukaryotic cells, the chemotaxis system rather depends on a spatial analysis of a gradient along the cell (*169*).

1.3.1 Signaling pathway of the *E. coli* chemotaxis system

The chemotaxis pathway of *E. coli* is well characterized on a structural and biochemical level. It belongs to the family of two-component systems and can be divided into five essential components. In *E. coli,* the chemotaxis complex consists of specific chemoreceptors, the auto phosphorylating sensor histidine kinase CheA, the small adaptor protein CheW, the response regulator CheY, the methyltransferase CheR and the methyl esterase CheB.

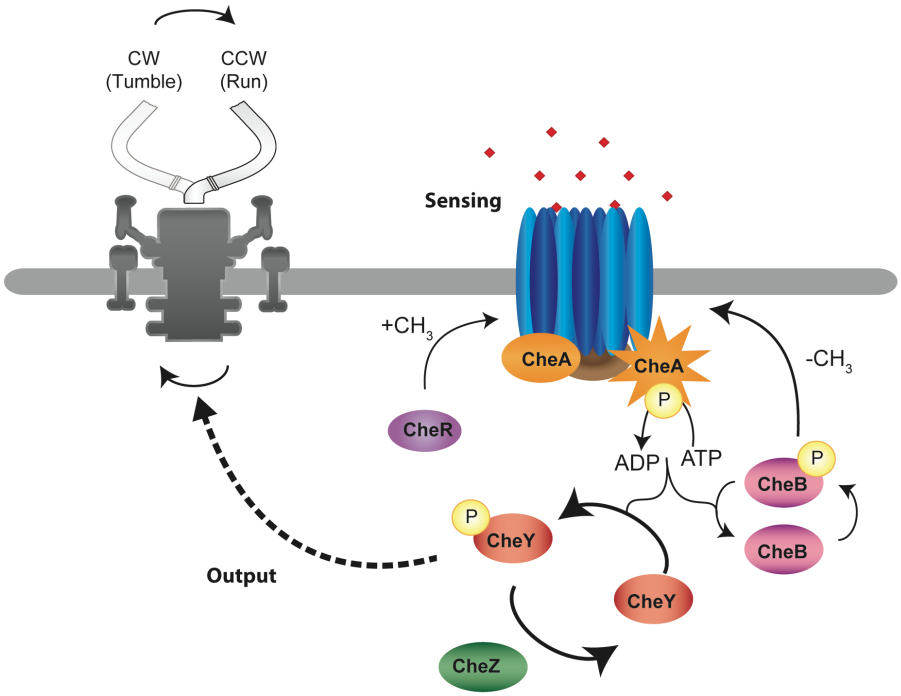

Figure 5. Chemotaxis signaling pathway in *E. coli*. Methyl-accepting chemoreceptors (MCP) form a sensory complex with CheA (histidine kinase) and CheW (adaptor protein). Ligand binding on the periplasmic site of the receptors regulates the autophosphorylation activity of CheA. A phosphoryl-group gets transferred to CheY (response regulator), controlling the flagellar rotation. CheY-P interacts with the motor switch complex, inducing tumbles due to a change from counterclockwise (CCW) to clockwise (CW) flagella rotation. CheY-P is dephosphorylated by CheZ (phosphatase)causing a response termination. CheB (methylesterase) and CheR (methyltransferase) control the sensory adaptation, by adjusting the level of receptor methylation.

In *E. coli,* the chemosensing (Figure 5) starts with the so-called methyl-accepting chemotaxis proteins (MCPs), which function as receptors for different ligands. The *E. coli* chemotaxis system is mainly regulated by CheA, which is anchored on the cytoplasmic side of the receptor using CheW as transducer (*161*). A conformational change of the receptor is triggered upon binding of chemo effectors on the periplasmic side of the MCP or due to changes in the receptor methylation modulated by the auto phosphorylation activity of CheA (*170, 171*). The activity of the kinase changes upon ligand binding. Attractant binding leads to a decrease in CheA activity, whereas binding of repellents leads to an enhancement of the auto phosphorylation activity. CheW is essential for this regulation; however, the exact manner remains unclear. With repellent binding, CheA transfers a phosphoryl-group to its response regulator CheY and with this subsequently leads to an increased level of CheY-P. The phosphorylated response regulator diffuses towards the flagella motor. This signal transmission leads to a direction change of the motor rotation from counter-clockwise to clockwise, causing tumbles. CheY-P gets dephosphorylated by CheZ. This protein acts as phosphatase, which is indispensable for the fast readjustment of bacterial behaviour (*172*). In the presence of chemo attractants, the increased receptor stimulation (receptor OFF state) leads to CheA inactivation and subsequently, to a rise in straight swimming section and a decrease in tumbling rate (*173*). As output, bacteria run smoothly when they are in a beneficial environment and start tumbling under potentially harmful conditions. The chemosensing pathway also includes an adaptation system allowing the cells to perform chemo sensing over more than four orders of magnitude of effector concentrations (*164*). This adaptation system is based on methylation and demethylation of four specific glutamate residues of the chemoreceptors (*174-176*) and controlled by CheR and CheB. A higher methylation grade of an attractant binding receptor, caused by CheR increases the CheA kinase activity. With this, the sensitivity towards the present stimuli decreases, resulting in the so-called sensory adaptation. The adaptation is reversed through demethylation of the receptor by CheB. The methyl esterase CheB is regulated by CheA through phosphorylation. This negative feedback sensory adaptation system allows the

cells to examine and react towards temporal changes of environmental stimuli (*177, 178*).

1.3.2 Chemoreceptors of *E. coli*

The sensing of outside stimuli is performed by several chemoreceptors. The genome of *E. coli* encodes two major and three minor receptors. The sensory complex is dominated by the major receptors with roughly 10000 expected copies per cell, in contrast to 1000 copies of the minor receptors (*179*). However, newer findings suggest that the difference in copy number is significantly smaller than previously estimated. It looks like minor receptors are more abundant than earlier expected and that they make up to one-quarter of the total amount of chemoreceptor per cell (*179*). The two high abundance receptors Tar and Tsr sense aspartate and serine, whereas *E. coli* uses the low abundance receptors Tap and Trg for sensing dipeptides, galactose and ribose (*180, 181*). For sensing with the major receptors, the ligands get mainly bound directly. Whereas the effectors for the minor receptors get bound indirectly, with the help of periplasmic binding proteins (BPs). The chemoreceptor Tar of *E.coli*, build-up of 553aa, is sensing the attractants aspartate through direct binding and maltose via binding of a periplasmic maltose-binding protein (*182*), as well as the repellents nickel and cobalt. The second major chemoreceptor of *E. coli* Tsr, is sensing L-serine and related amino acids such as cysteine, L-alanine and glycine as attractants and, e.g. acetate, benzoate, indole and L-leucine as repellents (*183*). The minor receptor Tap interacts with the periplasmic dipeptide-binding protein DppA to convey the sensing of di- and tripeptides (*184*). The other low abundance receptor Trg is sensing ribose and galactose by interaction with the periplasmic ribose- or galactose-binding proteins (*185*). The two major receptors, as well as the two minor receptors, are reported to be thermosensitive (*186-188*). The homodimeric receptors Tar, Tsr, Tap and Trg consist of four main parts: the outer ligand-binding domain, two transmembrane domains (TM1 and TM2), a HAMP domain and the cytoplasmic domain for sensory adaption and protein interaction (Figure 6). Upon ligand binding on the sensory domain, a conformation change of the transmembrane domains is triggered. This signal is further transmitted to the receptors cytoplasmic part by the HAMP domain. The HAMP (Histidine kinase

adenylyl cyclase methyl-accepting chemotaxis protein–phosphatase) functions as a signal conversion domain. The cytoplasmic signalling domain includes a methylation helix (MH) bundle, a flexible bundle, and a protein contact region that interacts with the kinase for its activity regulation. The fifth receptor, Aer, is structured differently: the periplasmic domain is missing, but therefore an additional PAS (Per-Arnt-Sim) domain can be found at the N-terminus. With this, the receptor belongs to the family of PAS domain proteins, which are involved in sensing oxygen, redox potential and light (*189, 190*). However, the aerotactic response is methylation independent and the Aer receptor does not get methylated in contrast to the other receptors (*191*). Mutations in different regions of the receptors are used to analyse distinct features of the receptor signalling, e.g. HAMP domain regulation, signalling control and cytoplasmic signalling of the hairpin tip (*192-196*). It has been shown that sequence changes (e.g. elongation or reduction) in the TM2 region of Tar lead to an inverted response (attractant/repellent) towards sensed amino acid ligands (*197*).

1.3.3 Formation of chemoreceptor clusters in *E. coli*

In general, chemoreceptor clustering is conserved amongst all studied prokaryotic chemotaxis systems (*198*). For *E. coli*, the assembly of homodimeric chemoreceptors (MCPs) in highly ordered arrays has been a research focus for several years. MCPs span the cytoplasmic membrane as homo-dimers and associate in trimers of dimers as the smallest building block for chemoreceptor clustering (*199-201*). Reconstitution of chemotaxis proteins within lipid nanodiscs revealed two receptor trimers of dimers, associated with a dimeric CheA coupled with two molecules of CheW, are forming the core signalling complex of the *E. coli* chemotaxis system (*202, 203*). Each monomer of the CheA dimer consists of 5 functionally different domains: a phosphorylation site (P1), a site for CheB and CheY binding (P2), a dimerization domain (P3), a catalysis domain (P4) and a site with two subdomains for receptor/CheW coupling (P5). For forming the core unit of receptor clustering, a CheA dimer is expected to connect two trimers of dimers via the P5 domain. Additionally, CheW binds to a receptor dimer in each trimer of dimers. The P3 domain of CheA is localising between the receptors,

without physical interaction. The P5 domain of CheA is homologous to the P5 domain of CheW. P5 subdomain 1 of CheA binds CheW at the P5 subdomain 2 and with this CheA gets linked with the receptor dimers of the locally opposite trimer of dimer. These two interactions, the dimerization of the CheA P3 domains and the two CheA–P5-CheW heteromers are responsible for bridging the two trimers of dimers (*171*). The key parts for interactions between the receptor dimers are similar to all receptors of *E. coli*, allowing the arrays to be formed with mixed receptors. This core signalling complex forms the basic building block for receptor assembly in high ordered complexes of about ~250 nm2 in size or ~6500 MCPs in number (Figure 6) (*204*). Robust clustering of MCPs requires CheA and CheW, still, CheA- or CheW- independent clustering can be observed, even though, it is more diffusive (*205, 206*). Recent studies explaining the subcellular localisation and chemoreceptor clustering in the absence of CheA and CheW, are based on possible interactions between the receptors and their TM regions with the lipid bilayer. This suggests that the receptors can organise themselves in membrane areas, where the TM length matches the size of the membrane. This can lead to a deformation of the bilayer and thereby acts as an attractive force for receptor clustering. Membrane protein clustering can generally be facilitated by the aforementioned hydrophobic mismatch (*125, 207*). Additionally, it has been shown that the TM regions of the receptor clusters anchoring the receptor in the membrane, is able to mediate cluster formation within the membrane by themselves (*208*). Only the high abundance of the receptors Tar and Tsr can form clusters independently, the minor receptor Tap and Trg might still localize at the cell poles, but are not capable of forming clusters by themselves without the major receptors (*209, 210*).

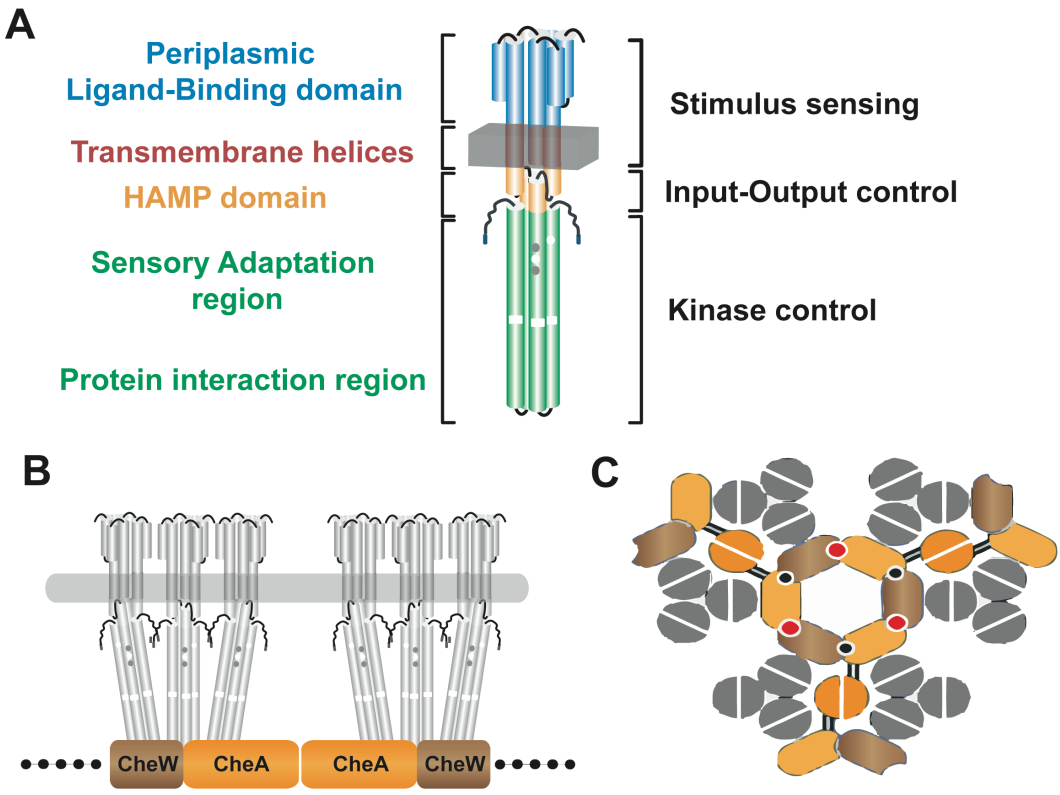

Figure 6. Chemoreceptor clustering in *E. coli*. Schematic drawing of a methyl-accepting chemoreceptor. Stimulus sensing occurs through ligand binding at the periplasmic receptor domain. Two transmembrane helices are anchoring the receptor in the membrane. The cytoplasmic part contains the HAMP domain as input/output control, as well as the sensory adaptation and protein interaction regions for kinase control (A). Adapted from Bi *et al*., 2016, (*211*). Schematic of the minimal core signaling complex, consisting of two receptor trimers of dimers (light grey), a CheA (orange) dimer and two CheW moieties (brown) (B). Display of a receptor array. Illustrating interactions between the P5 subdomain 2 and CheW subdomain 1 forming the hexagonal P5-CheW rings. These rings are interconnecting three core complexes (C). Adapted from Piñas et al., 2016, (*212*).

The chemoreceptors are associated with the cytoplasmic membrane of *E. coli* and are mainly localized at the cell poles (*213*) and along the cell body (*214*), named as polar and lateral chemoreceptor clusters. These receptor clusters are thought to be formed by stochastic self-assembly, which means that the new individual receptors are inserted in the membrane along the entire cell and then either joining an existing receptor cluster or forming new ones (*215*). Clusters are extremely stable formations with high stability lasting even longer than a cell generation (*216*). The exchange rate of the clusters match the signalling function of the chemotaxis proteins (*217*). This dependency of cluster formation and

signalling might allow the regulation of chemotaxis protein stoichiometry and receptor size dependent on response upon stimulation (*218*). However, the process of array-complexes finding their position remains partially unclear. A recent study could show that the membrane localization of the chemoreceptors is highly sensitive to membrane curvature. The authors found that the cone-shaped trimers of dimers (ToD) do form clusters that are highly enriched in outwards arched curved membrane regions. the authors propose that chemoreceptor ToD adapt a curved cone shape to maximize conformational entropy (*219*).

1.4 Comparison of the chemotaxis systems of *E. coli* and *B. subtilis*

E. coli as well as *B. subtilis* direct their motion towards favourable and away from disadvantageous conditions. This is possible, due to adjustment of their movement using runs and tumbles. The chemotaxis pathways of these two microbes vary at some points. The response to extracellular signals is regulated by CheA (histidine kinase) activity. The binding of chemoattractant in *E. coli* leads to an inactivation of CheA, whereas attractant binding in *B. subtilis* leads to an activation of CheA (*220, 221*). CheA phosphorylates CheY. CheY-P binds to the flagellar motor resulting in an increase of tumble frequency in *E. coli* and in runs for *B. subtilis* (*222, 223*). Both organisms use receptor methylation to adjust the CheA sensitivity towards attractants. This is performed by CheR and CheB (*177, 224*). Whereas for *E. coli* the activity of CheA is proportional to the methylation of the receptors, for *B. subtilis* the CheA activity is dependent on the location of the methylated residues. The *E. coli* phosphatase CheZ, does not exist in *B. subtilis*. Therefore, *Bacillus* has three more chemotaxis proteins: CheC, CheD and CheV. CheC is involved in the negative regulation of receptor methylation (*225*), contrary CheD is the positive regulator of receptor methylation (*226*). CheV is predicted to negatively regulate the receptor activity and is a CheW response regulator fission (*227*). FliY, the motor switch protein (C-ring) and CheY-P phosphatase of *B. subtilis* has no homolog in *E. coli* (*228, 229*). *B. subtilis* has two soluble

chemoreceptors (HemAT, YfmS) for Aero taxis and chemotaxis control as well as and several membrane-bound chemoreceptors (McpA, McpB, McpC, TlpA, TlpB, TlpC, YoaH, YvaQ). McpA and McpB are used as pH sensor, McpB is additionally used in asparagine taxis (*230, 231*). McpC controls the taxis towards the amino acids proline, threonine, glycine, serine, lysine, valine and arginine (*232*). TlpA senses acidic environments, vice versa TlpB senses alkaline environments (*231*). The sensing properties of TlpC, YoaH and YvaH remain still elusive.

2 AIMS OF THIS STUDY

The study on bacterial cell membranes is more and more emerging as field of interest in microbial research. Primary function of the membrane is the protection of the cell. However, the cytoplasmic membrane also contains a various number of proteins acting as transport proteins, cell adhesion proteins, enzymes and also receptors. Aims of this study was to elucidate the influence of the cytoplasmic membrane composition on different membrane associated systems in the gram-negative organism *E. coli* and the gram-positive *B. subtilis*. Main focus of this research project was to examine the effect of cardiolipin, a phospholipid of the cytoplasmic membrane, on the chemotaxis system of *E. coli*. In detail, the influence of cardiolipin on the assembly of higher ordered chemoreceptor complexes and their signalling function as well as the relation between cardiolipin and the mobility of chemoreceptors within the membrane. Additional interest was to investigate the correlation between cardiolipin and the motility system of *E. coli*. Another area of interest was the effect of cytoplasmic membrane alterations in *E. coli* and *B. subtilis* on growth, chemotaxis and the motility system.

3 MATERIAL AND METHODS

3.1 Chemicals and consumables

A List of all chemicals and consumables used for this study is listed in Table 1.

Table 1. Chemicals and consumables used in this study.

Substrate	Supplier
Acrylamide mix	Sigma-Aldrich
Agar bacteriology	AppliChem
Agarose ultra-pure	Difco
Ammonium Nitrate (NH_4NO_3)	Roth
Ammonium Sulfate ($(NH_4)_2SO_4$)	Sigma
Ampicillin	AppliChem
APS	Roth
Bacto tryptone	BD Biosciences
Bacto yeast extract	BD Biosciences
$CaCl_2$	Roth
Casamino-acids	BD Biosciences
Chloramphenicol	AppliChem
Collistin	Sigma-Aldrich
D-glucose	AppliChem
Dimethyl sulfoxide (DMSO)	Sigma-Aldrich
EDTA	Merck
Fe[III]-ammonium-citrate	Sigma-Aldrich
Glacial acetic acid	Sigma-Aldrich
Glycerol 99.5%	Gerbu
Glycine	Roth
Isopropyl-β-D-thiogalactoside (IPTG)	Roth
Kanamycin sulphate	Sigma-Aldrich
L-Serine	Acros Organics
Lactic acids	Fluka
Macrolide-lincosamide-streptogramin (mls)	Sigma-Aldrich
Magnesium sulfate ($MgSO_4$)	Sigma-Aldrich
Methionine	Sigma-Aldrich
Nicl2	Sigma-Aldrich
Poly-L-Lysine	Sigma-Aldrich
Polymyxin B	Sigma-Aldrich
Potassium citrate	Sigma-Aldrich
potassium glutamate	Sigma-Aldrich
Potassium phosphate dibasic (K_2HPO_4)	Sigma-Aldrich

Potassium phosphate monobasic (KH_2PO_4)	Sigma-Aldrich
Proteinase K	ThermoFisher
SDS	Roth
Sodium chloride (NaCl)	Roth
Sodium citrate dihydrate ($C_6H_5Na_3O_7$)	Sigma-Aldrich
sodium lactate	Sigma-Aldrich
Sodium salicylate	Sigma-Aldrich
TEMED	AppliChem
Tetracyclin	Roth
Tris base	Roth
Tryptone	Roth
Tryptophan	Fluka
Yeast Extract	AppliChem
α-methyl-DL-aspartate (MeAsp)	Sigma-Aldrich

3.2 Media and Buffer solutions

3.2.1 Media, plates and media additives

All Media, if not indicated differently, were autoclaved for 20 min at 121°C and 20 bar. If necessary, agar was added prior to autoclaving.

Luria broth (LB) medium

10 g Bacto tryptone

5 g Bacto yeast extract

5 g NaCl

Adjusted with NaOH to pH 7 and ddH_2O was added up to a total volume of 1 L.

Tryptone broth (TB) medium

10 g Bacto tryptone

5 g NaCl

Adjusted with NaOH to pH 7 and ddH_2O was added up to a total volume of 1 L.

Luria broth (LB) plates

1.5 g Agar/ 100 mL LB medium

TB Soft agar plates

0.27 g Agar (Bactoagar) / 100mL TB medium

MN medium

136 g K_2HPO_4 (x3 H_20)

60 g KH_2PO_4

10 g Na-citrate (x2 H_20)

MNGE medium (100mL), sterile filtered

9.2 mL 10xMN medium

82.8 mL water

10 mL Glucose (20%)

500 µL K-Glutamate (40%)

500 µL Fe[III]-ammonium-citrate (2.2 mg/mL)

1 mL Tryptophan (5mg/mL)

300 µL $MgSO_4$ (1M)

Expression mix, sterile filtered

5 mL Yeast extract (5%)

2.5 mL Casamino-acids (CAA) (19%)

2.5 mL Water

500 µL Tryptophan (5 mg/mL)

Antibiotics and solutions for induction used in this study are listed in table 2.

Table 2. Antibiotics and solutions.

Antibiotics/Inducers	Stock solution
Ampicillin	100 mg/mL in ddH_20
Chloramphenicol	34 mg/mL in 70% ethanol
Kanamycin	50 mg/mL in ddH_20
Collistin	20 mg/mL in ddH_20
Polymyxin B	20 mg/mL in ddH_20
IPTG	100 mM in ddH_20
Sodium Salicylate	100 mM in ddH_20

3.2.2 Buffers

Lysis Buffer

50 mM	EDTA
0.1 M	NaCl

Adjusted to pH 7 using NaOH.

TE buffer

10 mM	TRIS base
1 mM	EDTA

Adjusted to pH 8 using HCl.

Tethering buffer

5 mL	1 M K_2HPO_4
5 mL	1 M KH_2PO_4
0.2 mL	0.5 M EDTA
0.1 mL	10 mM Methionine
1 mL	90% lactic acid

Adjusted to pH 7 using NaOH and ddH_20 added up to a volume of 1L.
For indicated experiments Tethering Buffer without EDTA was used.

Chemotaxis buffer (*B. subtilis*)

10 mM	K_3PO_4
0.1 mM	EDTA
0.14 mM	CaCl
0.3 mM	$(NH_4)_2SO_4$
5 mM	sodium lactate
0.05 %	(v/v) glycerol

Adjusted to pH 7 using NaOH.

P1 Buffer

10 mM	$MgSO_4$
5 mM	$CaCl_2$

sterile filtered

TAE Buffer

242 g	TRIS base
57.1 g	glacial acetic acid
100 ml	0.5 M EDTA (pH 8)

ddH_20 added to a total volume of 1L

10x SDS Running Buffer

250 mM	TRIS Base
1.92 M	Glycine
1%	SDS

12% SDS resolving gel

1.7 mL	ddH_20
2 mL	30 % Acrylamide mix
1.3 mL	1.5 M Tris (pH 8.8)
50 µL	10 % SDS
50 µL	10 % APS
2 µL	TEMED

5% SDS stacking gel

0.68 mL	ddH_20
0.17 mL	30 % Acrylamide mix
0.13 ml	1.5 M Tris (pH 6.8)
10 µL	10 % SDS
10 µL	10 % APS
1 µL	TEMED

10x TBS

250 mM Tris base

1.5 M NaCl

pH 7.5

for 1x TBST: added 1mL of Tween20 to 1 L 1xTBS

10x Western Transfer Buffer

250 mM Tris base

1.92 M Glycine

for 1x Transfer buffer 10% Methanol was added.

3.2.3 Reaction Kits

The Reaction Kits listed below were used in this study, the guidelines given by the supplier were followed.

- GeneJET DNA Purification Kit, ThermoFisher Scientific, Dreieich
- GeneJET Gel Extraction Kit, ThermoFisher Scientific, Dreieich
- GeneJET Plasmid Miniprep Kit, ThermoFisher Scientific, Dreieich

3.3 Bacterial strains

Table 3. *E. coli* strains used in this study.

E. coli	Description	Source
NS2	VS367 *ΔybhO*	This study
NS3	VS367 *ΔymdC*	This study
NS54	VS367 *ΔclsA*	This study
NS8	VS367 *ΔybhO ΔymdC*	This study
NS89	VS367 *ΔclsA ΔybhO ΔymdC*; Kan^R	This study
VS367	RP437 *Δtar*-tap DE4530 *Δtsr* DE5547 *Δaer* DE1 *ygjG*::Gm *Δtrg* DE4543	Sandy Parkinson
VS558	W3110 *rpoS*+	Regine Henge

Table 4. *B. subtilis* strains used in this study.

B. subtilis	Description	Source
***WT*168**	trpc2 attSpß	Sourjik lab
AMP213	trpc2 attSpß *Δ (mcpA mcpB tlpA tlpB)101::cat mcpC4::erm tlpC::cat yvaQ::erm yfmS::erm yoaH::erm yhfV::erm*	Ordal lab (*233*)
HB5343	trpc2 attSpß *ΔpsdA*::Mls^R	Helmann lab (*87*)
HB5361	trpc2 attSpß *ΔpssA*::Spec^R	Helmann lab (*87*)
HB5362	trpc2 attSpß *ΔywnE*::Cm^R	Helmann lab (*87*)
HB5337	trpc2 attSpß *ΔmprF*::Kan^R	Helmann lab (*87*)
NSB12	trpc2 attSpß *ΔywnE*:: Cm^R *ΔywjE*:: Mls^R	This study
NSB17	trpc2 attSpß *ΔywnE*:: Cm^R *ΔywiE*:: Mls^R	This study
NSB18	trpc2 attSpß *ΔywnE*:: Cm^R *ΔywjE*:: Mls^R *ΔywiE*:: Kan^R	This study

3.4 Plasmids and oligonucleotides

Table 5. Plasmids used in this study.

Self-propagating plasmids	Description	Source
pAMP13	pKG116, Tar-TM1(I24G)-sfGFP-TM2; Cm^R	(*208*)
pAMP14	pKG116, Tar-TM1(I24T)-sfGFP –TM2; Cm^R	(*208*)
pAMP20	pKG116, Tar-TM1-sfGFP (-3)- TM2; Cm^R	(*208*)
pAMP22	pKG116, Tar-TM1-sfGFP (-1)- TM2; Cm^R	(*208*)
pAMP23	pKG116, Tar-TM1-sfGFP (+1)- TM2; Cm^R	(*208*)
pAMP24	pKG116, Tar-TM1-sfGFP (+3)- TM2; Cm^R	(*208*)
pAMP4	pKG116, Tar-TM1-sfGFP-TM2; Cm^R	(*208*)
pCP20	FLP$^+$; Amp^R Cm^R	(*234*)
pKG110	expression vector, p15A ori, nahG promotor, Cm^R	Sandy Parkinson
pKG116	expression vector, pACYC184 ori; Cm^R	
pNS1	pKG110 derivate; expression of ClsA; Cm^R	This study
pNS14	*fliC* reporter; Amp^R	This study
pNS15	*fliA* reporter; Amp^R	This study
pNS16	*fliC* reporter; Cm^R	This study
pNS17	*fliA* reporter; Cm^R	This study
pNS18	short Tar (TM2 -1) –YFP; Amp^R	This study
pNS19	short Tar (TM2 +1) –YFP; Amp^R	This study
pNS2	pKG110 derivate; expression of PssA; Cm^R	This study
pNS20	short Tar (TM2 +3) –YFP; Amp^R	This study
pNS26	short Tar (TM2 -2) –YFP; Amp^R	This study
pNS3	pKG110 derivate; expression of PsD; Cm^R	This study
pNS4	pKG110 derivate; expression of YwjE; Cm^R	This study
pNS5	pKG110 derivate; expression of PgsA; Cm^R	This study

pNS6	pKG110 derivate; expression of YwiE; Cm^R	This study
pNS7	pKG110 derivate; expression of MprF; Cm^R	This study
pNS8	pKG110 derivate; expression of CdsA; Cm^R	This study
pTrc99A	expression vector, pBR ori, trc promoter, Amp^R	Sourjik lab
pUA66-*fliA*	pUA66-*fliA*-gfpmut2; pSC01 ori, Kan^R	(*235*)
pUA66-*fliC*	pUA66-*fliC*-gfpmut2; pSC01 ori, Kan^R	(*235*)
pVS1092	Tar(QEQE) in pLC113; Cm^R	Sourjik lab
pVS132	pTrc99A-RBS, eYFP; Amp^R	Sourjik lab
pVS160	pACYC based tsr expression vector; pPa114; Cm^R	Sandy Parkinson
pVS216	pTrc99a derivative, CheW-eYFP; Amp^R	Sourjik lab
pVS263	pTrc99A-RBS, Tar-eYFP; Amp^R	(*236*)
pVS332	pTrc99A-RBS, tetR-eYFP; Amp^R	Sourjik lab
pVS419	pTrc99A-RBS, Tar (1-397) -eYFP; Amp^R	(*236*)
pVS448	pTrc99A-RBS, mtlA-eYFP; Amp^R	Sourjik lab
pVS457	pTrc99A-RBS, lacY-eYFP; Amp^R	Sourjik lab
pVS483	pTrc99A-RBS, Hns-eYFP; Amp^R	Sourjik lab
pVS576	pTrc99A-RBS, nagE-eYFP; Amp^R	Sourjik lab
pVS686	pTrc99A-RBS, Tsr -eYFP; Amp^R	(*237*)
pVS88	pTrc99a derivative, CheY-eYFP / CheZ-eCFP; Amp^R	(*166*)

Integrative plasmids	**Description**	**Source**
pCH7	pDR111 derivate; Integration vector; integrates into *amyE* locus of *B. s*. genome; Amp^R in *E. coli*; $Spec^R$ in *B.s*.; gen-expression from hyper-spank promoter is chemically inducible by IPTG	Master thesis, Carolin Höfler, 2011

Table 6. Primers used in this study.

Primers	**Sequence**	**Restriction site**	**Target**	**Source**
Bi-Tar-A198I199I-F	attattGTGGTGGTATTGATTCTGCTGG	-	Tar TM helix (+2 nt) fwd	Shanghyu Bi (*238*)
Bi-Tar-A198I199I-R	CAGCGCGATAACCGCCAG	-	Tar TM helix (+2 nt) rev	Shanghyu Bi *238*)
Bi-Tar-A199I-F	attGTGGTGGTATTGATTCTGCTGG	-	Tar TM helix (+1 nt) fwd	Shanghyu Bi *238*)
Bi-Tar-A199I-R	CAGCGCGATAACCGCCAG	-	Tar TM helix (+1 nt) rev	Shanghyu Bi *238*)
Bi-Tar-d198199-F	GTGGTGGTATTGATTCTGC	-	Tar TM helix (-2 nt) fwd	Shanghyu Bi *238*)
Bi-Tar-d198199-R	GATAACCGCCAGTTGCCA	-	Tar TM helix (-2 nt) rev	Shanghyu Bi *238*)
Bi-Tar-d199-F	GTGGTGGTATTGATTCTGCTG	-	Tar TM helix (-1 nt) fwd	Shanghyu Bi *238*)

Bi-Tar-d199-R	CGCGATAACCGCCAGTTG	-	Tar TM helix (-1 nt) rev	Shanghyu Bi *238*)
Bi-TarA198I199I200I-F	tattGTGGTGGTATTGATTCTGCTGG	-	Tar TM helix (+3 nt) fwd	Shanghyu Bi *238*)
Bi-TarA198I199I200I-R	ataatCAGCGCGATAACCGCCAG	-	Tar TM helix (+3 nt) rev	Shanghyu Bi *238*)
prNS1	CATATGGCGGCCGCGTGAATTACATCCCCTGTATGATTACG	NotI	*pssA* fwd	This study
prNS10	TCCGGTCTGCAGGGAGGCGGCCTAATTCCATCTCCCAGACTCCAG	PstI	*pssA* rev	This study
prNS11	TCACTGCTGCAGGGAGGCGGCGTGAGTATTTCTTCCATCCTTTTATCAC	PstI	*clsA* fwd	This study
prNS17	CATATGGCGGCCGCatgTTTAACTTACCAAATAAAATCACAC	NotI	*pgsA* fwd	This study
prNS18	TCCGGTGGATCCttaGTTAGATGTTTTTAACGCTTCC	BamHI	*pgsA* rev	This study
prNS23	CATATGGCGGCCGCatgAAGGTATTTATCGTGATTATGATC	NotI	*ywjE* fwd	This study
prNS24	TCCGGTGGATCCttaTAAGAAATAAGATAATGCCCTGC	BamHI	*ywjE* rev	This study
prNS240	atagccGAGCTCctccacctccggatcc	SacI	Linker Tar YFP rev	This study
prNS241	cgctagGAATTCagcggccgcgactcta	EcoRI	fwd eYFP Tar	This study
prNS25	CATATGGCGGCCGCatgTTTAATACGGCTGTAAAGATTCTG	NotI	*psd* fwd	This study
prNS250	atagccggatccggaggtggag	BamHI	fwd linker between Tar and eYFP	shanghys constructs
prNS251	cgctagGAATTCacccatggcacactcc	EcoRI	rev before Tar	This study
prNS252	atagccggatccatgATTAACCGTATCCG	BanHI	fwd Tar	This study
prNS253	cgctagGAATTCAAATGTTTCCCAGTTTGG	EcoRI	rev Tar	This study
prNS26	TCCGGTGGATCCttaTTCTTCGTAACCTATCAGTTCTC	BamHI	*psd* rev	This study
prNS27	CATATGGCGGCCGCatgCTGAAAAGGAGACTGGAATTTTTC	NotI	*ywiE* fwd	This study
prNS28	TCCGGTGGATCCttaCAGAACACCTGAAAACAGGCG	BamHI	*ywiE* rev	This study
prNS29	CATATGGCGGCCGCttgCTGATTAAAAAGAATGCTTTATCAATATTAAA	NotI	*mprF* fwd	This study
prNS30	TCCGGTGGATCCttaGACGGAGTCTTTTTTGCTTTTGCC	BamHI	*mprF* rev	This study
prNS31	CATATGGCGGCCGCatgGTGGACATGAAACAAAGAATTTTTGAC	NotI	*cdsA* fwd	This study

prNS32	TCCGGTGGATCCttaTGAAAAAAGGGCAAGCAGAAAGTAC	BamHI	*cdsA* rev	This study
prNS33	CAGCGAACCATTTGAGGTGATAGGctgccattcatccgcttattatcac	-	Cm^R fwd LFH	This study
prNS34	CGATACAAATTCCTCGTAGGCGCTCGcgtaagaggttccaactttcacc	-	Cm^R rev LFH	This study
prNS35	GCACTCGACACACGCGTATAGATC	-	*ywjE* up fwd LFH	This study
prNS36	CAAGCAGAATCAAGGCAAAGAAAATAACGCCTATCACCTCAAATGGTTCGCTG	-	*ywjE* up rev LFH	This study
prNS37	CGAGCGCCTACGAGGAATTTGTATCGGCGCACATTCAGGCAGCGCC	-	*ywjE* down fwd LFH	This study
prNS38	CTATTTTTGCACATTTATGACTTCCATTGC	-	*ywjE* down rev	This study
prNS39	GGGACTGCTGTGCGTTGTCGG	-	*ywiE* up fwd LFH	This study
prNS40	CCGGAAAAAACCAAATGACATATGCCCCCTATCACCTCAAATGGTTCGCTG	-	*ywiE* up rev LFH	This study
prNS41	CGAGCGCCTACGAGGAATTTGTATCGGAGGTGTGGCTGACCGGACAAAA	-	*ywiE* down fwd LFH	This study
prNS42	CCCGCGATCCCCCTCGGATA	-	*ywiE* down rev LFH	This study
prNS43	CAGCGAACCATTTGAGGTGATAGGGgtggcacttttcggggaaatgtgcgcggaacccc	-	Kan^R fwd LFH	This study
prNS44	CGATACAAATTCCTCGTAGGCGCTCGctcagtggaacgaaaactcacgttaa	-	Kan^R rev LFH	This study
prNS53	CAGCGAACCATTTGAGGTGATAGGGCTGACGAATCATCGTCTGTC	-	Mls^R fwd LFH	This study
prNS64	CGATACAAATTCCTCGTAGGCGCTCGGCCGACTGCGCAAAAGACATAATCG	-	Mls^R rev LFH	This study
prNS70	CAGCGAACCATTTGAGGTGATAGGGttgcaatggtgcaggttgttc	-	Tet^R fwd LFH	This study
prNS71	CGATACAAATTCCTCGTAGGCGCTCGgaattcctgttataaaaaaggatcaa	-	Tet^R rev LFH	This study
prNS78	TatgccccATGGCAACCGTTTATACGTTGGTGAGTTGGT	-	P1 *clsA* check fwd	This study
prNS79	ccaataggatccCAGCAACGGACTGAAGAAGTAAAACAGTCGC	-	P1 *clsA* check rev	This study
prNS8	GCAGCTGCGGCCGCTTATAAGATCGGCGACAACAGCCG	NotI	*clsA* rev	This study
prNS80	tat gtt ccatgg caATGAAATGTAGCTGGCGCGAAGGCAATA	-	P1 *ybhO* check fwd	This study
prNS81	ggcataggatccGGGTTTTACCCCCGTGTTTTCAGTTTCTA	-	P1 *ybhO* check rev	This study

prNS82	gagtctccatggctTTGCCCCG GCTGGCGAGCGCGGTGC TGCC	-	P1 *ymdC* check fwd	This study
prNS83	Ccgataggatcc CAATAACCATTCCACGGG CAATATCGAC	-	P1 *ymdC* check rev	This study

3.5 Molecular cloning

3.5.1 Preparation of chromosomal DNA from *B. subtilis* cells

Cells from 10 mL overnight culture were harvested and resuspended in 0.5 mL Lysis buffer and incubated with 1 mg/mL lysozyme for cell lysis. The lysate was extracted with phenol: chloroform solution. For chromosomal DNA precipitation 40 µL of 3 M sodium acetate and ethanol was added. The precipitated DNA was harvested by centrifugation and washed with 70% ethanol. Afterwards the pellet was air-dried overnight, before resolving in TE buffer.

3.5.2 Polymerase-Chain-Reaction

The PCR reactions were performed in the thermocyclers TPersonal (Biometra) and peqSTAR (PEQLAB). The resulting fragments were analysed using agarose gel electrophoresis. If necessary DNA was purified using the Gene JET DNA Purification Kit or the Gene JET Gel Extraction Kit.

3.5.2.1 Single Colony PCR

25 µL	DreamTaq Green PCR Master Mix (2x)
1 µL	forward primer (10 pmol/µL)
1 µL	reverse primer (10 pmol/µL)
DNA template	colony picked from plate
up to 50µL	ddH_2O

Table 7. Thermocycler conditions for single colony PCR.

Step	Temperature (°C)	Time	Cycles
Precycle	95	5 min	1
Denaturation	95	30sec	30
Annealing	55	30 secs	30
Extension	72	variable (1min/kb)	30
Post-Extension	72	5 min	1
Hold	16	variable	1

3.5.2.2 PCR with Phusion High-Fidelity DNA Polymerase

10 µL	Phusion HF or GC buffer (5x)
1 µL	dNTPs (10 mM)
2.5 µL	forward primer (10 µM)
2.5 µL	reverse primer (10 µM)
variable	DNA template
1.5 µL (optional)	DMSO
0.5 µL	Phusion DNA Polymerase
up to 50 µL	nuclease free water

Table 8. Thermocycler conditions for Phusion Polymerase.

Step	Temperature (°C)	Time	Cycles
Precycle	98	30 sec	1
Denaturation	98	30 sec	35
Annealing	45-72	30 sec	35
Extension	72	variable (30sec/kb)	35
Post-Extension	72	10 min	1
Hold	16	variable	1

3.5.3 Agarose gel electrophoresis

The agarose gel electrophoresis was used to separate DNA-fragments based on their size. DNA-samples were mixed with 6x DNA-loading dye (New England Biolabs,

Germany) and loaded on a 1 % agarose gel (1 % agarose in TAE-buffer; 0.005 % peqGreen, Biozym, Germany). The DNA-fragments were separated at 125V in a gel chamber filled with TAE-buffer and visualised via UV-light.

3.5.4 Spectrophotometric determination of DNA concentration

The purity and concentration of DNA were determined via NanoDrop2000 Spectrophotometer. For this, the absorption spectrum of the solution between 220 to 350 nm was detected. The quotient 260 nm/280 nm served as a measure of DNA purity. A quotient of 2 corresponded to pure DNA. For an estimation of the DNA concentration the following formula was used: OD_{260}*50 µg/mL= DNA concentration in µg/mL.

3.5.5 Restriction

All enzymes used for restriction digests were purchased from NEB (New England Biolabs), if available as High-Fidelity Restriction Endonucleases. Restriction digests were performed as described below:

1 µg	DNA
5 µL	CutSmartBuffer (10x)
1µL	Restriction Enzyme (each)
to 50 µL	ddH_2O

The mixtures were incubated for one to three hours at 37°C, afterwards the DNA was purified using the Gene JET DNA Purification Kit, according to the provided protocol.

3.5.6 Ligation

Linearized DNA fragments were ligated using the T4 DNA Ligase from NEB as described below:

2 µL	T4 DNA Ligase Buffer (10x)
50 ng	Vector DNA
variable	Insert DNA (molar ratio 1:3)
1 µL	T4 DNA Ligase
to 20 µL	nuclease free water

All Ligations were performed either for 1 h at room temperature or overnight at 16°C. Followed by heat inactivation for 10 min at 65°C.

3.5.7 Competent cells

For producing competent cells two different procedures, dependent on the organism were used:

3.5.7.1 Chemical component *E. coli* cells with calcium chloride

For the chemical method, 50 µL cells of a LB overnight culture were diluted into 10 mL fresh LB media and grown at 37 °C to an OD_{600} = 0.4. The cells were harvested by centrifugation for 5 min at 4000 rpm, the pellet was resuspended in 10 mL ice-cold 0.1 M $CaCl_2$ and incubated on ice for 5 min. Subsequently the cells were centrifuged for 5 min at 4000 rpm and the pellet was resuspended again in 10 mL ice-cold 0.1 M $CaCl_2$, followed by 2 more washing and incubating steps. Next, the cells were centrifuged as previous and resuspended in up to 600 µL ice-cold 0.1 M $CaCl_2$, aliquoted and kept on ice for the following transformation.

3.5.7.2 MN- competent *B. subtilis* cells

For producing competent *B. subtilis* cells 10 mL MNGE medium were inoculated with a 1/100 dilution from an overnight culture in LB. The cells were grown at 37°C at 200 rpm until OD_{600} = 1.1-1.3.

3.5.8 Transformation

3.5.8.1 Transformation of chemical competent *E. coli* cells

For transformation, 1-2 µL of plasmid DNA and 100 µL of freshly prepared ice-cold competent cells were mixed and incubated on ice for 30-45 min. Cells were given heat shock at 42°C for 60 s and kept on ice for 2 min. 1 ml LB was added to the mixture and cells were shaken at 600 rpm for 1-2 h at 37°C. The cells were then centrifuged and the pellet was resuspended in 100 µL. The resuspended pellet was plated on LB agar plates (with antibiotics if required). Plates were incubated over night at 37°C.

3.5.8.2 Transformation of MN- competent *B. subtilis* cells

400 µL of freshly cells were used per transformation. DNA (up to 10 µL) was added to the cells and let grown at 37°C. After 1h 100 µL Expression Mix was added, followed by an additional growing phase at 37°C with agitation. The cells were harvested by centrifugation and plated in selective media.

3.6 P1 Transduction

To derive gene deletions using transduction with the P1 phage the kanamycin resistant single-gene deletion strains from the Keio collection (*239*) were used as donor strains, into the VS367 background. For the procedure of P1 phage transduction the published protocol of Thomason, Costantino and Court (*240*) was followed. The resulting strains were tested for correct insertion of the FRT-site flanked kanamycin cassette into the genome, using gene and kanamycin cassette specific primers (Table 6, prNS78-prNS82). The kanamycin cassette was removed from the deletion strains using the temperature sensitive pCP20 plasmid encoding a FLP recombinase (*234*) and tested for the loss of antibiotic resistance after two rounds of growth on LB plates without any antibiotic at 43°C.

3.7 Glycerol stock for storage of bacterial strains

Relevant bacterial cells were grown in 10 ml LB/TB medium with appropriate antibiotics for about 15h (overnight) at 37 °C and 200 rpm. The culture was pelleted and resuspended in 2mL LB/TB + 20 % glycerol. The stocks were stored on ice is necessary and then frozen at -80°C.

3.8 SDS Page

For protein analysis *E. coli* cells from an overnight culture (30°C and 200 rpm) were diluted to an $OD_{600} \approx 0.1$ in a total volume of 10mL TB with supplemented antibiotics and inducers. The cells were harvested at an OD_{600} of 0,6. The cells were washed twice in Tethering buffer and resuspended to a final OD_{600} of 10. SDS loading/sample buffer was added and the solution was boiled for 5 min at 95°C. Afterwards 5 µL of sample was added on the SDS gel. For the SDS gel a 12% resolving gel and a 5% stacking gel were used.

3.9 Western Blot

For transferring the proteins separated via SDS Gel, Whatman paper, nitrocellulose membrane and the Gel were cut to the area of proteins of interest (here between 38 and 70kDa). Additionally, the Gel as well as the Whatman paper and the membrane were soaked in 1x Transfer buffer. Afterwards the transfer sandwich was assembled and mounted in the tank with 1x Transfer buffer and transferred overnight at 30 V at 4°C. After the transfer the membrane was blocked with 5%milk powder in TBST for 30 min with gentle shaking. Following the membrane was washed for 10 min with 1xTBST three times. The membrane was incubated using primary monoclonal mouse GFP-specific antibody diluted 1: 5000 in 1 % milk powder- TBST for 1 h, followed by a washing step three times for 5 minutes with 1x TBST. Secondary fluorescently labelled IRDye™700DX anti-mouse IgG goat antibody (Rockland) was used for detection with a dilution of 1:10000. Fluorescence signals were detected using an infrared LI-COR

scanner (Odyssey).

3.10 Growth experiments

3.10.1 Growth curves and analysis

For growth experiments *E. coli* cells from an overnight culture (variable temperature and 200rpm) were diluted to an OD_{600} ≈ 0.1 in a total volume of 900 µL TB with supplemented antibiotics and inducers if necessary. Growth of the cultures was analysed in a 24-well plate using a plate reader (Tecan Infinite M1000 or M200, Tecan Deutschland GmbH, Crailsheim, Germany) for 20-40 h at variable temperatures between 30°C and 42°C and a shaking speed of 100 rpm or 180 rpm. The growth curves were generated using Microsoft Excel (2011).

3.10.2 Colony Forming Unit (CFU) Assay

For evaluating the ability of different strains on giving rise to colonies at different temperatures and after different growth conditions in liquid media, CFU assays were performed. In an ideal case the number of colonies is proportional to the number of viable single cells. 1 mL of *E. coli* cells from a certain culture were diluted in 9 mL Tethering Buffer (10^{-1}) and vortexed thoroughly. The dilution steps were continued until a total dilution of 10^{-7} was reached. 100 µL of dilutions 10^{-5}, 10^{-6} and 10^{-7} were plated on LB plates with according antibiotics and left for growth overnight at corresponding temperatures. The colonies on each plate were counted, the CFU per mL was calculated and averaged over the different dilutions per origin culture. The calculation was done using Microsoft Excel (2011), the results were displayed in a Column chart.

3.11 Soft Agar Assay

Viable *E. coli* and *B. subtilis* cells, having a functional chemotaxis and motility system are spreading on soft agar. By metabolizing nutrients in the agar, a gradient of attractants is arising, whereupon the bacteria spread circular. Soft Agar plates were prepared from 100 ml of TB with 0.27 % agar, and the required antibiotics and inducers. The plates were inoculated by pipetting between 1 µL

(overnight) or 5 µL (5-6h) dependent on their incubation time into the agar. The strains of interest were analysed together with suitable positive and/or negative controls applied on the same plate as reference. The plates were incubated at various temperatures between 30°C and 42°C. For analysis, the plates were imaged, the spreading diameter was measured and all calculations and graphical illustrations were done using Microsoft Excel (2011). The spreading diameter of all mutants was normalized to the diameter of the positive control (*WT*).

3.12 Microscopy

To study the effect of various phospholipids on the chemotaxis system of *E. coli* and *B. subtilis* it was made use of several different microscopy related techniques like fluorescence imaging, FRET, and FRAP.

3.12.1 Cluster analysis by fluorescence imaging

3.12.1.1 Preparation of cells

Overnight cultures were grown in 3 mL TB supplemented with appropriate antibiotics at 30°C. 10 mL day cultures were prepared by reinoculating 100 µL of overnight cultures into fresh TB and grown at different temperatures and 200 rpm, supplemented with appropriate antibiotics and inducers. Cells were harvested at OD_{600} 0.4 or 0.6 by centrifugation (4000 x *g* for 5 min; at specific growth temperature). Afterwards the cells were placed on an agar pad (1% agar in Tethering buffer) and imaged at respective growth temperature.

3.12.1.2 Data acquisition and analysis

Images were taken with a Nikon Eclipse microscope, taking two/three-layer images in phase contrast, as well as YFP (and CFP) channels. To automatically quantify the data sets, Oufti (*241*) was used for segmentation of the cells using phase contrast images. Subsequently for the cluster detection SpotFinderZ out of the toolbox of Microbetracker (*242*) was used. The following statistical analysis was accomplished with MATLAB (*243*). Roughly 1000 cells per strain were used

for the quantitative cluster analysis. For manual analysis, the number of clusters per cells was counted for roughly 200 cells per condition.

3.12.2 FRET

The technique of Förster Resonance Energy Transfer (FRET), permits determination of the approach between two fluorescent proteins, when the emission band on the first covers the absorption band of the second (*244, 245*). This technique was used to monitor the intracellular response of the chemotaxis pathway towards certain compounds. The assay used in this study relies on the phosphorylation-dependent interaction between CheY fused to a yellow fluorescent protein (CheY-YFP) and the phosphatase CheZ fused to a cyan fluorescent protein (CheZ-CFP) (*166, 177*).

3.12.2.1 Preparation of cells

Overnight cultures were grown in 3 mL TB supplemented with appropriate antibiotics at 30°C. 10 mL day cultures were prepared with by reinoculating 200 µL of overnights cultures into fresh media and grown in a rotary shaker at 34°C and 275 rpm, supplemented with appropriate antibiotics and inducers. Cells were harvested at OD_{600} 0.6 by centrifugation (4°C, 4000 x *g* for 5 min), washed with cold tethering buffer and stored at 4°C for 20-30 min to inhibit protein synthesis. Circular coverslips (Ø 12 mm) were prepared with 50 µL of poly-L-lysine and let stand for 15 min before rinsing with ddH_20. To prepare the samples for FRET measurements, the culture was centrifuged (4°C, 4000 x *g* for 7 min) and resuspended in 200 µL of cold Tethering buffer. The concentrated cells were attached to the poly-lysine-coated coverslip for 10 min and then mounted into a flow-chamber, that was maintained under constant flow of 0.3 mL/min of tethering buffer using a syringe pump (Harvard Apparatus).

3.12.2.2 Preparation of stimulus solutions

All stimulus solutions were prepared in tethering buffer at a concentration between 5M (e.g. $NiCl_2$) and 100 mM (MeAsp) dependent on their solubility. The pH of all chemical solutions was adjusted to pH=7. For pH testing the pH level of tethering buffer was adjusted between pH=6 and pH=8.3. All stock solutions were stored at 4°C and if used diluted freshly to the desired work concentration in tethering buffer.

3.12.2.3 Data acquisition and analysis

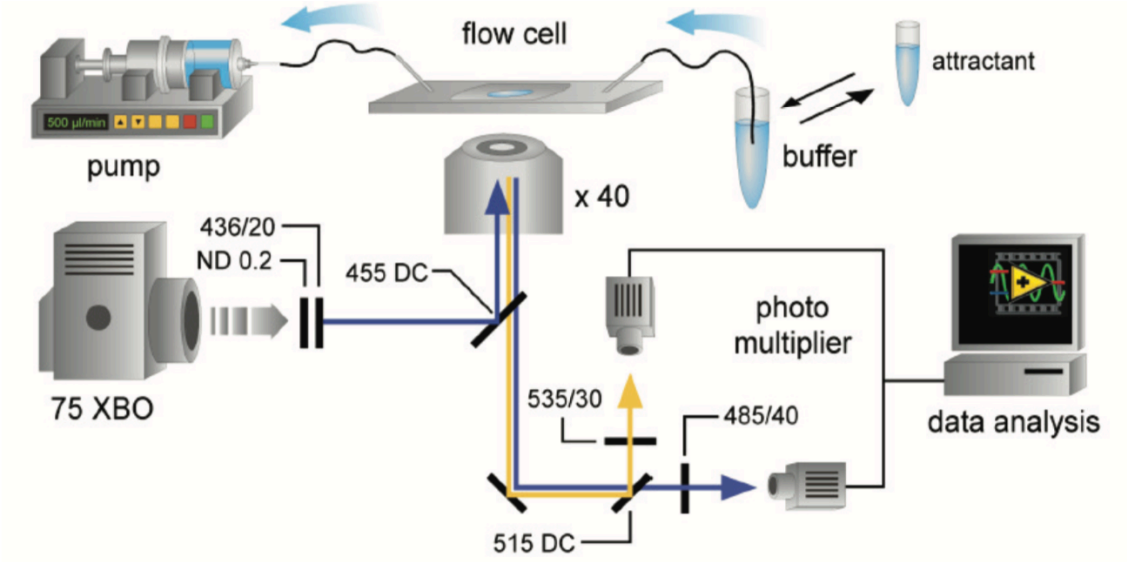

Figure 7: Flow-FRET assay apparatus

An exemplary setup of the experimental setup for FRET is shown in Figure 7. After a certain acclimatization time for the samples, the cells were excited at a CFP-specific wavelength of 436/20 nm by a 120W Hg-Lamp (EXFO X-Cite® 120) attenuated 500-fold with neutral density filters (upright microscope). A 455 nm dichroic mirror was utilized to separate excitation from emission light and a second, 515 nm dichroic mirror was used to split up emission light in two spectral parts *per* second. Cells were focused with a 40x objective (Zeiss Plan-Neofluar 40x/0.75) and a section of a dense and uniformly attached monolayer comprising of 500-600 cells was chosen for data acquisition. The fluorescence of the cells

was continuously recorded in the cyan and yellow channels using photon counters with a 1.0 s integration time and a PCI-6034E counting board connected to a computer with LabView7/Template software for data acquisition as counts of detected photons *per* second. Cells were allowed to adapt to the flow conditions in tethering buffer for at least 15 min. Solutions of different stimuli or repellents at different concentrations (respectively indicated) were exchanged with the buffer reservoir, and the change in YFP/CFP ratio was continuously monitored while the experiment. Stimulation with an attractant results in a rapid decrease in the FRET ratio, while stimulation with a repellent solution is followed with a rapid increase in FRET ratio. Because continuous stimulation leads to adaptive changes in receptor methylation that gradually equalizes the effects of the stimulants, the FRET ratio typically tentatively overshoots upon removal of the chemo effector (Appendix-Figure 1) (*166, 177*). FRET response was measured as the change in the ratio of YFP/CFP as reaction upon addition or removal of increasing concentration steps of the indicated compound and subsequent the changes in FRET Ratio between different strains were compared.

3.12.3 FRAP (Fluorescence Recovery after Photobleaching)

FRAP (Fluorescence Recovery After Photobleaching) is a biophysical method to determine diffusion kinetics of proteins within single cells. Therefore, the protein of interest was tagged with a fluorophore (YFP or GFP) so that the mobility of the certain protein could be followed via TIRF microscopy. The fluorescence intensity of up to 6 single cells was followed at the same time. The fluorophores at a small area at the pole region of a cell was irreversibly bleached with a laser forming a non-fluorescent dark area. Over time the diffusion of the still bright fluorophores within the cell is followed partially replacing the non-fluorescent bleached proteins while diffusing thorough out the cell and with this forming again a uniformly fluorescence intensity over the whole cell. By measuring the return of fluorescence in the previously bleached cell-pole area the *in vivo* diffusion values of specific proteins constructs were determined.

3.12.3.1 Preparation of cells

For FRAP experiments cells were grown in TB over night at 30°C. Overnight cultures were diluted 1:100 into fresh medium with a specific induction with IPTG and grown for 3.5 h at 275 rpm at 34°C. After 3h of growth 10 % Cephalexin was added. Cells were harvested by centrifugation at 4000 rpm for 5 min, washed and resuspended in tethering buffer prior to attaching the cells on poly-lysine treated 8 well glass bottom µ-slide (ibidi).

3.12.3.2 Data acquisition and analysis

Sequences were recorded using a Nikon Eclipse TIRF microscope and a Laser (Visitron Systems) of 515nm for the bleaching and protein-YFP imaging and a Laser of 488 nm for bleaching and imaging of GFP labelled constructs with 400-800 ms exposure time. The frame interval was between 0.5 and 2 sec. The experiments were followed over up to 500 sec depending on the diffusion speed of the constructs. All measurements were performed at indicated temperatures using a water bath (Lauda. RE104), connected to an heatable slide holder.
Data was acquired with the VisiView (Visitron systems) software and was subsequently analysed using FiJi (*246*). Further quantifications were performed using Microsoft Excel and Kaleidagraph. Curve fitting was performed using Kaleidagraph. To get the recovery rates of the tagged proteins of interest we fitted all averaged fluorescence recovery curves, using exponential curve fitting:

$$f(x) = c + a(1 - \exp(-bx))$$

with the parameters:
a: slowly recovery fraction
b: recovery rate
c: rapidly recovery fraction

For simplification and more reliability of the recovery rate of the fit we assumed the plateau of the recovery curves is always reaching 1, what simplifies the equation to:

$$f(x) = c + (1 - c)(1 - \exp(-bx))$$

with the parameters:
b: recovery rate
c: rapidly recovery fraction

3.13 Flow Cytometry

Flow cytometry is a laser-based technique used for quantitative determination of different characteristics while rapid analysing large amounts of single cells (up to 10 000 cells per minute). After sample injection from a tube into the machine the cell suspension passes the flow cell. After addition of sheath fluid, the suspension passes a nozzle where the cells get aligned via termed hydrodynamic focusing, followed by a single cell passing the laser beam(s). The refracted light as well as the fluorescence is channelled by filters towards the detector and split into their ranges of wavelength. Here, the resulting fluorescence from the sample is collected by photomultiplier tubes (PMTs), that converts the light to a voltage or electrical output being proportional to the original fluorescence intensity so that the data can be recorded digitally and quantified.

3.13.1 Preparation of cells

To measure the intensity of fluorescence dyes or reporters, cells were either grown in liquid TB at various temperatures and rotation or grown of soft agar (see 3.11) at various temperatures. The cells were harvested at different time point of the growth phase up to an hourly sampling and diluted minimum 5-fold in tethering buffer and GFP was measured by FACS machine.

3.13.2 Data acquisition and analysis

Fluorescence-activated cell analysis (10,000 cells per sample) was carried out on a BD LSRFortessaTM SORPflow-cytometer (BD Biosciences, NJ, USA). The

fluorescent protein GFP was excited using a 488-nm laser (blue) at 100 mW for excitation and a 510/20 bandpass filter. The forward and side scattered light was used for identify the cells in the FSC/SSCplot. The acquired data, collected in FCS 3.0 file format was analysed using BDFACSDiva TM software version 8.0 (BD Biosciences) and FLOWJO (10.5.3).

3.14 Software

Adobe Illustrator CS6 (version 16.0.4) Adobe Systems
DNA Star Navigator (version 12.0.0.222) DNA Star
FiJi (version 2.0.0) Creative Commons License
FlowJo (version 10.5.3) BD Biosciences
KaleidaGraph (version 4.5.2) Synergy Software, USA
LabView (Version 7) Template software
Matlab (version R2014B 8.4.0.150421) MathWorks
Microsoft Office for Mac2011, Microsoft, USA
NIS Elements, Nikon
Oufti (version 1) Jacobs-Wagner Lab
SerialCloner (version 2.6.1) Serial Basics
Spotfinder Z (Version 0.50) Microbetracker
VisiView, Visitron Systems

4 RESULTS

4.1 The role of cardiolipin in *E. coli*

In *E. coli* three synthases, encoded by the genes *clsA*, *ybhO* and *ymdC*, are responsible for the biosynthesis of the anionic phospholipid cardiolipin. The significance of each of these proteins is dependent on the growth phase, whereas ClsA represents the main synthase. We were interested in gaining insights on the effect of cardiolipin on *E. coli*, especially the influence of cardiolipin on the chemosensing and chemotaxis system. Therefore, we created a CL null mutant in a strain lacking receptors to maintain the opportunity for observing the influence of CL on individual chemoreceptors, especially the main receptors Tar and Tsr. We investigated the influence of cardiolipin on growth, motility, the sensing behaviour of the receptors, the chemoreceptor cluster formation and the receptor diffusion within the cytoplasmic membrane.

4.1.1 Influence of cardiolipin alterations on the growth, viability and morphology of *E. coli*

Examination of bacterial growth can improve the understanding of various extra and intra cellular effects on the viability of a microbial population. To better understand the physiological relevance of the *E. coli* cell membrane on their viability, we performed growth experiments. The gained growth curves are a graphical representation of how a particular strain grows and subsequently dies over time.

4.1.1.1 Cardiolipin has no adverse influence on growth irrespective of temperature

For investigating the effect of CL on the viability of *E. coli*, we started performing growth experiments at different temperatures. The experiments were performed

as described in Materials and Methods 3.10. We used a plate reader to follow the cells growth. The results of the growth experiments with VS367 as *WT* (+cardiolipin, + CL), several single and double cardiolipin synthase knockout strains and the triple knockout strain (VS367 *ΔclsAybhOymdC*) lacking CL (- CL), are summarized in Figure 8.

We could see that the single deletions impair the growth, especially in the lag phase (Figure 8A). All three mutants carrying a single knockout showed a more prolonged lag phase. In addition, the single knockouts are reaching stationary phase partly at a lower level.

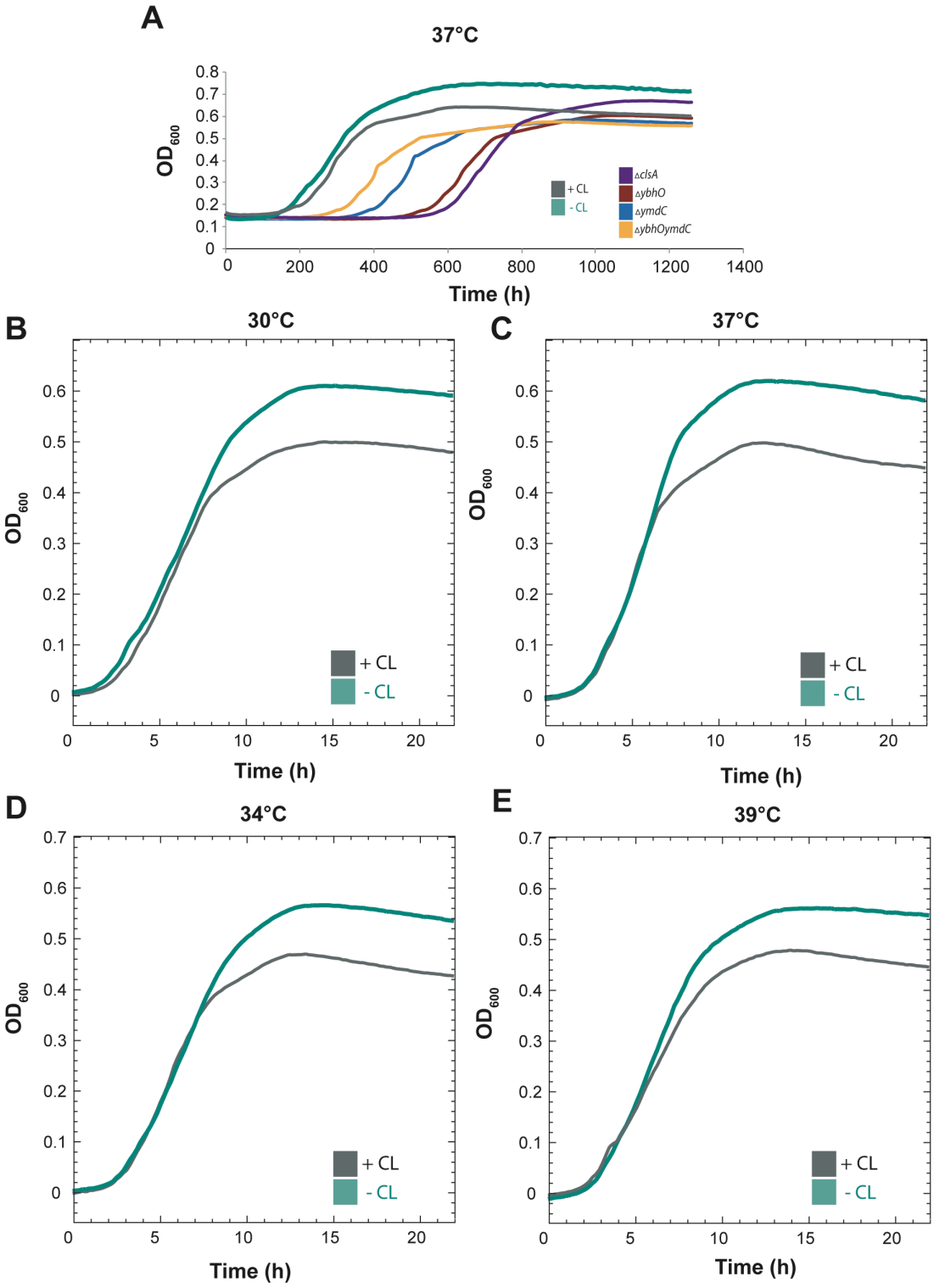

Figure 8. Growth curves at different temperatures. Growth curves of several cardiolipin synthase knockouts at 37°C (A) and growth curves of *E. coli WT* (+CL, grey) and *E. coli* Δ*clsAybhOymdC* (-CL, green) at 30°C (B), 34°C (C), 37°C (D) and 39°C (E). All growth experiments were repeated minimum twice.

When comparing the cardiolipin deficient strain to the *WT*, there are no differences in lag and exponential growth phase, independent of the incubation temperature detectable. The doubling time of both strains is here roughly 120 min. Even though the CL knockout strain (*ΔclsAybhOymdC*) shows no difference in growth during lag phase as well as during logarithmic phase, when compared to the *WT*, there is a significant difference for the stationary phase detectable. As it is shown in the displayed growth curves, the mutant grows to a higher OD_{600} independent of the respective experimental temperatures. At 37°C is the most significant difference in cell density for attaining the stationary phase ascertainable (Figure 8D).
Our results indicate an impairing effect of single knockouts versus the enhanced growth of the triple knockout is due to a possible dysregulation in knockout compensation.

4.1.1.2 Influence of cardiolipin on growth of *E. coli* under stress conditions

For most bacteria, the cell envelope sustains a certain level of ambient osmolality. However, above a certain level of osmolality, the cells need to adapt to changes of surrounding conditions. Generally, for most microbes, an increase in osmolality concludes a decrease in growth rate. Cells actively adapt the distribution of certain substances across the cytoplasmic membrane to overcome unhealthy effects caused by osmolality (*247*). Many bacteria use redundant osmoregulatory systems and channels to overcome osmotic stress. For example, *E. coli* makes use of the chemosensory transporter ProP, whose polar localization is expected to be cardiolipin promoted (*248*). The transporter senses increasing levels of osmolality and help accumulating osmolytes like proline, glycine betaines of ectoine in the cytoplasm (*249*). The deletion of cardiolipin synthases and the consequent lack of cardiolipin changes the composition of the inner membrane of *E. coli*. As the cell envelope is involved directly (e.g., obtaining the turgor pressure) and indirectly (e.g., localization of osmosensory channels) in opposing osmolality, we want to see how growth under osmolar conditions is affected by the lack of cardiolipin. Therefore, we performed growth experiments (as

described in 3.10) with supplementation of sodium chloride, sucrose, proline and betaine to the growth media.

Using high levels of salt (NaCl) in growth media leads to a water loss in cells due to osmosis. Different species can have alternate tolerance levels for salt levels. By adding increasing levels of NaCl to the growth media, we wanted to find out whether the presence or absence of cardiolipin influences the salt tolerance of *E. coli* (see Figure 9A). We used two concentrations of NaCl (300 mM, 600 mM) for our growth experiments. The experiments were performed as described before at 30°C growth temperature. We could show that already 300 mM NaCl decreases the OD level when reaching stationary phase. However, the effect is comparable for both examined membrane conditions. An increase in salt concentration (600 mM) shows a more drastic effect on the growth of both tested strains. The lag phase of both strains is slightly elongated and the WT strain seems to grow slightly better than the cardiolipin deficient strains during exponential growth phase. The transition to stationary phase is reached already at an OD_{600} of 0.4 compared to $OD_{600=}$0.8 without salt treatment. Additionally, we determined, that the cells do lyse faster after reaching stationary phase. However, at high salt concentrations (600 mM) a lack of cardiolipin might slightly impair growth, in particular the exponential phase. For a final statement, though, closer steps of NaCl concentrations, need to be examined.

Varying sugar concentration can lead to a higher or lower osmolality of different solutions, e.g. growth media. With adding sucrose in raising concentrations (10 mM, 30 mM and 100 mM) to the growth media, we could detect a decreasing slope of growth curves (Figure 9B). Additionally, with a rise in sugar concentration, the stationary phase levels are reached at lower levels. Independent of added sugar concentration the *CL*- strain is reaching stationary phase at a slightly higher OD_{600} comparable to the *WT*. This finding, is in line with the previously presented results at different growth temperatures (see 4.1.2.1).

Bacteria can use osmoprotectants acting as osmolytes. These substances are helping the cells to survive extreme osmotic conditions and can even raise the bacterial growth under stressful conditions e.g. high salinity. (*250, 251*). Proline is one of the major compatible solutes in bacteria used to maintain the cellular

osmotic pressure (*252*). Betaine and other compounds also have osmoprotective effects preventing the cells from dehydration and stabilising the enzyme activity under high ionic pressure (*253, 254*). General working concentrations of betain as osmoprotectant are in low millimolar range (1-2 mM) (*255, 256*). We were interested whether osmoprotectants would hinder the growth of *E. coli* in growth medium without provoked salt stress in dependency of cardiolipin. Therefore, we tested two compounds with different concentrations in our growth experiments. Three different concentrations of proline (10, 30 and 100 mM) and four different concentrations (1, 3, 10, and 30 mM) for betaine were used. The results are shown in Figure 9C.

For proline, we could not detect a cardiolipin-dependent effect on growth of *E. coli*. We could see that the addition of proline aligns the growth curve of the *WT* to the one of the *CL*- strain, which is usually reaching a higher OD_{600} in stationary phase (Figure 9, C). However, if this effect is due to the osmoprotective manner of proline or its usage possibility as energy and nitrogen source needs to be further evaluated. The stationary phase aligning effect of proline could not be detected when using betaine as an additive to the growth medium. Early studies show that extra cellular glycine betaine is stimulating the growth rate of *Escherichia coli*, in media with high salt concentrations (*256*). This could not be detected in carbon or nitrogen free minimal media. Concentrations of 1 mM, 3 mM and 10 mM betaine do not show any negative effect on growth, when compared to the growth of these strains without additional osmoprotectant. An addition of 1 mM and 3 mM betaine reduces the lag phase comparable for both strains. An addition of 10mM betaine the stationary growth phase of both strains is reached at a higher OD_{600}, whereas the lag phase is similarly slightly delayed. Neither the *WT* nor the *CL*- strain is able to grow with a concentration of 30 mM betaine in the growth medium (Figure 9D). 30 mM betaine constitutes a very high concentration, which may be already toxic to the cells. With these growth experiments, we could show that osmoprotectants do not influence the growth of *E. coli* in dependence of cardiolipin, but for a more explicit assertion, further experiments with smaller increasing steps of concentrations would be appropriate. Considering the results of our osmolar growth experiments, we

cannot detect a clear effect of cardiolipin on the resilience of *E. coli* towards osmotic influences.

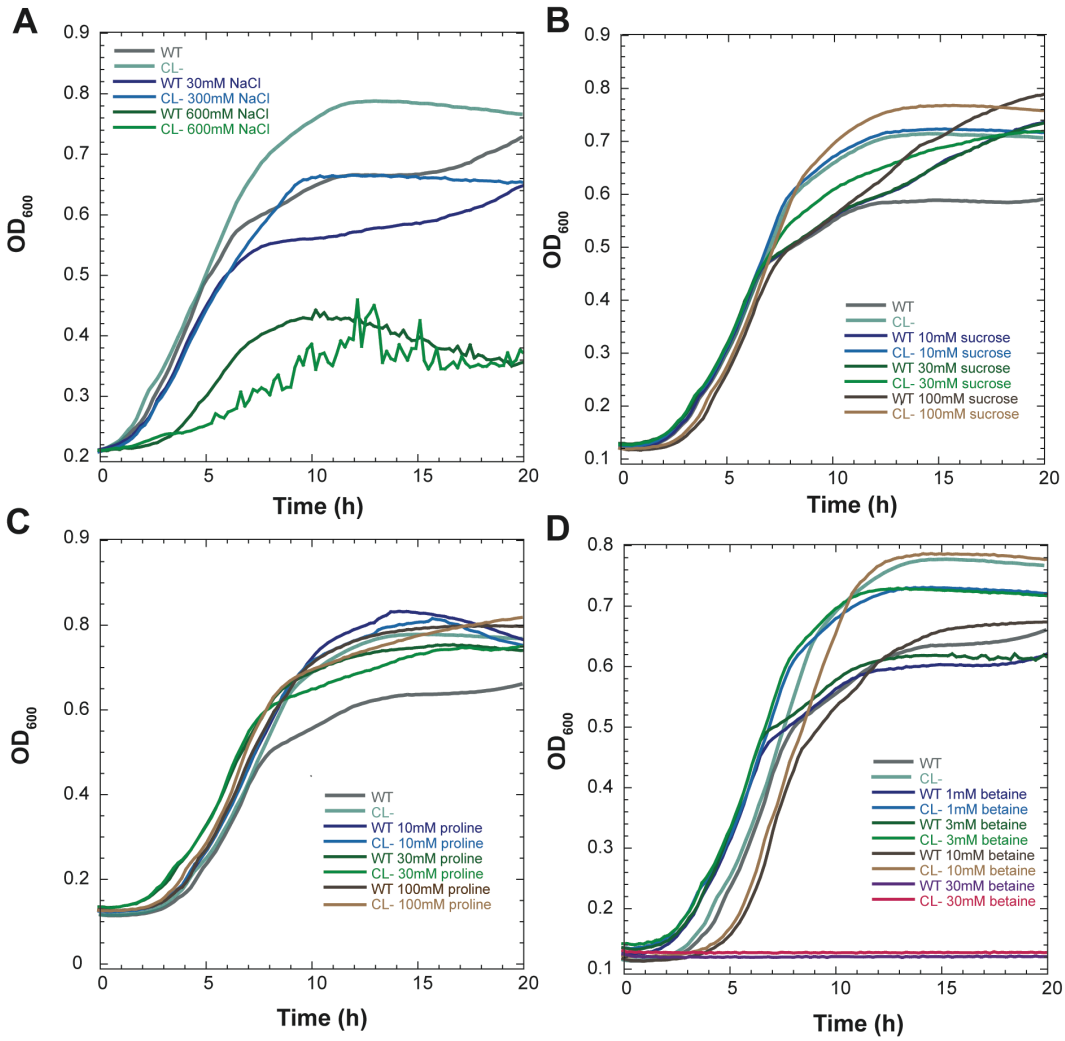

Figure 9. Growth curves under stress conditions. The curves show the growth of *E. coli WT* (grey) and *E. coli* Δ*clsAybhOymdC* (green) with the supplementation of NaCl (A), sucrose (B), proline (C) or betaine (D) to the growth media. Used concentrations are indicated.

4.1.1.3 Cardiolipin-dependent susceptibility for membrane targeting antibiotics

Antibiotics can be classified in two groups of action: bactericidal and bacteriostatic. A bactericidal antibiotic has the ability to kill bacteria, whereas bacteriostatic agents do only inhibit growth. Antibiotics have different point of

action, e.g. cell wall and membrane synthesis, protein and nucleic acid synthesis as well as metabolic processes. Cardiolipin, our lipid of interest is located mainly in the inner membrane of *E. coli* sustaining the idea that its presence or absence can change the potency of antibiotics with membrane target. Polymyxins, a group of polypeptide antibiotics derived from *PaeniBacillus (Bacillus) polymyxa*, are used for the treatment of gram-negative bacteria. Two Polymyxins, Polymyxin B and Colistin (Polymyxin E), are used under clinical conditions as a last resort for multiresistant infections with gram-negative bacteria (*257*). They bind lipopolysaccharides (LPS) which are located in the outer membrane of gram-negative bacteria. This is causing a disruption of the inner and outer membrane due to the hydrophobic tail precipitating detergent like membrane damage (*258*). A study with cardiolipin and lauric acid in combination with the effect of Polymyxin B suggests a higher ionic permeability of a cardiolipin and lauric acid harbouring membrane in the presence of Polymyxin B (*259*). To determine the effect of cardiolipin on the susceptibility or resistance towards membrane-targeting antibiotics, we performed growth experiments in LB and TB medium at low (30°C) and high (39°C) temperature (see material and methods, 3.10) using increasing concentrations of Polymyxin B and Colistin as treatment. Antibiotic concentrations from 0.002 µg/mL to 0.3 µg/mL µm were used. Acquired data is presented in Figure 10.

In LB medium at 30°C, our *E. coli* strains (*WT*, *CL*-) can grow adequately, unaffected by the different used concentrations of Polymyxin B (Figure 10A). The stationary phase is reached on average at an OD_{600} of 0.7 to 0.9. However, with an increase in growth temperature to 39°C Polymyxin B has an influence on the growth of *E. coli*. Concentrations of 0.1 µg/mL and 0.2 µg/mL of the membrane acting antibiotic impair *WT* growth. The cardiolipin-lacking strain, however, shows a delayed growth in 0.1 µg/mL of Polymyxin B. The prolonged lag phase is followed by an average growth behaviour. At a concentration of 0.2 µg/mL Polymyxin B also the cardiolipin deficient strain is unable to grow. When using TB as growth media, we could determine approximately similar Polymyxin B concentration limits for the growth of *E. coli* as shown before with LB (Figure 10B). At 30°C *E. coli* grows normally until a concentration of 0.2 µg/mL independent of cardiolipin presence or absence, attaining the stationary phase at an OD_{600} of 0.5

- 0.6. 0.2 µg/mL of Polymyxin B leads to a slightly longer lag phase for the CL- strain, comparing to the regular growing *WT*. At a concentration of 0.25 µg/mL, the cardiolipin lacking strain has a comparatively long lag phase of 42h, whereas the *WT* is not viable under these conditions. Concentrations of 0.3 µg/mL cannot be tolerated by either the *WT* nor the *CL*- strain. An increase in temperature to 39°C drops the tolerance level for Polymyxin B drastically. At high temperature, *WT* fails to grow ascending from a concentration of 0.12 µg/mL. At the concentration level of 0.12 µg/mL the *CL*- is still viable, however, the lag phase is slightly elongated here and the stationary phase is reached at ½ of the OD_{600} compared to unaffected growth. The cardiolipin deficient strain is impaired in cell growth, starting from an increasing concentration of 0.16 µg/mL of Polymyxin B.
Even though Colistin has a similar structure to Polymyxin B, there are distinct differences between the formulas. Colistin is traded as structural inactive prodrug, whereas Polymyxin B is considered as an active antibacterial compound (*260, 261*). We used Colistin to carry on the investigation of membrane targeting antimicrobial substances in *E. coli* dependent on the absence or presence of cardiolipin (Figure 10C). We tested the influence of similar concentrations as used for Polymyxin B, also at 30°C and 39°C growth temperatures. At the lower growth temperature, Colistin is suppressing growth from an increasing concentration of 0.2 µg/mL. For lower concentrations, no drastic differences between cardiolipin presence and absence could be detected. The only noticeable difference is the longer lag phase of the *CL*- strain with a concentration of 0.16 µg/mL. Here the lag phase is roughly 2h longer compared to the *WT*. A raise in growth temperature to 39°C, leads to a more effective impact of Colistin on the growth of *E. coli*. Up to a concentration of 0.04 µg/mL we could not detect any effect in growth, independent of cardiolipin absence or presence. 0.08 µg/mL affects the growth of the WL as well as the *CL*- strain. However, the *WT* is only delayed in growth, visible due to an elongated lag phase, whereas the cardiolipin-deficient strain suffers from a more extended lag phase. Additionally, the growth of the cardiolipin-deficient strain is inhibited when reaching stationary phase at a low OD_{600} of 0.25. A concentration of 0.12 µg/mL has similar effects on the *CL*- strain, while the *WT* growth is completely inhibited. These inconsistent growth curves at concentrations of 0.08 µg/mL and 0.120 µg/mL Colistin need to be

further examined. However, we can state that these concentrations are lying around the MIC (minimal tolerable concentration) of our *E. coli* strains towards Colistin. Lack of cardiolipin might lead to a broader MIC range where the growth is decreased but still possible. Further investigations with more datapoints between 0.08 and 0.12 µg/mL would be necessary to find the exact MIC concentration, however this was not the scope of this work. Higher concentrations are suppressing the growth comparably for both strains.

Contrary to clinical experience of Polymyxin B being more efficient than Colistin, we observed opposite effects under laboratory conditions. Summarized, we can say that Colistin is more effective in the treatment of our strains than Polymyxin, at a higher temperature the two used agents are more effective, and a cardiolipin deficiency leads to a higher tolerance level of Polymyxin B and Colistin.

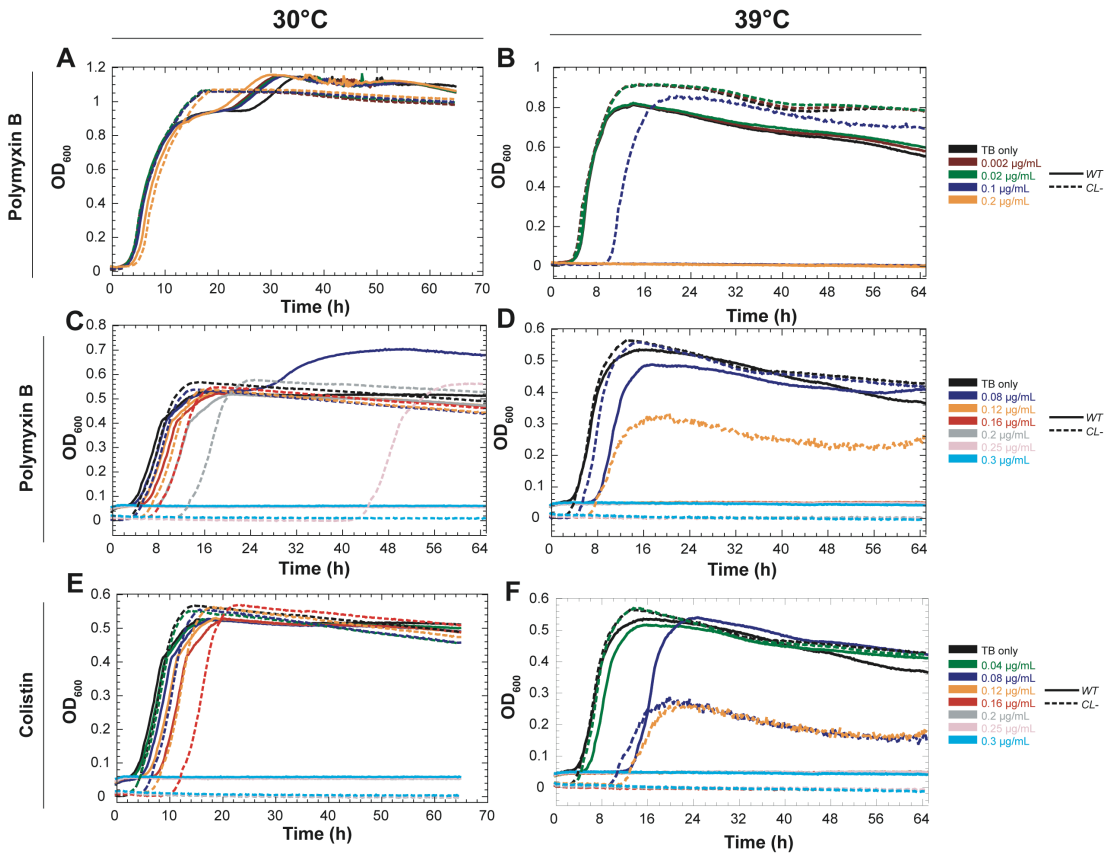

Figure 10. Growth curves with membrane targeting antibiotics. The curves show the growth of *E. coli WT* (grey) and *E. coli* Δ*clsAybhOymdC* (green) with the supplementation of Polymyxin B in LB growth media (A,B), Polymyxin B in TB growth media (C,D) and Colistin in TB growth media (E,F) at 30°C and 39°C. Concentrations are indicated. Experiments were repeated twice.

4.1.1.4 Viability of *E. coli* under presence or absence of cardiolipin

While the analysis of growth curves can give hints about bacterial growth kinetics, CFU can give reference about bacterial survival ability regarding different conditions like temperature, pH or osmolality. A colony-forming unit assay is used to estimate the number of viable, multiplying cells within a sample (*262*). With this assay (see materials and methods, 3.10.2), we wanted to evaluate the effect of cardiolipin in the cell membrane of *E. coli* on the viability. The experiments were performed at increasing temperatures from 30°C to 42°C. The cultures were sampled and diluted correspondingly after 24 h and 96 h of growth. The evaluated results are displayed in Figure 11, showing the number of CFU per mL per strain and condition. Irrespective of incubation time and temperature, the cardiolipin deficient strain is more viable. However, with increasing temperature, the difference in the viability of the *CL*- strain compared to its *WT* is decreasing, reaching equality at 39°C. As we have also seen a higher OD_{600} for the stationary phase of the *CL*- strain compared to the *WT*, one can argue that the difference seen in CFU are based on the growth ability; however, the difference in stationary phase OD_{600} seems too small to function as sufficient explanation. With these results, we can propose that the lack of cardiolipin increases the viability of *E. coli* cells in connection with growth temperature; for lower growth temperature, more than for high ones. Additionally, these findings confirm the results of the growth experiments (see 4.1.1.1). The cardiolipin knockout strain grows irrespective of temperature to a higher OD_{600} at stationary phase compared to the *WT* (CL+). Consistent, the cardiolipin deficient strains forms more colony forming units independent of growth temperature and sampling time point while stationary phase, than the cardiolipin comprising *WT*.

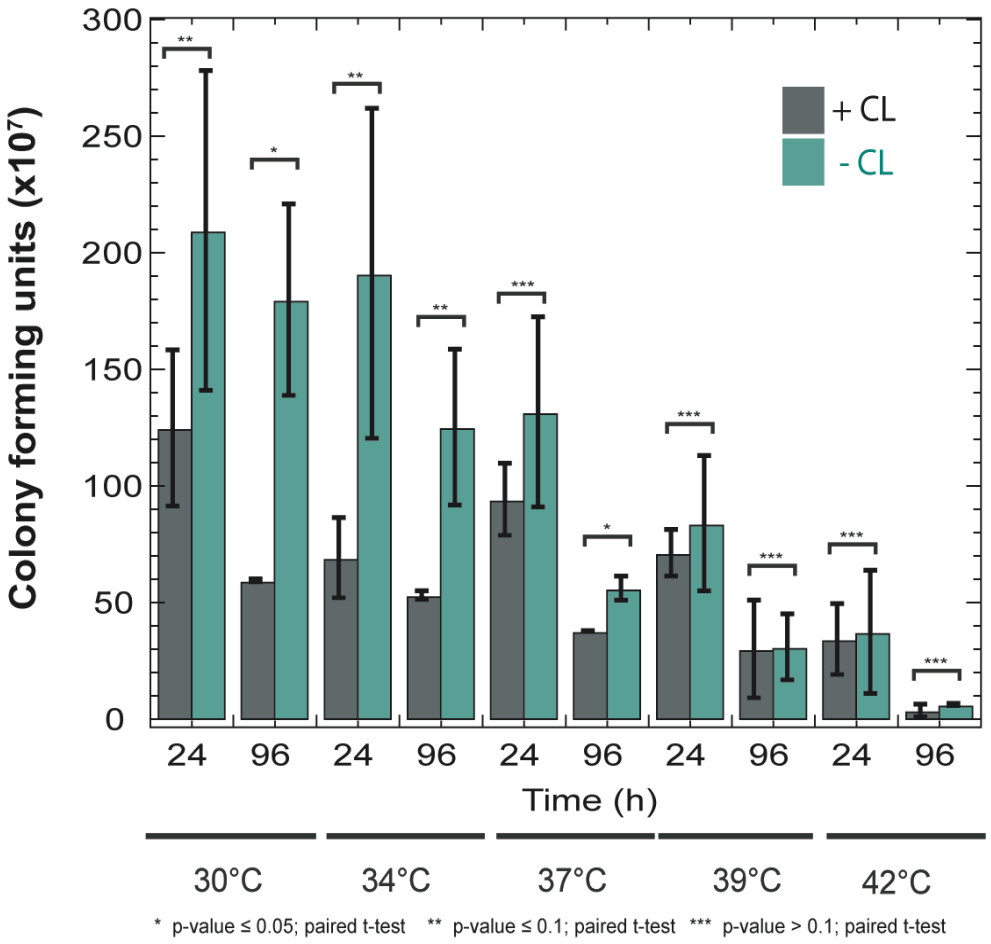

Figure 11. Colony forming units. The figure shows the CFUs of *E. coli WT* (grey) and *E. coli* Δ*clsAybhOymdC* (green) at various indicated temperatures (30°C to 42°C). Error bars indicate the standard deviation of three replicates, significance analysis by paired t-test. Cells were grown in TB at indicated temperatures, harvested after 24h or 96h, dilution series were plated on TB and CFUs were examined.

4.1.1.5 Single knockouts of cardiolipin synthases affect cell morphology

Cell morphology is an important aspect of the cells phenotype and is critical in regulation of cell activities. When looking at the morphology of certain cells, one can evaluate different factors, e.g. size, width, length and symmetry (*263*). Different environmental factors can force bacteria to adapt their morphology. For example, nutrient limitations generally lead to shorter *E. coli* cells. Different morphological changes can also derive from antimicrobial treatments or genetic mutations (*264*). A microscopic observation can be used to look for effects/functions of certain genes/proteins within the cell. We examined the

generated single cardiolipin synthase knockouts and the triple knockout to investigate whether these deletions cause morphological changes, as this can be an indicator for cellular stress.

As shown already for the growth experiments (see results 4.1.2.1), single knockouts of cardiolipin synthases are responsible for growth malfunctions. With morphological examinations, we could also detect an adverse effect of single cardiolipin synthase knockouts. We used flow cytometry to examine various population within a strain as well as the cell size of populations. The results are plotted as SSC-A (side scatter) vs. FSC-A (forward scatter) and SSC-H vs. SSC-W plots. The ratio between cell size and wavelength of the laser alters the scatter behaviour. The measurement of the forward scatter allows to discriminate the cells by size, whereas the side scatter provides information about the internal complexity. The height (H) parameter is directly affected by PMT (photomultiplier tubes) voltage changes and is the parameter for the highest signal. The Width (W) parameter represents the duration time of the signal and directly correlates with the cell size and is independent of the voltage change. We could detect that the single-deletion YbhO leads to a subpopulation with elongated cells (Figure 12, green). The other single deletions do not lead to obvious morphological changes. Further, we could show, that the triple knockout (*ΔclsAybhOymdC*) exhibits the same appearance than the *WT* (Figure 12 A, B). These finding could be confirmed by microscopic imaging (Figure 12 C).

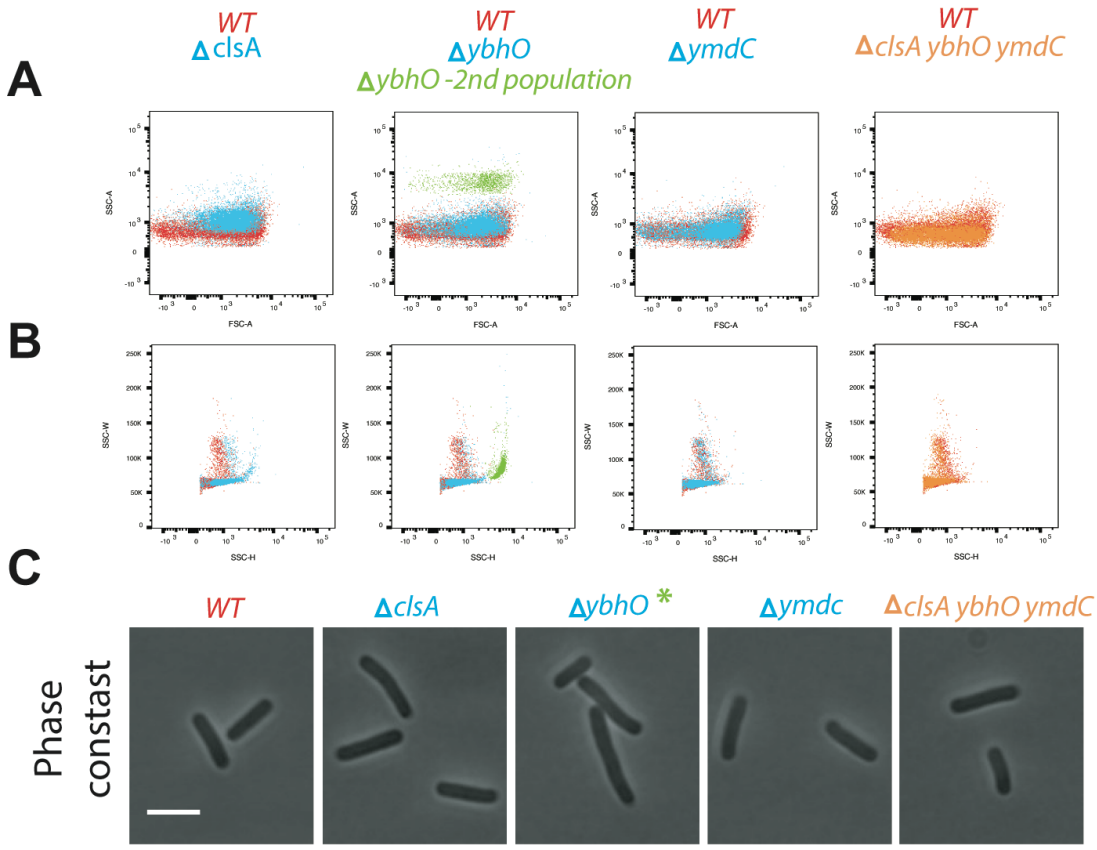

Figure 12. Morphological changes by single CL synthase knockouts. FSC-A vs. SSC-A (A) and SSC-H vs. SSC-W scatter plots showing sample evaluation of *E. coli* mutants Δ*clsA*, Δ*ybhO*, Δ*ymdC*, *ΔclsAybhOymdC* populations in TB at 34°C as measured by flow cytometry. Color scale indicates WT (red), single cardiolipin synthase knockouts (blue), additional population of *E. coli* Δ*ybhO* (green), *ΔclsAybhOymdC* (CL-) (orange). Exemplary microscopic phase contrast images (C) of *E. coli* WT (CL+), *E. coli* Δ*clsA*, *E. coli* Δ*ybhO*, *E. coli* Δ*ymdC*, *E. coli ΔclsAybhOymdC (*CL-*) strains*.

4.1.1.6 Cardiolipin has no impact on the cell size

As a basis for further experiments, we wanted to further confirm that cardiolipin has no effect on the cell size. Therefore, we used phase-contrast images of the *WT* and the cardiolipin depletion strain to examine their cell size. The cells were grown at 34°C in TB media and imaged at an OD_{600} of 0.4 and OD_{600} of 0.6. Subsequently, the images were analysed, the cell outlines were tracked, and the volume per cell was examined using FiJi (*246*). Further calculations were performed using Kaleidagraph (*265*). The results are shown in Figure 13. With cell size analysis of the *WT* and the corresponding *CL-* strain we could not detect a significant difference in cell size, by that we can say the lack of all three cardiolipin synthases in *E. coli* does not lead to a change in cell size. These

findings support our idea of a generated dysfunction with the single deletion of a cardiolipin synthase as it seems single knockouts do influence not only the growth ability but also the morphology of the cells.

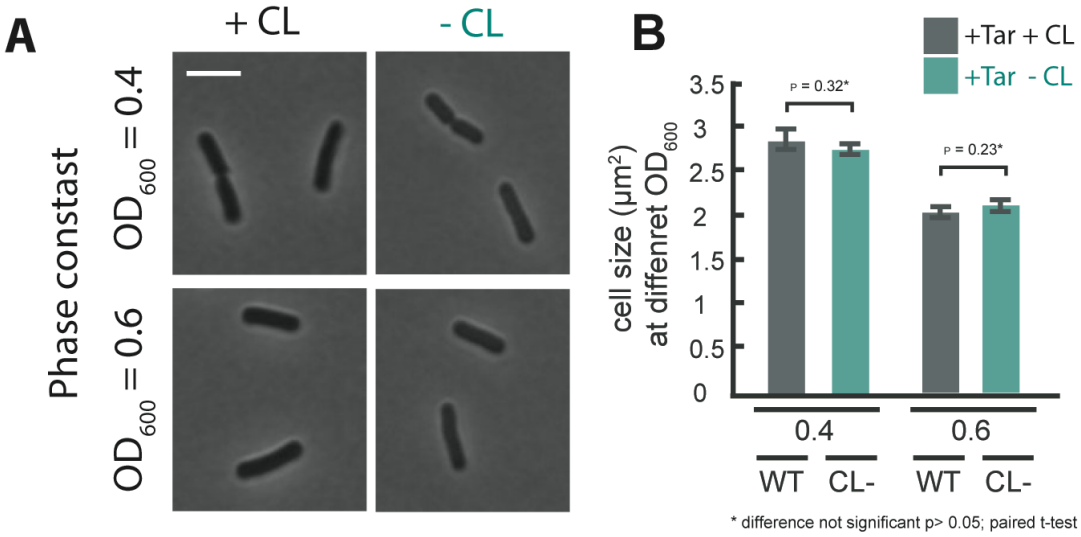

Figure 13. Cell size evaluation of *E. coli*. Exemplary microscopic images (A) of *E. coli WT* (+CL) and *E. coli* Δ*clsAybhOymdC* (CL-). Cell size evaluation (B) of *E. coli WT* (CL+, grey) and *E. coli* Δ*clsAybhOymdC* (CL-, green). Cells were grown at 34°C in TB until OD_{600}=0.4/0.6. Minimum 200 cells per strain were evaluated. Calculations were performed with FiJi and Microsoft Excel. Scale bar indicates 2µm.

4.1.2 Influence of cardiolipin on the swimming behavior of *E. coli*

Soft agar assays were first introduced as a useful tool for studying chemotaxis (*266*). However, this assays gives not only information about the chemotactic behaviour of the observed cells, but also about the functionality of their motility system and their growth ability (*267*). Inoculated into the soft agar with its polysaccharide network, the cells can spread through the agar pores. Unlike in liquid medium, in the soft agar the cells can get stuck in the pores and need to change their swimming direction to effectively free themselves. The cells need their chemotaxis system to compare spatiotemporal differences of nutrients in order to control their flagella rotation. Is this system impaired, two phenotypes are conceivable: the cells either exhibit a smooth swimming phenotype where they get stuck in the agar pores due to failure in tumbling and reorientation or the cells display a tumbling phenotype caused by a high tumbling frequency and with this,

the cells are hardly moving away from the inoculation point. Additionally, the cells grow, which leads to an establishment of a local nutritional gradient incipient at the inoculation point outwards, due to take up of nutrients available in the used TB medium. Cells can determine this gradient with their functional chemotactic system. We made use of this assay (see Material and Method, 3.11), for examining the influence of cardiolipin on the capability of growth and the functionality of the chemotaxis and motility system. Obtained results on soft agar plates are shown in Figure 14. The experiments were performed using a receptorless strain, harbouring or lacking cardiolipin with additional expression of Tar or Tsr from plasmid (*Tar+; Tsr+*). The experiments were performed at different temperatures in the range of 30°C to 39°C, consistent with the performed growth experiments (see 4.1.2.1). Figure 14A shows the swimming ability on agar plates of the cardiolipin null Tar-only (*CL- Tar+)* mutant compared to the *Tar+* (*WT*) wildtype strain at different temperatures. Similarly, Figure 14C shows the swimming ability on agar plates of the cardiolipin null Tsr-only (*CL-Tsr+)* mutant compared to the *Tsr+* (*WT*) wildtype strain. The swimming diameters were measured and normalized to the respective *WT* (+CL). Arithmetical results are displayed in Figure 14B (for *Tar+*) and 14D (for *Tsr+*). The lack of cardiolipin enhances the ability to form swimming rings independent of temperature for both chemoreceptors of interest. Looking at the Tar receptor (Figure 14, B) at 30°C, the diameters of swimming rings are the same with and without cardiolipin in the membrane, whereas the increase to 34°C leads to an enlargement of the swimming diameter by 50% for the cardiolipin lacking strain. At 39°C, the cardiolipin deficient strain shows swimming rings more than doubled the size compared to the *WT* in the same condition. The swimming ring diameters for the *Tar+ WT* are decreasing with increasing temperature. Contrariwise, the measured diameters of swimming rings formed by the mutant lacking cardiolipin and expressing Tar as only chemoreceptor are increasing with rising temperature. When visually examining the Tsr receptor at 30°C, a significant difference is visible. The cardiolipin-lacking *Tsr+* mutant is forming a 70% larger ring. At 37°C, the benefit of cardiolipin deficiency leads to an increase of the swimming ability of around 170% in swimming ring size, compared the *WT Tsr+*. Whereas at 37°C the *WT Tsr+* is hardly forming any detectable swimming ring,

at 39°C the *WT Tsr*+ is not able to form swimming rings in soft agar plates anymore. In contrast to the *Tsr*+ *WT* at these temperatures, the *CL*- mutant is still able to grow and form swimming rings. For both, the *Tsr*+ *WT* and the *Tsr*+ *CL*- mutant, the diameters of formed swimming rings are decreasing with temperature, contrary to the *Tar*+ strains. However, the decrease up to stagnation of swimming ability is way faster reached for the *Tsr*+ *WT* than for the *Tsr*+ *CL*- mutant.

Additionally, we examined the effect of single cardiolipin synthase knockouts on the ability to form swimming rings on soft agar plates (Figure 14, E). The three examined knockouts are deteriorating the behaviour of the cells expressing Tar as chemoreceptor by minimum 10% and maximum 40%. These findings support our already mentioned assertion of a created dysregulation with single or double knockouts of cardiolipin synthase genes.

The lack of cardiolipin leads to increased swarming diameter for both receptors (Tar and Tsr), when compared to their *WT*, however Tar shows to be stronger influenced here. A soft agar assay doesn't only depend on the growth, but also on the chemotaxis and motility system. So far we could not explain the increased swimming rings of the cardiolipin deficient cells just by the growth shown in previous experiments. Therefore, we continued to investigate further factors like the chemotaxis and motility system.

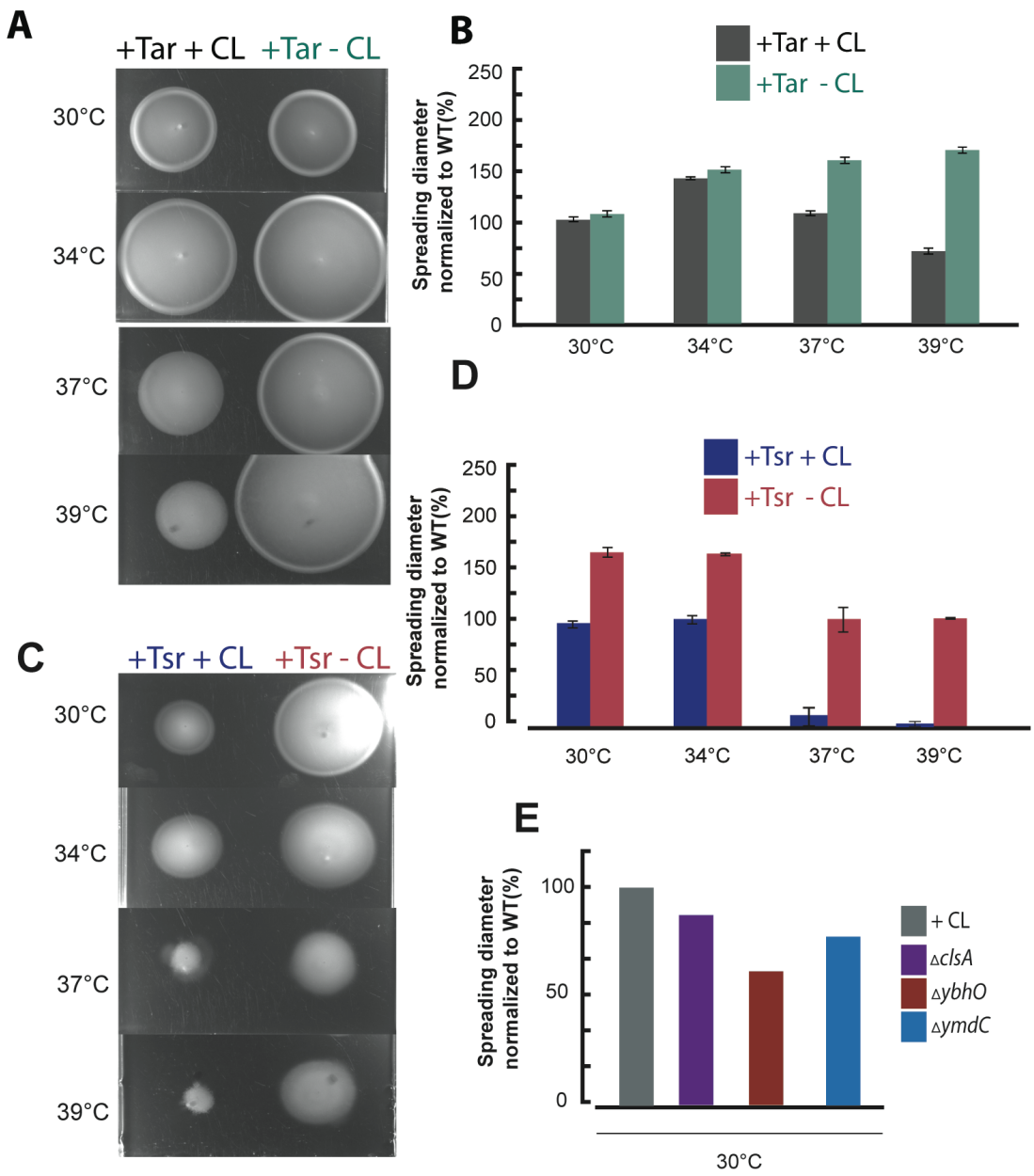

Figure 14. Soft agar assays of *E. coli*. Exemplary images of swimming rings of *E. coli WT* and *E. coli* Δ*clsAybhOymdC* with either expressing Tar (A) or Tsr (B) as only chemoreceptor at different indicated temperatures. Evaluation of minimum three replicas of Tar (C) and Tsr (D) expressing *E. coli WT* and *E. coli* Δ*clsAybhOymdC*, growing on 0.27% soft agar TB plates at various temperatures, normalized to the corresponding *WT* at 30°C. Tar expression from plasmid induced with 1 μM salicylate, Tsr expression induced with 0.4 μM salicylate. Evaluation of *E. coli WT*, *E. coli* Δ*clsA, E. coli* Δ*ybhO* and *E. coli* Δ*ymdC* growing on 0.27% soft agar TB plates at 30°C. Experiment was performed once (E).

4.1.4 Influence of cardiolipin on the chemotaxis system of *E. coli*

To analyse the possible effect of presence or absence of cardiolipin on the chemotaxis system of *E. coli*, we made use of three different experimental setups. First, we focused on the cardiolipin influence on the chemosensing by intracellular observations using a FRET assay. Second, we used fluorescence imaging for quantifications of chemoreceptor clustering in dependency of cardiolipin. Finally, as the chemoreceptors are anchored in the cytoplasmic membrane, we used a FRAP approach to examine the receptor diffusion within the inner membrane with reliance on cardiolipin.

4.1.4.1 Effect of cardiolipin on the plasmid-based expression of Tar and the expression of native chemotaxis genes

For our experiments, we used a receptorless strain (VS367; RP437 Δ*tar* Δ*tsr* Δ*trg* Δ*tap* Δ*aer*) as background and deleted all three cardiolipin synthases to prevent the cells from producing cardiolipin. The respective receptor (Tar) was expressed from plasmid. Before going on with further experiments, we wanted to validate that deficiency of cardiolipin does not influence the plasmid-based chemoreceptor expression in our working strains. Since all plasmids used in this study have the same backbone, we utilised the Tar expression plasmid (pVS1092) as an example. To evaluate the expression of Tar, we performed a Western Blot (see material and methods, 3.9). The cells were grown at 34°C in TB and harvested at an OD_{600} of 0.6. The results are shown in Figure 15. As expected, we could detect a similar amount of Tar chemoreceptor in the two strains (*WT*, *CL*-). With this, we could prove that the lack of cardiolipin does not influence the plasmid-based expression of chemoreceptors. Additionally, by that we can exclude that the following results are erroneously based on differential expression levels of the plasmid-based chemoreceptors in our tested strains. Furthermore, we analysed by flow cytometry the gene expression of native *fliC* using a GFP tagged promoter-reporter. Examination of the native *fliC* expression can be used to monitor the expression of several generally accepted Class 3 operons including the chemotaxis operons *tar-tap-cheRBYZ* and *motAB-cheAW*. For this reason, we used *fliC* as representative of native chemotaxis

gene expression. Flow cytometry results of the GFP tagged *fliC*-promoter reporter, examined in the *WT* and the cardiolipin deficient strain are shown in Figure 15, B. At 34°C, we could not detect a drastic difference of *fliC* expression in the two strains of interest. The expression of native *fliC* in the cardiolipin deficient background is slightly lower than in the *WT*. However, this difference is too small to explain the later shown results of chemosensing and chemoreceptor clustering (see chapters 4.1.4.2 and 4.1.4.3).

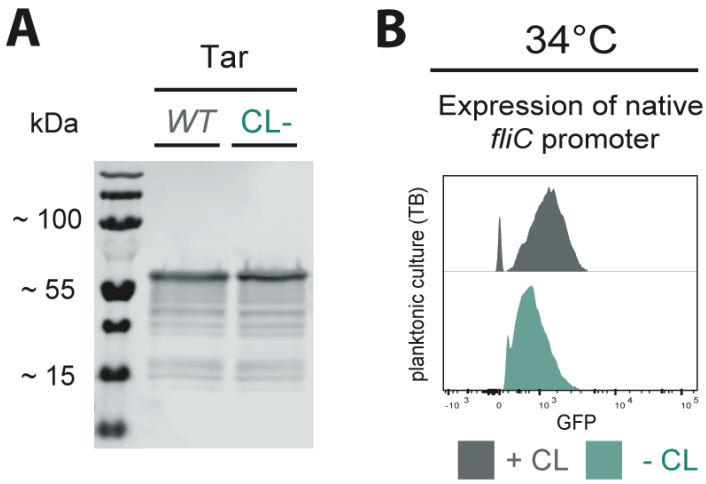

Figure 15. Gene expression analysis. Analysis of Tar expression from plasmid in *E. coli WT* and *E. coli* Δ*clsAybhOymdC via Western Blot (A)*. Flow cytometry-based examination of native *fliC* expression using a GFP tagged promoter reporter (B).

4.1.4.2 Influence of cardiolipin on the chemosensing of *E. coli*

To examine the effect of cardiolipin on protein interactions upon stimulation with an attractant or repellent in *E. coli*, we used a stimulus-dependent FRET assay. As described before (see Material and Methods, 3.12.2), the Förster (fluorescence) Resonance Energy Transfer (FRET) assay relies on a phosphorylation-dependency of the interaction between the response regulator CheY fused to the yellow fluorescent protein (CheY-YFP) and its phosphatase CheZ fused to the cyan fluorescent protein (CheZ-CFP) (*166, 268*).
That enables the analysis of the intracellular pathway response towards certain chemotactic stimuli. More accurately, this assay (illustrated in Supplementary Figure S1) can be used to monitor the activity of the kinase CheA upon stimulation. We determined the amplitudes and dose-response curves by

continuous stimulation of the cells with increasing serial dilutions of the compound of interest, with concentrations ranging from below the limit of response to those exceeding the maximum FRET response. From obtained dose-response curves, the EC50 value was calculated corresponding to the ligand concentration triggering the half-maximum response. This value can be utilised to precisely analyse the sensitivity of certain strains (CL +/-) under different conditions (e.g. temperature). For all experiments concentrations of 0.01 µM to 100 µM for methyl-aspartate (MeAsp), 0.01 µM to 3 mM serin, and 0.03 µM to 100 µM for $NiCl_2$ were used. For pH-dependent experiments, a range from pH 6 to 8.3 was used. The experiments were carried out at 22°C and later also at 18°C, due to obtained protein diffusion results in FRAP experiments (see 4.1.5). Results are summed up in Figure 16, A-G.

We could show that at 22°C experimental temperature, the cardiolipin deletion mutant expressing Tar as only chemoreceptor is responding differently in the FRET assay compared to *WT*-Tar (Figure 16, A). The response curve of the cardiolipin knockout strain seems not to be monotonic but biphasic. The response amplitude of the mutant is smaller than the response amplitude of the *Tar*+ *WT* strain at attractant concentrations higher than 3 µM MeAsp. For lower concentrations, the mutant strain lacking cardiolipin (*CL*- *Tar*+) is significantly more sensitive. For attractant levels, lower than 0.1 µM MeAsp the *WT*-Tar is not responding whereas the *CL*- *Tar*+ is still sensing. The *Tar*+ strain has an EC50 of 2 µM MeAsp, and the *CL*- deletion *Tar*+ mutant exhibits an EC50 of 0.6 µM MeAsp. The time the cells need to adapt to certain different attractant (MeAsp) concentrations are shown in Figure 16, C. For example, for an attractant concentration of 1 µM MeAsp the *Tar*+ strain needs around 400 seconds to adapt, whereas the *CL*- *Tar*+ mutant is adapting in roughly 200 seconds. The differences in adaptation time might result from different response intensities. This can be seen in Figure 16, D, where the adaptation time is plotted against the relative response of the Tar receptor towards MeAsp. At smaller response values until approximately 0.6, the cardiolipin knockout mutant adapts faster than the *WT* with unmodified membrane composition, whereas at relative response values higher than 0.6 up to 0.9 the *WT* adapts faster. At a relative Tar response of 1, the *WT* needs twice as long to adapt than the cardiolipin deficient mutant. However,

further experiments regarding the adaptation modalities would be necessary to obtain more precise insights into the fluctuation adaptation behaviour of the cardiolipin knockout strain. So far our results indicate a slightly better sensitivity of Tar in the cardiolipin deficient strain, especially at lower attractant concentration. As we could detect a difference in attractant sensing of the Tar receptor, we also tested the influence of cardiolipin on the repellent sensing using $NiCl_2$ (Figure 16, E) as ligand. Initial experiments show a continuously smaller response amplitude of the cardiolipin lacking mutant compared to the *WT*. The *WT* is sensing the repellent in a low nanomolar range, whereas the mutant starts sensing in a range higher than 1µM. The EC50 values are 1.3 µM for the *WT* and 2.7 µM for the mutant. To get further insights into the effect of cardiolipin on the chemosensing behaviour of Tar, we carried out further experiments, examining the receptor response towards step-wise changes of the external pH (Figure 16, F). Generally, the pH-taxis of *E. coli* used to obviate acidic or basic external conditions likely depends on the opposing pH sensing behaviour of the two main chemoreceptors Tar and Tsr (3, 4). Previous observations reported an attractant response of Tar for more acidic pH values lower than seven and a repellent response for basic pH levels higher than 7 (4-6). Throughout the attractant as well as the repellent side of our FRET experiment, the amplitudes of the cardiolipin deficient strain are smaller. However, these preliminary results do not seem to be conclusive when comparing to the results with attractant (MeAsp) and repellent ($NiCl_2$).

After detecting the influence of cardiolipin on the Tar receptor, we were additionally testing the influence of cardiolipin on the second main receptor in *E. coli*, Tsr. With our experiments, we could show that for Tsr no significant difference in attractant response is detectable (figure 16, G). The EC50 values are here 30 µM serin for *Tsr*+ and 27 µM serin for the CL null *Tsr*+ mutant. These results are leading to the idea that cardiolipin has an influence on the Tar receptor but not on the Tsr receptor of *E. coli*.

As described earlier, the chemoreceptors constitute an essential part of the bacterial chemotaxis system and are located in the cytoplasmic membrane. It is known that lipid bilayers, such as the cytoplasmic membrane, are temperature-

dependent regarding their fluidity and phase transition (7). Corresponding results to the temperature dependency of the interplay between the cell membrane fluidity and the chemoreceptors diffusion are shown later (Results, 4.1.5). In this context, we repeated the *Tar*+ FRET experiments at a slightly lower experimental temperature of 18°C, to investigate the influence of this temperature shift on the sensing abilities of the receptor. The results are shown in Figure 16, B. In contrast to the results at 22°C, here the curve of the *CL*- strain curve is continuously below the *WT* one. This means the response amplitudes are generously smaller compared to the cardiolipin containing *WT*. Additionally, the cardiolipin-deficient strain is less sensitive at lower concentrations of MeAsp. At 18°C, the Tar receptor expressed in the *CL*- strain is not sensing MeAsp concentrations lower than 0.1 µM, whereas the *WT* starts sensing already at this concentration level. The EC50 of the *WT Tar*+ strain is 0.32 µM, for the *CL*- *Tar*+ strains its 0.67 µM MeAsp. Comparing the two temperatures, some differences in Tar response can be detected. For *WT* as well as for the *CL*- strain at 18°C, the response amplitude is in the maximum, at 50% of the response amplitude at 22°C. Additionally, at 22°C, it seems the *CL*- strain is with regards to the Tar response more sensitive at lower MeAsp concentration. However, at 18°C, the cardiolipin deficient strain is throughout the response curve less sensitive and showing lower amplitudes, compared to the corresponding *WT*.

With our experiments, we could show that the attractant sensing of Tar can be affected by membrane composition and the external temperature additionally influencing the membrane fluidity. A temperature shift leads to a difference in response amplitudes and also the sensitivity changes.

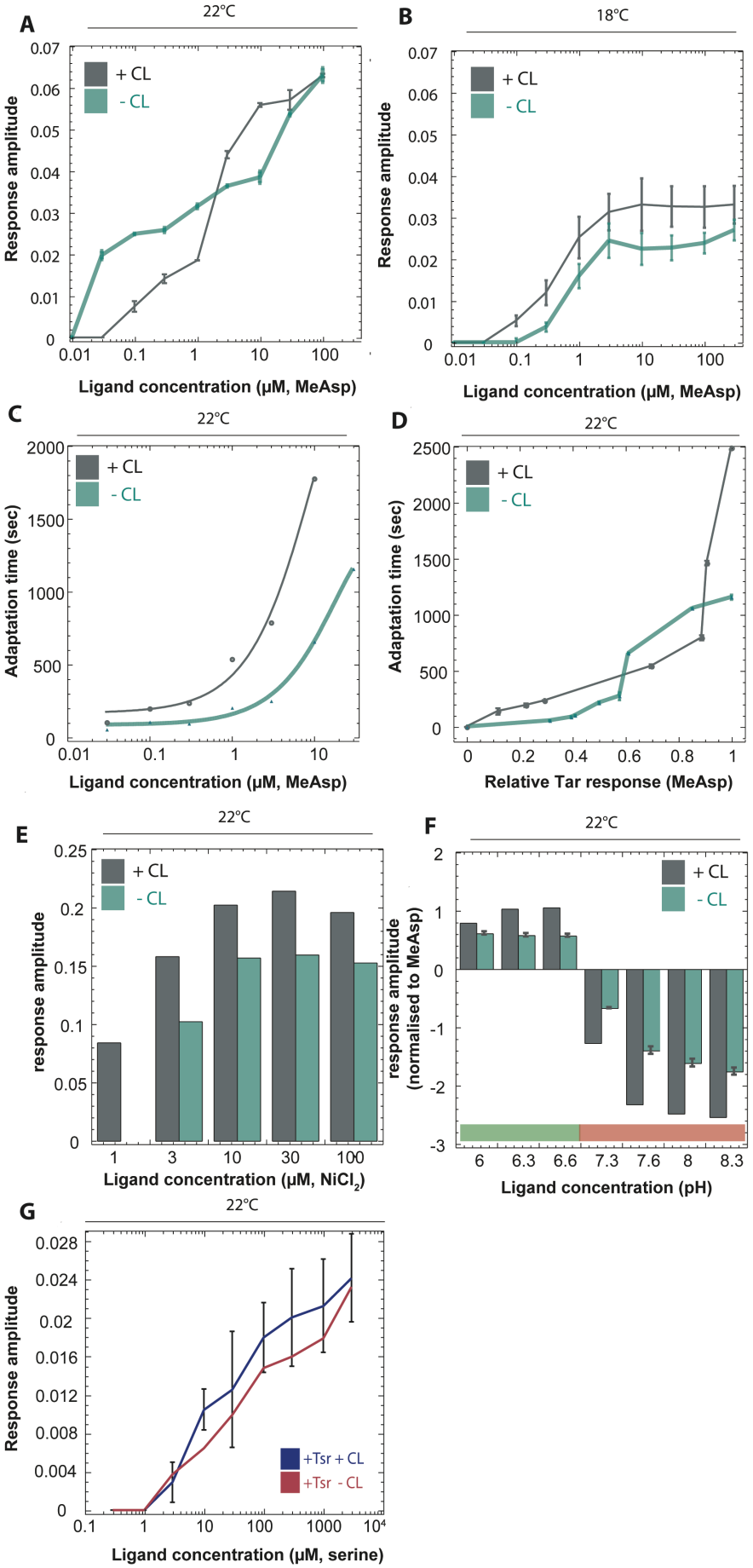
A
22°C
+ CL
- CL
Response amplitude
Ligand concentration (µM, MeAsp)
B
18°C
+ CL
- CL
Response amplitude
Ligand concentration (µM, MeAsp)
C
22°C
+ CL
- CL
Adaptation time (sec)
Ligand concentration (µM, MeAsp)
D
22°C
+ CL
- CL
Adaptation time (sec)
Relative Tar response (MeAsp)
E
22°C
+ CL
- CL
response amplitude
Ligand concentration (µM, NiCl2)
F
22°C
+ CL
- CL
response amplitude (normalised to MeAsp)
Ligand concentration (pH)
G
22°C
+Tsr + CL
+Tsr - CL
Response amplitude
Ligand concentration (µM, serine)

Figure 16. Chemotaxis in *E. coli*. FRET amplitude response curves of *E. coli WT* (grey) and *E. coli* Δ*clsAybhOymdC* (green) expressing Tar as only chemoreceptor at 22°C (A) and 18°C (B). Each point represents the values of response amplitudes, measured from the buffer-baseline, for at least three independent experiments. Error bars indicate the standard error. Preliminary adaptation curves of *E. coli WT* (grey) and *E. coli* Δ*clsAybhOymdC* (green) to MeAsp(C). Plotted adaptation time against amplitudes for *E. coli WT* (grey) and *E. coli* Δ*clsAybhOymdC* (green), one biological replicate (D). Measures response amplitudes of *E. coli WT* (grey) and *E. coli* Δ*clsAybhOymdC* (green) to $NiCl_2$, one biological replicate (E). Measures response amplitudes of *E. coli WT* (grey) and *E. coli* Δ*clsAybhOymdC* (green) towards pH, one biological replicate for the *WT*, three biological replicates for *CL*-. Error bars indicate standard error (F). Dose response curve of *E. coli WT* (grey) and *E. coli* Δ*clsAybhOymdC* (green) expressing Tsr from plasmid towards serine (G). Each point represents the mean kinase activity, normalized by the baseline in buffer, from three biological replicas for the *WT* and one replicate *CL*-, error bars indicating the standard error.

4.1.4.3 Cardiolipin enhances chemoreceptor clustering

4.1.4.3.1 Influence of cardiolipin on the clustering of Tar and Tsr

Methyl-accepting chemotaxis proteins (MCPs) together with several chemosensing-relevant proteins (e.g. CheA, CheW) form supramolecular structures, which are expected to localise mainly at cell poles and septa (*213, 269*). So far, the interaction and dependency of chemoreceptor clustering on the lipid structure of the cytoplasmic membrane remained poorly understood. In this work, we used fluorescent protein fusions to study cluster localisation *in vivo* and to elucidate the role of the cardiolipin in the inner membrane on chemoreceptor clustering. For observing the localisation and number of chemotaxis clusters in *E. coli*, CheY and CheZ were fluorescently labelled with YFP and CFP, respectively and expressed from the same plasmid with 10μM IPTG induction, further CheW tagged with YFP was induced with 10μM IPTG. CheY and its phosphatase CheZ localise only indirectly to the receptor while phosphorylation and dephosphorylation upon ligand binding, whereas CheW binds directly to the receptor. As we work in a chemorecetorless background strain, the receptors of interest were expressed from a plasmid. The Tar receptor was induced with 1 μM salicylate, and the Tsr receptor was induced with 0.4 μM salicylate. For experimental setups and data analysis see material and methods 3.12.1. Results are shown in Figure 17.

Exemplary fluorescence images (Figure 17, A) display clusters on almost all cell poles of the *Tar*+ cells, as well as sporadically along the cells (either at mid septum position, or at cell quarters). Visual observation of the cardiolipin deletion strain (*CL*- *Tar*+) shows a decreased amount of visible chemotaxis clusters compared to the *WT*. For the Tsr receptor is by eye no difference in cluster formation detectable (images not shown).

Manual analysis of the chemoreceptor clusters revealed a halved number of clusters detected in the cardiolipin deficient strain compared to the *WT*. This is consistent throughout all tested growth temperatures from 30°C to 39°C and the tested OD_{600} 0.4 and 0.6, respectively. However, with increasing temperature, the general number of clusters per cell is decreasing. We could confirm these results, with the quantitative cell analysis of 2000 cells per tested OD_{600}=0.4 at 34°C. The results are shown in Figure 17, C. Here the detected cluster number per cell for the cardiolipin lacking strain is also about half compared to the *WT*. Additionally, we used the automated cell analysis to quantify the normalised cluster intensity, representing the cluster size (14, 16) for the two tested membrane compositions (*WT*, *CL*-). The cells expressing Tar as the only chemoreceptor were grown at 34°C and imaged at OD_{600} 0.4. The cluster intensity distribution (Figure 17, D) of the *WT* is slightly broader than the *CL*- strain one. The cardiolipin deficient strain exhibits more Tar chemoreceptor clusters with lower intensity (0 to 0.3), whereas the *WT* shows more clusters with a larger size (0.3 – 0.7).

With the manual analysis of Tsr receptor clustering, we could detect a marginal effect of cardiolipin depletion. The analysis shows a weakly significant difference of Tsr clustering with 1.1 Tsr clusters detected in the *WT* and 0.9 detectable Tsr clusters in the *CL*- strain. By a quantitative analysis of the Tsr expressing strains, the visual inspection (see above), as well as the manual counting results, could be confirmed. Cardiolipin has a small effect on the receptor clustering of Tsr, however the difference is minor (Figure 17, E).

Additionally, to chemoreceptor cluster examinations of cells grown in liquid media, we evaluated the amount of Tar chemoreceptor clusters under ‘active’ chemotactic conditions, with cells grown on soft agar plates, at 34°C (Figure 17, F). On these semi-solid plates, the cells form an outwardly expanding swimming ring to overcome the decreasing nutrient concentration due to metabolism. *WT*,

as well as *CL*- cells, were sampled from the outer precisely formed swimming ring. The imaging and evaluation process agrees with the experiments in liquid media (see material and methods 3.12.1). Here, consistently with previous cluster analysis results, the cardiolipin deficient strain has around half the amount of Tar receptor clusters than the *WT*.

With these experiments, we could prove that cardiolipin promotes the clustering of Tar in *E. coli* at various growth conditions.

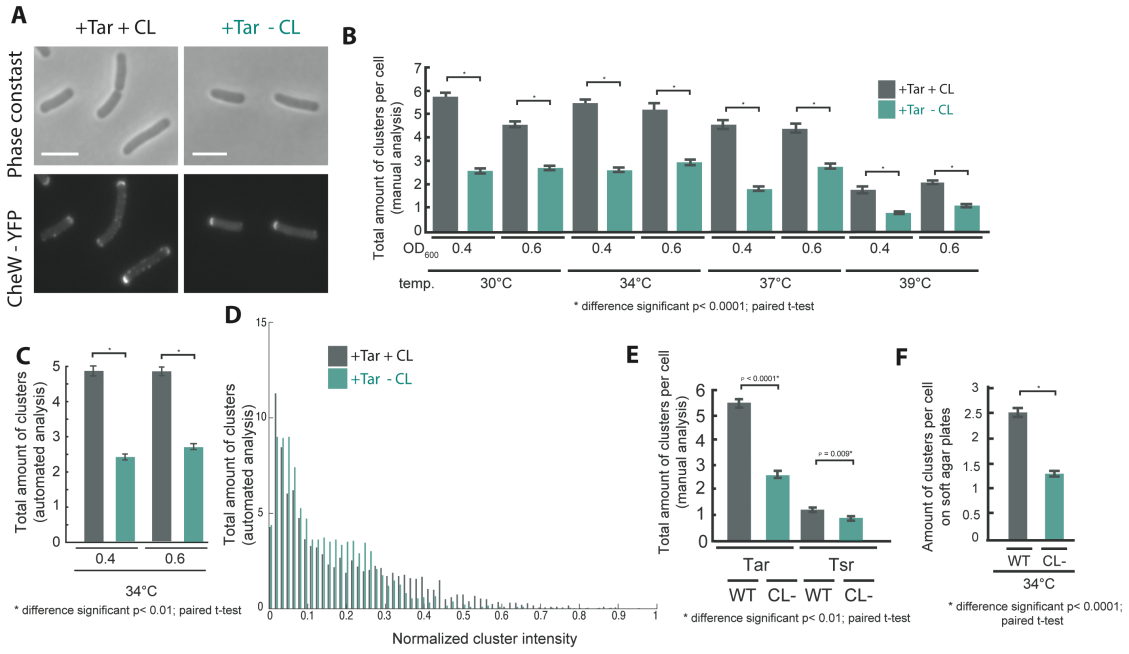

Figure 17. Chemoreceptor clustering in *E. coli*. Exemplary images of chemoreceptor clusters visualized with CheW-YFP in *E. coli WT* and *E. coli* Δ*clsAybhOymdC* (A). Manual analysis of the amount of Tar chemoreceptor clusters in *E. coli WT* (grey) and *E. coli* Δ*clsAybhOymdC* (green) at different indicated temperatures and at mid (OD_{600}=0.4) or late exponential phase (OD_{600}=0.4) (B). Minimum 200 cells per strain and condition were evaluated. Error bars indicate the standard error of the mean and corresponding significance t-test values are specified in the plots. Automated cell analysis of Tar chemoreceptor clusters at 34°C and OD_{600}=0.4 and 0.6 for *E. coli WT* (grey) and *E. coli* Δ*clsAybhOymdC* (green) (C). Normalized cluster intensity as indicator of cluster size for *E. coli WT* (grey) and *E. coli* Δ*clsAybhOymdC* (green), examined by automated cell analysis (D). Manual analysis of the amount of Tsr chemoreceptor clusters in *E. coli WT* (grey) and *E. coli* Δ*clsAybhOymdC* (green) at different indicated temperatures and at mid exponential phase (OD_{600}=0.4), in comparison to the amount of Tar receptor clusters (E). Manual analysis of Tar chemoreceptor clusters in *E. coli WT* (grey) and *E. coli* Δ*clsAybhOymdC* (green) sampled from soft agar plate, grown at 34°C (F). Scale bar indicates 2µm.

4.1.4.3.2 Modification of trans membrane domains restores cardiolipin-dependent effect on receptor clustering

Recent models suggest that the clustering and localisation of chemoreceptors in the absence of CheA and CheW is based on the interplay between the chemoreceptors and the cytoplasmic membrane. These interactions of the membrane-anchored chemoreceptors with the phospholipid bilayer can lead to deformations of the membrane. The hydrophobic mismatch created by that might play a crucial role in the localisation and stability of the receptor clusters (*125, 207, 270*). Due to this fact, we investigated the stability of chemoreceptor localisation and chemoreceptor cluster formation by creating hydrophobic mismatches between the Tar TM domains and the cytoplasmic membrane. For this, we made use of plasmid-based Tar constructs with various modified TM2 domains. In these constructs, the Tar TM2 helix was either shortened by deletion of amino acids or elongated by addition of isoleucine (I). These modifications of Tar result in different chemosensing outputs towards MeAsp (*238*). With the addition of one isoleucine or removal of one amino acid, the modified Tar receptor is still mediating an attractant response towards MeAsp. An addition of two or three isoleucine resulted in an inverted (repellent) response towards MeAsp. In contrast, the modified Tar receptor with two deleted amino acids in the TM2 helix impairs the sensing of MeAsp. The cells were grown in TB at 34°C with 1 µM salicylate induced expression of the respective receptor and IPTG induction of 10 µM for expressing CheY-YFP for the analysis of chemoreceptor cluster localisation. Apart from indicated deviations, the clusters were visualised and quantified using CheY-YFP. The experiment and analysis were performed equivalent to previous investigations (3.12.1), and results are shown in Figure 18, A. Additional noteworthy is the relatively huge change in the absolute number of detected chemoreceptor clusters between the unmodified Tar receptor and the constructs with modified transmembrane domains. This confirms published findings of lower cooperability of the modified Tar constructs compared to the unmodified receptor, as it can be seen by a lower Hill coefficient and the examined higher EC50 values (*238*). Consistent with earlier findings for the unmodified Tar receptor, the Tar TM2+1 construct showed twice as many

clusters, when expressed in the *WT* than in cardiolipin deficient strain. The elongation of the Tar TM2 domain by two isoleucines (Tar TM2+2), increases the ratio of detectable clusters between the two strains. We could detect roughly 1.4 clusters per cell for the *WT*, whereas the cardiolipin lacking strain exhibits only 0.45 clusters per cell. The deletion of one amino acid, within the TM2 helix of Tar, aligns the examined number of chemoreceptor cluster between the cardiolipin comprising and deletion strain. For the *WT*, we could detect around 2.3 clusters per cell, and for the *CL-* strain 2.4. The difference in cluster number for this construct is not significant, which confirms that a reduction of the Tar TM2 domain by one amino acid residue might compensate for the effect of cardiolipin on the clustering of Tar. With the deletion of two amino acids within the Tar TM2 helix, we were unable to detect any chemoreceptor clusters using CheY-YFP. Surprisingly, CheZ-CFP is localising with the chemoreceptor clusters, enabling the evaluation of chemoreceptor clusters (Figure 18, B). The *WT* has an average 0.4 clusters per, and the cardiolipin deficient strain exhibits 0.3 clusters per cell. However, this does not constitute a significant difference in cluster number of our evaluated strains. These results indicate that even with two deleted amino acids in the transmembrane domain, the receptor is still capable of forming clusters, even though the number is small.

A shortening the TM2 domain of Tar by two amino acid residues disabling the receptor from sensing MeAsp, and our finding that this construct is still able of cluster formation, but at the same time the localization of CheY with the receptor is not detectable, leads us to the assumption that this modification results in an impaired interaction of CheY with CheA (*238*). This disturbed localisation of CheY can be caused by a conformational change of the receptor array generated by the reduction of the transmembrane domain by two amino acid residues. Nevertheless, the modification of the TM2 region of Tar, decreases the number of detectable receptor clusters, compared to the unmodified construct.

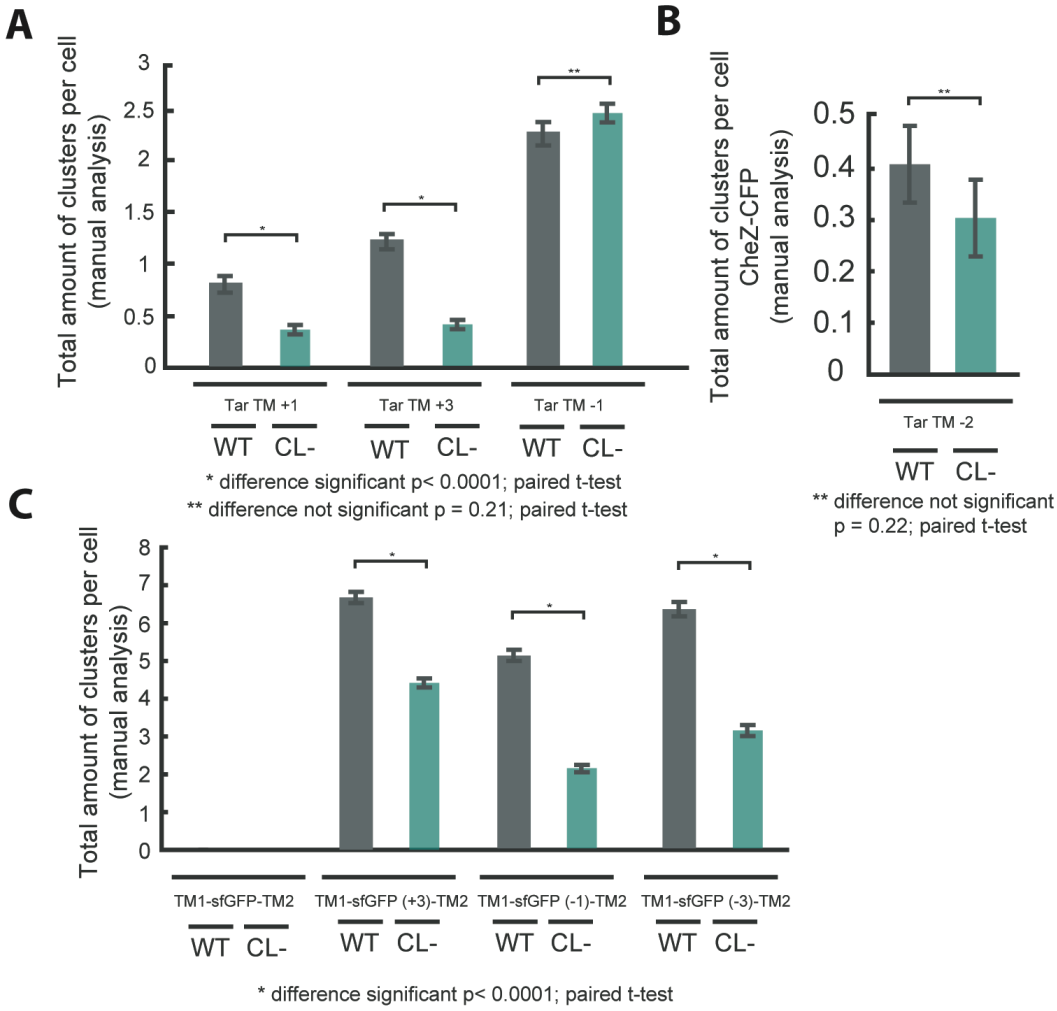

Figure 18. Clustering of Tar with modified transmembrane domains. Manual analysis of the amount of chemoreceptor clusters of Tar with modified transmembrane domain in *E. coli WT* (grey) and *E. coli* Δ*clsAybhOymdC* (green) at 34°C and at mid exponential growth phase (OD_{600}=0.4), labelled with CheY-YFP (A). Amount of chemorceptor clusters of Tar with TM2 domain shortened by two amino acids in *E. coli WT* (grey) and *E. coli* Δ*clsAybhOymdC* (green) at dif34°C and mid exponential growth phase (OD_{600}=0.4), labelled with CheZ-CFP (B). Number of cluster like structures of the modified transmembrane domains of Tar labelled with sfGFP in *E. coli WT* (grey) and *E. coli* Δ*clsAybhOymdC* (green) (C). Minimum 200 cells per strain and condition were evaluated. Error bars indicate the standard error of the mean and corresponding significance t-test values are specified in the plots.

It was published recently that the membrane-anchored TM domains of Tar are capable of forming cluster-like structures by themselves (*208*). Therefore, we continued examining the cluster formation capability of modified Tar transmembrane domains, in correlation with cardiolipin presence (figure 18, C). For this, we made use of different constructs comprising only the TM1 (residue 1-43) and the TM2 (residue 184-214) domain of Tar in various lengths linked by

five amino acids and sfGFP. Most of these constructs are capable of forming cluster like associations in *E. coli* cells by themselves (*208*). For the unmodified Tar TM construct, we could not detect any cluster-like structures, consistent with previously published data (*208*), suggesting that the Tar-TM construct is only capable of forming clusters in the presence of a major native chemoreceptor. For the elongated version TM1-sfGFP(+3)-TM2, we could detect around 6.8 cluster-like patches per *WT* cell and 4.5 in the cardiolipin deficient strain. For this construct, the ratio of identified clusters formed in the *WT*, to the cluster number in the cardiolipin deficient strain is smaller compared to the native version of Tar but still significantly different. For the shortened constructs TM1-sfGFP(-1)-TM2 and TM1-sfGFP(-3)-TM2 the doubled ratio of cluster number in the *WT* compared to the cardiolipin lacking strain is consistent. Our results suggest that the modified TM helices of Tar are capable of forming clusters independent of cardiolipin. Consistent with the finding of the Tar full version clustering, the *WT* has more cluster-like patches than the cardiolipin deficient strain. However, the significant difference in the detectable number of cluster-like patches for the shortened versions TM1-sfGFP(-1)-TM2 and TM1-sfGFP(-3)-TM2 are not matching the previously examined Tar constructs with reduced TM regions. For the full-length Tar versions with the modified transmembrane domain, we could not detect a significant difference in cluster number in dependency of cardiolipin. We suspect that a shortening of the TM2 helix of Tar leads to a conformational change of the receptor, caused by the provoked mismatch between receptor and membrane. This mismatch might overcome the effect evoked by the absence of cardiolipin. The results of the tested construct comprising only the TM helices suggest that the localisation/clustering of the TM region itself might be stabilised by cardiolipin. We assume that the presence of cardiolipin in the cytoplasmic membrane influences the chemoreceptor cluster size, but not the number of actually present Tar chemoreceptor clusters. We expect cardiolipin to stabilise the formed chemoreceptor clusters, as well as the lipid might influence the mobility of the membrane inserted chemoreceptors. Possibly this difference in size of the Tar chemoreceptor clusters is based on a difference in membrane fluidity and resulting in a changing diffusion of the single receptors within the membrane.

4.1.5 Cardiolipin mediated enhancement of receptor mobility

Protein mobility is a key part for the cellular process, especially as bacteria lack an active protein transport and therefore rely on a passive diffusion mechanism for protein mobility within the membrane (*237*). In the previous chapter, we proposed that the difference in detectable amount or size of chemotaxis clusters might be a matter of chemoreceptor diffusion within the membrane, possibly arising from changes in phospholipid composition caused by the depletion of cardiolipin. To examine this, we carried out various FRAP (Fluorescence Recovery After Photobleaching) experiments monitoring protein mobility in the cytoplasmic membrane. An exemplary fluorescence recovery curve (FRAP) is shown in Supplementary Figure S2.

We made use of the FRAP approach to investigate the mobility of the two main chemoreceptors Tar and Tsr within the cytoplasmic membrane, concerning cardiolipin presence or absence (*271*). Additionally, we evaluated the membrane diffusion of two randomly selected membrane proteins of *E. coli* (see material and methods, 3.12.3). For our experimental approach, we used YFP labelled fusions expressed from a plasmid in our *WT* and the cardiolipin knockout strain. For improving the experimental resolution, we elongated cells by a treatment with the cell-division inhibiting antibiotic cephalexin for approximately 30 minutes (*272, 273*). The cells were harvested and resuspended in tethering buffer. After attachment of the cells on the temperated microscopy slide as described in material and methods, and adaptation of the samples to the experimental conditions for minimum 20 minutes to ensure full maturation of the fluorescent proteins, the experiments were performed at different temperatures from 8°C to 30°C. The fluorescence fusion protein of interested was bleached at the polar region of a cell. Subsequently, the recovery of fluorescence was followed by acquiring serial images in distinct time intervals (see Material and Methods). Throughout our experiments, most of the observed membrane protein fusions were distributed evenly along the membrane. Because full-length chemoreceptors form mostly polarly located chemoreceptor clusters, we additionally performed our experiments with YFP tagged shortened versions of the chemoreceptor Tar, which are incapable of cluster formation. The usage of

short-Tar-YFP constructs facilitates the examination of clustering unaffected chemoreceptor diffusion within the cytoplasmic membrane.

4.1.5.1 Cardiolipin related temperature dependency of Tar diffusion

Initially, we observed the diffusion of the full and truncated version of Tar at four different temperatures (8°C, 18°C, 22°C, 30°C), the results are presented in Figure 19, A. Although temperature might generally influence the diffusion of membrane proteins due to changes of the membrane viscosity, our data suggest a temperature-dependent specific effect of cardiolipin on the diffusion of Tar within the cytoplasmic membrane. Figure 19, C, a-b, shows normalised fluorescence recovery curves of the full-length Tar receptor labelled with YFP at different experimental temperatures. The corresponding recovery rates and the values indicating the extent of recovery are shown in Table 9. Recovery rates are calculated by a simplified exponential curve fitting of the examined fluorescence recovery curves, using Kaleidagraph (see Material and Methods 3.12.3). The recovery rate values (parameter b of the exponential curve fit) represent the speed of fluorescence recovery by means of protein diffusion. The extent of recovery indicates the total amount of fluorescence recovery in the strain of interest after photo bleaching.

Table 9. Recovery rates and extent of recovery values of Tar-YFP in VS367 (*WT*) and NS89 (*CL-*) at 8°C, 18°C, 22°C and 30°C.

		Recovery rate ($x10^{(-3)}$)		Extent of recovery (%)	
Construct	**Experimental temperature (°C)**	***WT***	***CL-***	***WT***	***CL-***
full-Tar-YFP	8	0.32136	0.35163	60	64
full-Tar-YFP	18	0.52917	0.23957	75	55
full-Tar-YFP	22	0.48375	0.4241	77	70
full-Tar-YFP	30	0.27638	0.35163	57	52

At 8°C, 22°C and 30°C, no clear difference in diffusion of the full-length construct in the *WT* compared to the cardiolipin deficient strain is detectable. However, at 18°C there is visually a difference in diffusion depending on cardiolipin perceptible. The receptor is diffusing faster in the *WT* than in the *CL*- strain. Also, for all temperatures the extent of recovery is larger in the *WT* then in the cardiolipin deficient strain. At 18°C the difference is the largest, whereas the full-Tar construct in the *WT* recovers to around 75%, the extent of recovery in the *CL*-strain is only 55%. Exemplary microscopic time lapse images of the full length-Tar-YFP construct in the *WT* and the cardiolipin deficient strain are shown in Supplementary Figure 19, A. The full-length construct of Tar is capable of complex cluster formation, which decelerates the average diffusion of the receptor. Further diffusion examinations of cluster forming receptors would require a more extended recording of the experiment necessary, leading to an increase in sample bleaching. Due to that, the precise fluorescence recovery rate might become indistinct. To overcome this effect, we examined the cardiolipin-dependent effect on the mobility of a truncated version of Tar. This version is incapable of cluster formation but still localising smoothly distributed within the cytoplasmic membrane as shown in Figure 19, B.

Consistent with the temperature and cardiolipin-dependent results of the full-length construct, we could also see slower diffusion for the short version at 18°C, however, the differences between the *WT* and *CL*- strain are even more drastic. Figure 19, D shows the normalised fluorescence recovery curves of the short-Tar-YFP construct in the *WT* (grey) and the cardiolipin lacking strain (green). The values of the corresponding recovery rates and the extent of recovery are listed in Table 10. Similar to just described results of the full Tar version, at 8°C, 22°C and 30°C, no drastic difference in receptor diffusion for the two strain is detectable. However, at 18°C, the difference is unambiguous, similarly to full-length receptors. While the diffusion of the short-Tar-YFP construct in the *WT*, at 18°C, is even faster than at other tested temperatures, the diffusion in the *CL*-strain is drastically decelerated. The *WT* is partially recovering after 65 s, whereas for the cardiolipin mutant strain even after 240 s, hardly any recovery is

detectable. The values indicating the extent of recovery confirm these observations. The comparison of the fluorescence recovery of the two constructs (long and short Tar-YFP) in the *WT* (Figures 19, C and D), illustrates the accelerated recovery due to faster diffusion of the short Tar-YFP construct.

Table 10. Recovery rates and extent of recovery values of short Tar (1-319)-YFP in (*WT*) and NS89 (*CL*-) at various temperatures.

		Recovery rate ($x10^{(-3)}$)		Extent of recovery (%)	
Construct	**Experimental temperature (°C)**	***WT***	***CL-***	***WT***	***CL-***
short-Tar-YFP	8	1.4759	1.1667	95	94
short-Tar-YFP	14	2.067	1.504	95	93
short-Tar-YFP	16	3.4344	0.5509	98	68
short-Tar-YFP	17	2.4147	0.60015	94	70
short-Tar-YFP	18	3.0646	0.3363	99	58
short-Tar-YFP	19	4.5217	2.2517	99	95
short-Tar-YFP	20	5.0313	5.4022	98	98
short-Tar-YFP	22	1.2901	1.2358	87	96
short-Tar-YFP	30	2.0918	1.5543	95	95

We continued examining the slower fluorescence recovery of the Tar receptor at temperatures around 18°C. Therefore, we performed further FRAP experiments examining the receptor recovery with tightly defined temperature steps around 18°C, namely 14°C, 16°C, 17°C, 19°C, 20°C. For better clarity, all relevant FRAP results of the short Tar-YFP construct examined in the two strain (*WT*, *CL*-) backgrounds are summarised and displayed in Figure 19, E. As shown already for 8°C, also at 14°C, we could not determine any effect of cardiolipin on the

recovery of the truncated receptor (short-Tar-YFP). With approaching the temperature of 18°C, we could detect a comparable cardiolipin-dependent difference in fluorescence recovery of the short receptor version. At 16°C as well as 17°C, the short-Tar-YFP construct diffuses faster in the *WT* than in the cardiolipin deletion strain. Still, at 18°C the difference in recovery is the most prominent. This can also be seen the extent of recovery, at 18% the fluorescent short-Tar construct in the cardiolipin deficient strain recovers only to almost 60%. At 16°C and 17°C the extent of recovery is around 70%. Surprisingly, with an increase of only 1°C, the cardiolipin-dependent effect on the diffusion of the chemoreceptor Tar disappears. At 19°C and 20°C, we couldn't detect any differences in the fluorescence recovery of the short Tar-YFP construct. At temperatures, higher than 18°C the fluorescent truncated Tar construct is recovering to an extent of 95% and higher.

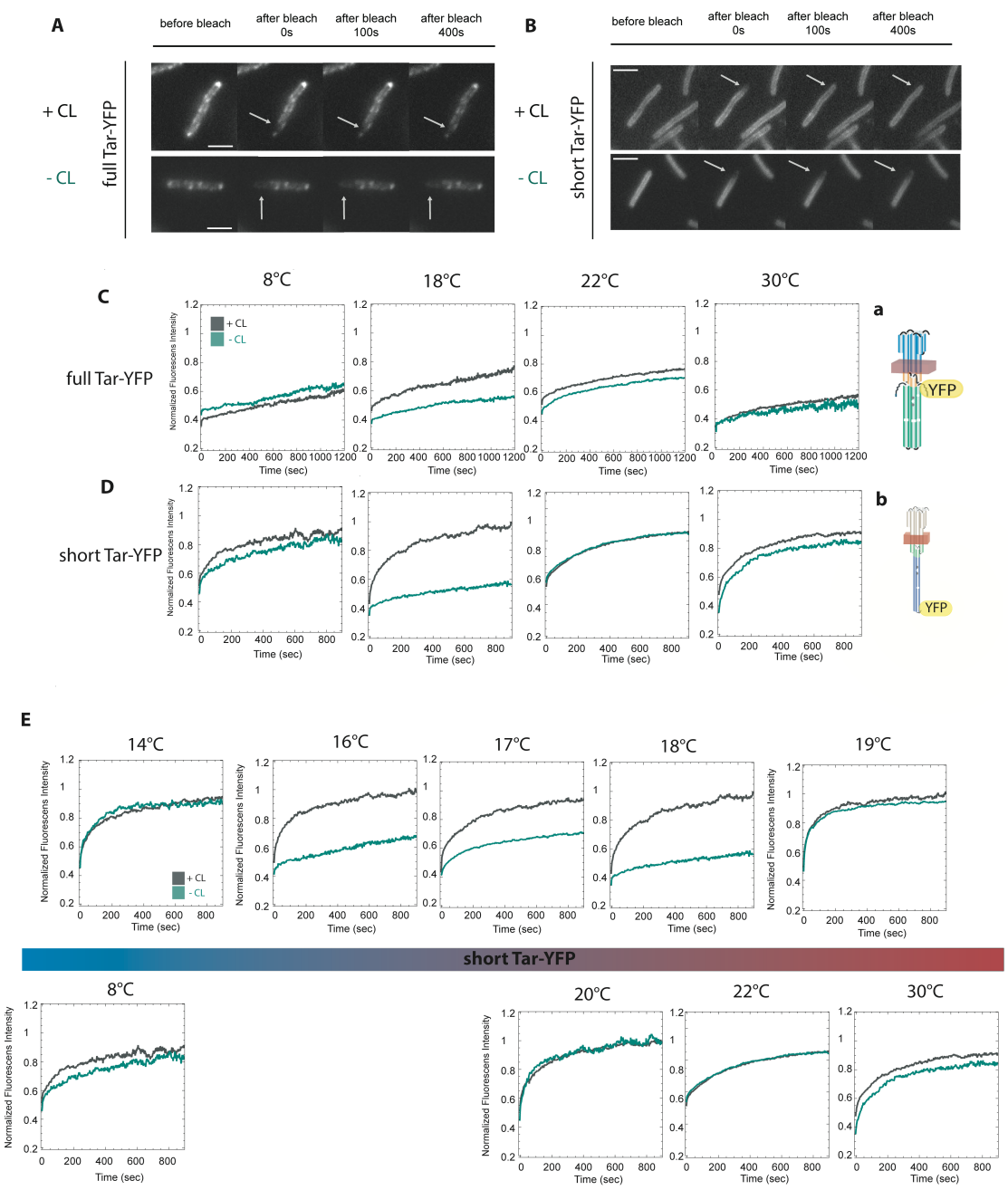

Figure 19. FRAP diffusion experiments with full and short Tar receptor. Selected FRAP recovery images for the full-Tar-YFP construct (A) and the short-Tar construct (short-Tar (1-319)-YFP) (B) in CL+ and CL- cells. Fluorescence recovery curve of the full-length Tar receptor labelled with YFP (a) in *E. coli WT* (grey) and *E. coli* Δ*clsAybhOymdC* (green) at 8°C, 18°C, 22°C and 30°C experimental temperature (C). Fluorescence recovery curve of the short-length Tar receptor (1-319) labelled with YFP (b) in *E. coli WT* (grey) and *E. coli* Δ*clsAybhOymdC* (green) at 8°C, 18°C, 22°C and 30°C experimental temperature (D). Fluorescence recovery curve of the short-length Tar receptor (1-319) labelled with YFP in *E. coli WT* (grey) and *E. coli* Δ*clsAybhOymdC* (green) at tight temperature steps around 18°C (E). Curves show averaged fluorescence recovery of minimum 15 different cells out of minimum three independent biological replicates.

4.1.5.2 BzA reverts cardiolipin related diffusion effects

Cardiolipin increases the membrane fluidity due to changing the ratio of more unsaturated hydrocarbon tails of membrane containing phospholipids in comparison to the phospholipid head groups. Additionally, the membranes mechanical stability decreases with an increasing amount of cardiolipin (*72*). Noteworthy, cardiolipin is also known for specific interactions with proteins, peptides and other entities (*67*). With the deletion of the three known cardiolipin synthases, we anticipate the cytoplasmic membrane to be less fluid. Based on our previous FRAP results, we assume the temperature-dependent effect on the diffusion of the chemoreceptor Tar is due to the absence of cardiolipin and the resulting decrease in membrane fluidity. To confirm our theory, we reversed the membrane fluidity by using benzyl alcohol (BzA), as it is known to increases membrane fluidity (*274*). The experiments were performed as previously described, and BzA was added to the samples. Treatment of the cells with BzA indeed abolishes the effect caused by the lack of cardiolipin. Corresponding diffusion values and the extent of recovery are indicated in Table 11. At 18°C, a concentration of 20 mM benzyl alcohol minimises the temperature-dependent impact on the diffusion of Tar caused by the lack of cardiolipin by half (Figure 20, B). With 40 mM BzA, the distinct effect of cardiolipin deficiency at 18°C on the fluorescence recovery of the short Tar-YFP construct can be abolished entirely (Figure 20, C). The increase in membrane fluidity by treating the cells with BzA can be observed by comparing the normalised fluorescence recovery curves of the short Tar-YFP construct in the *WT* with and without BzA treatment. When treated with BzA, the recovery curve is slightly steeper in the beginning, and a fast plateau formation is detectable when compared to untreated samples. These observations suggest faster mobility of the shortened receptor within the membrane as a result of an increased membrane fluidity.

Table 11. Recovery rates and extent of recovery values of short Tar (1-319)-YFP constructs with benzylalcohol in (*WT*) and NS89 (*CL-*) at various temperatures.

		Recovery rate ($x10^{(-3)}$)		Extent of recovery (%)	
Construct/additional chemicals	**Experimental temperature (°C)**	***WT***	***CL-***	***WT***	***CL-***
short-Tar-YFP 20mM BzA	18	2.9535	0.98073	99	82
short-Tar-YFP 40mM BzA	18	5.0779	7.5065	99	98
short-Tar-YFP 40mM BzA	20	6.1935	11.604	98	98

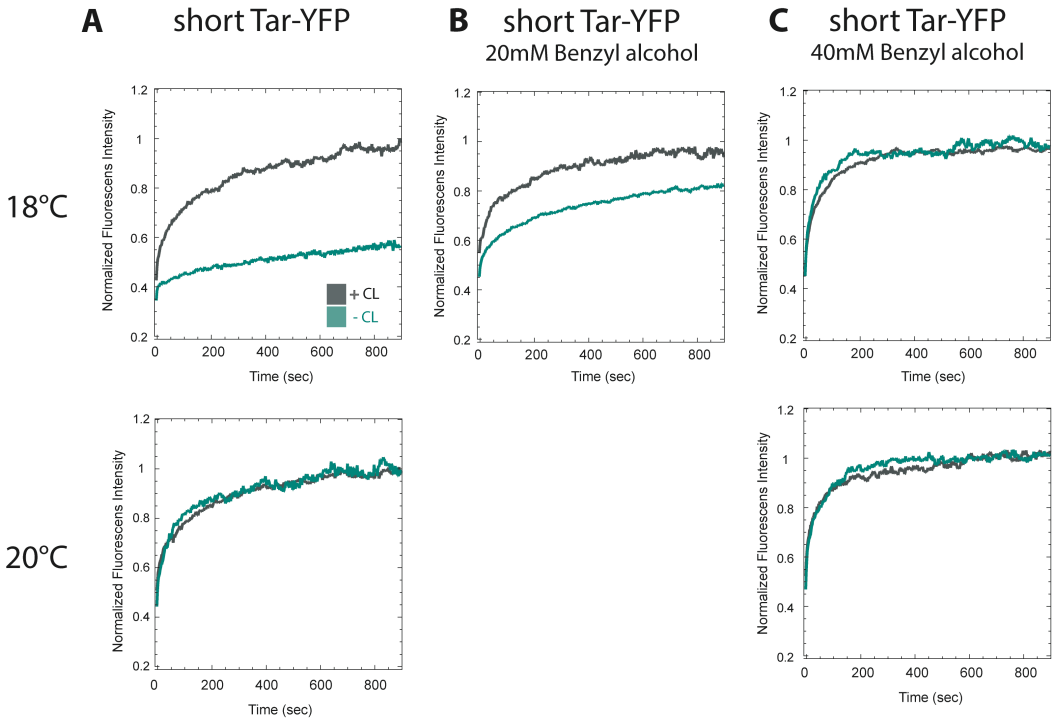

Figure 20. FRAP diffusion experiments with short Tar receptor and benzylalcohol (BzA). Fluorescence recovery curve of the short-length Tar receptor (1-319) labelled with YFP in *E. coli WT* (grey) and *E. coli* Δ*clsAybhOymdC* (green) at 18°C and 22°C experimental temperature, without BzA (A), with 20 mM BzA (B) and with 40 mM BzA (C). Curves show averaged fluorescence recovery of minimum ten different cells out of minimum three independent biological replicates.

4.1.5.3 Transmembrane domain modification of Tar restores cardiolipin-dependent diffusion effects

In addition to the just described Tar constructs (truncated and full length), we examined YFP tagged Tar receptors with elongated or shortened transmembrane helices, based on a recent publication (*238*). Exemplary fluorescence images are shown in Figure 21, A. With the thereby provoked possible changes of the receptor-membrane interaction through hydrophobic mismatch, we want to gain further insights into the temperature-dependent effect of cardiolipin on the diffusion of Tar. All experiments were performed as previously described, and the results are shown in Figure 21. Recovery rates and values indicating the extent of recovery are listed in Table 12. The experiments were carried out at 18°C and 22°C. At 18°C, reduction of the TM2 helix by two amino acids causes the same cardiolipin-dependent diffusion effect on the chemoreceptor as observed before for the unmodified Tar-construct (Figure 21, C, a). With a transmembrane helix elongation by two residues (TM+2), the temperature-dependent effect of cardiolipin at 18°C, can be eliminated. The fluorescence recovery curves, shown in Figure 21, D, a, show no difference of recovery between *WT* and the cardiolipin lacking strain. The elongation of the transmembrane region by three amino acids (TM +3) does not fully restore the effect of cardiolipin deficiency at 18°C like the one residue shorter version (TM2 +2). As shown in Figure 21, E, a, the recovery curves do slightly differ in their slope with a slower recovery of the modified receptor in the cardiolipin lacking strain. Compared to the unmodified version of this construct (Figure 19, D), the difference in slope has narrowed with the extension by three residues.

Table 12. Recovery rates and extent of recovery values of short Tar (1-319)-YFP constructs with modified TM2 domains in (*WT*) and NS89 (*CL*-) at various temperatures.

		Recovery rate x10$^{(-3)}$		Extent of recovery (%)	
Construct	**Experimental temperature (°C)**	***WT***	***CL-***	***WT***	***CL-***
short-Tar-TM(-2)-YFP	18	1.9965	0.40264	95	70
short-Tar-TM(+2)-YFP	18	1.8738	1.6157	93	93
short-Tar-TM(+3)-YFP	18	1.1359	0.47857	85	72
short-Tar-TM(-2)-YFP	22	2.0187	1.3729	95	90
short-Tar-TM(+2)-YFP	22	1.4194	0.77617	87	80
short-Tar-TM(+3)-YFP	22	0.73368	0.20705	80	55

At 22°C, the recovery of the unmodified short Tar-YFP construct does not differ in both strains (*WT*, *CL*-) (Figure 19, C). Similar results could be detected for the diffusion of the short Tar version with addition or reduction by two residues of the transmembrane helix (TM2 +2, TM2 -2) (Figure 21, Cb, Db). For these two constructs, the general slope is slightly smaller compared to the unmodified short Tar-YFP version. This indicates a generally slower diffusion of the modified constructs in the cytoplasmic membrane compared to the non-modified construct. With the elongation of the transmembrane domain by three residues (TM2 +3) (Figure 21, E, b), the difference in recovery of the modified receptor in the *WT* compared to the cardiolipin lacking strain is similar to the one of the unmodified short Tar-YFP version at 18°C. It seems that the elongation of the transmembrane domain of Tar by three residues at 22°C, leads to a similar effect of decelerated diffusion as the unmodified short Tar-YFP version at 18°C.

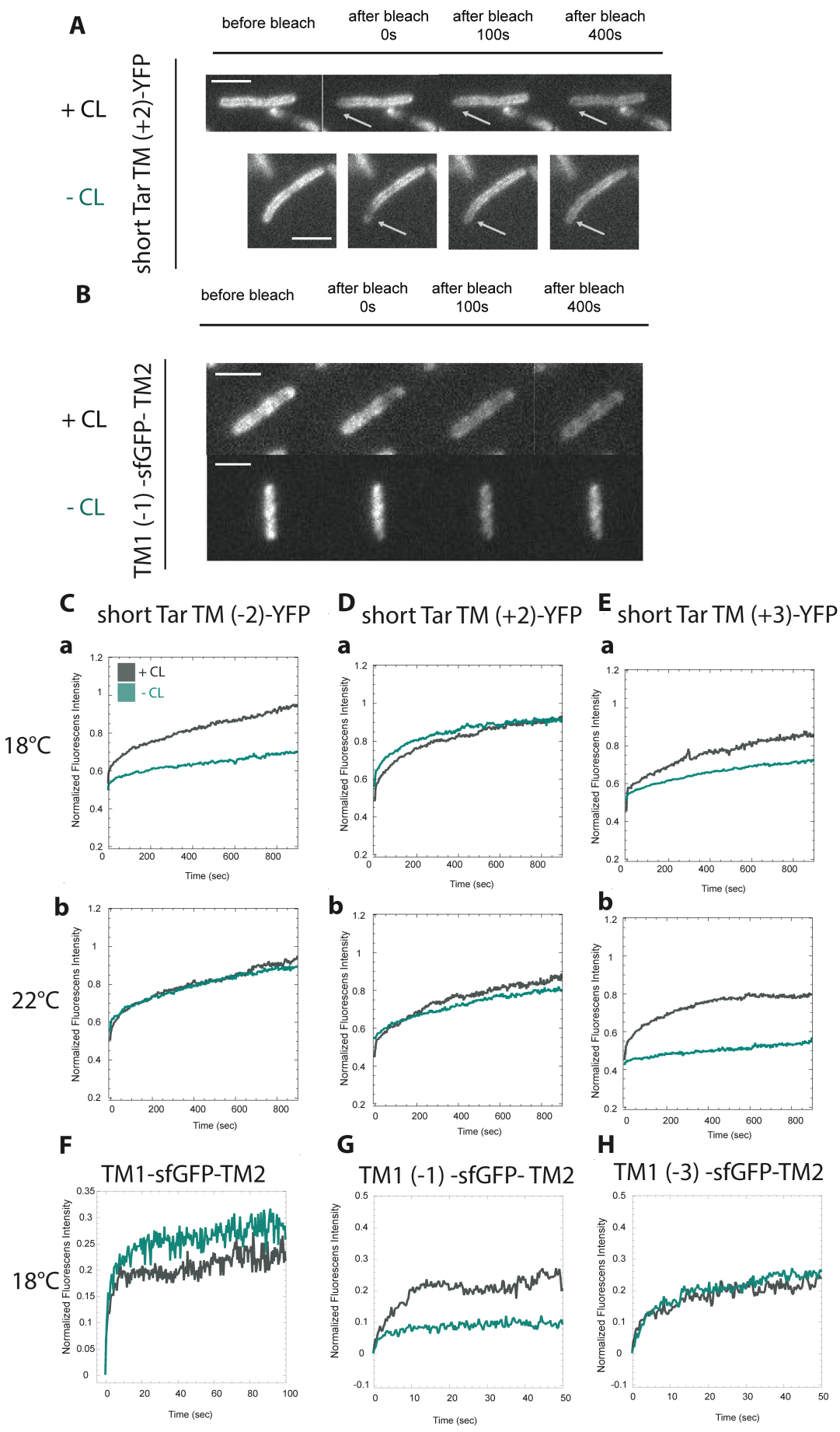
A
before bleach
after bleach 0s
after bleach 100s
after bleach 400s
+ CL
- CL
short Tar TM (+2)-YFP
B
before bleach
after bleach 0s
after bleach 100s
after bleach 400s
+ CL
- CL
TM1 (-1) -sfGFP- TM2
C
short Tar TM (-2)-YFP
D
short Tar TM (+2)-YFP
E
short Tar TM (+3)-YFP
a
b
18°C
22°C
+ CL
- CL
Normalized Fluorescens Intensity
Time (sec)
F
TM1-sfGFP-TM2
G
TM1 (-1) -sfGFP- TM2
H
TM1 (-3) -sfGFP-TM2
18°C

Figure 21. FRAP diffusion experiments with modified TM2 domain of the short Tar receptor. Selected FRAP recovery images for the short Tar TM (+2) -YFP construct (A) and the TM1-sfGFP (-1) TM2 construct (B) in CL+ and CL- cells. Fluorescence recovery curve of the short-length Tar receptor (1-319) with modified TM2 domain labelled with YFP in *E. coli WT* (grey) and *E. coli* Δ*clsAybhOymdC* (green) at 18°C and 22°C experimental temperature. Short-Tar TM2 -2 residues (C), short-Tar TM2 +2 residues (D), short-Tar TM2 +3 residues (E). Fluorescence recovery curve of modified Tar transmembrane domains labelled with sfGFP in *E. coli WT* (grey) and *E. coli* Δ*clsAybhOymdC* (green) at 18°C experimental temperature. Unmodified TM1-sfGFP-TM2 (F), TM1-sfGFP- (-1) TM2 (G), TM1-sfGFP- (-3) TM2 (H). Curves show averaged fluorescence recovery of minimum 12 different cells out of minimum three independent biological replicates.

In addition to those just described transmembrane helix modified short version of Tar, we worked with Tar-TM only constructs, just harbouring the two transmembrane helices of the receptor in a standard, elongated and shortened length of the TM2 fused with sfGFP (*208*). With this, we hope to gain further insights on how cardiolipin influences the membrane diffusion of Tar and the temperature dependency of this effect. These modified constructs are mostly capable of forming chemoreceptor cluster-like structures. We analysed the membrane diffusion of the initial construct (TM1-sfGFP-TM2) as well as of the by one residue shortened version (TM1-sfGFP (-1) TM2), and the (TM1-sfGFP- (-3) TM2) construct reduced by three amino acids, each at 18°C. For the unmodified construct (Figure 21, F), a small difference in fluorescence recovery between *WT* and the *CL*- strain is visible. For both strains, in the early phase of recovery, a rapid diffusion is detectable, whereas the curve flattens with time. As for other constructs like the unmodified short and full tar-YFP versions expressed in the *CL*- strain, the total recovery is lower than in the *WT*. However, the difference between the two curves here is decreased. The TM1-sfGFP (-1) TM2 construct expressed in the *CL*- strain is hardly recovering at all, whereas in the *WT* a slight recovery of 0.2 is detectable (Figure 21, G). Strikingly, for the even shorter version (TM1-sfGFP (-3) TM2) no difference in recovery is observed, when expressed in the *WT* and *CL*- strain and both recovery curves are similar (Figure 21, H). Compared to the unmodified construct, both shortened versions are recovering much slower in the *WT*, whereas only for the *CL*- strain the recovery of the (TM1-sfGFP (-1) TM2) constructs stagnates almost completely. We could show that already the modification of the sfGFP tagged transmembrane helices by removing up to three residues can influence the diffusion of the Tar membrane

domains. However, the general comparison of the (modified und unmodified) short and full Tar-YFP versions with the TM only-sfGFP constructs needs to be evaluated with caution. Additional possible conformational variabilities of the short and long variants of the receptor in contrast to the transmembrane only constructs should be noted. Due to this reason, a direct comparison of diffusion results of the modified or unmodified truncated and full-length receptor with the TM only constructs is difficult. We could show, that modification of the transmembrane helix two of Tar can partially restore the temperature-dependent slower diffusion of the receptor in the cardiolipin lacking strain.

4.1.5.4 Cardiolipin does not influence the diffusion of Tsr and other proteins

To determine whether the just described temperature and cardiolipin-dependent effect on protein diffusion within the cytoplasmic membrane, affects only the Tar receptor or also more globally other chemoreceptors and membrane proteins, we performed additional FRAP experiments. As shown in Figure 22, A, for the Tsr receptor tagged with YFP (Tsr-YFP), at 18°C, no cardiolipin-dependent difference in fluorescence recovery is detectable. Furthermore, we investigated the possible effect of cardiolipin- and temperature-dependent protein diffusion within the cytoplasmic membrane for two more random membrane proteins (LacY-YFP and NagE-YFP). LacY, the lactose permease of *E. coli*, is a symport system responsible for the beta-galactosides import and the concomitant proton uptake into the cell (*275*). NagE is coding for a phosphoenolpyruvate-dependent sugar phosphotransferase system and additionally catalysing the phosphorylation of incoming sugar substrates, combined with their translocation through the cell membrane (*276*). We performed the experiments similarly to previous ones at 18°C and 22°C. Neither for LacY-YFP nor NagE-YFP any cardiolipin or temperature-dependent difference in fluorescence recovery could be detected (Figure 22, B-C). For LacY-YFP and NagE-YFP, the normalised fluorescence recovery curved in both strain backgrounds (with and without cardiolipin) overlap, showing no significant difference. These findings suggest that the temperature-

dependent effect of cardiolipin on the diffusion of the chemoreceptor Tar is probably specific. The diffusion of other membrane proteins than Tar seems not to be influenced by cardiolipin.

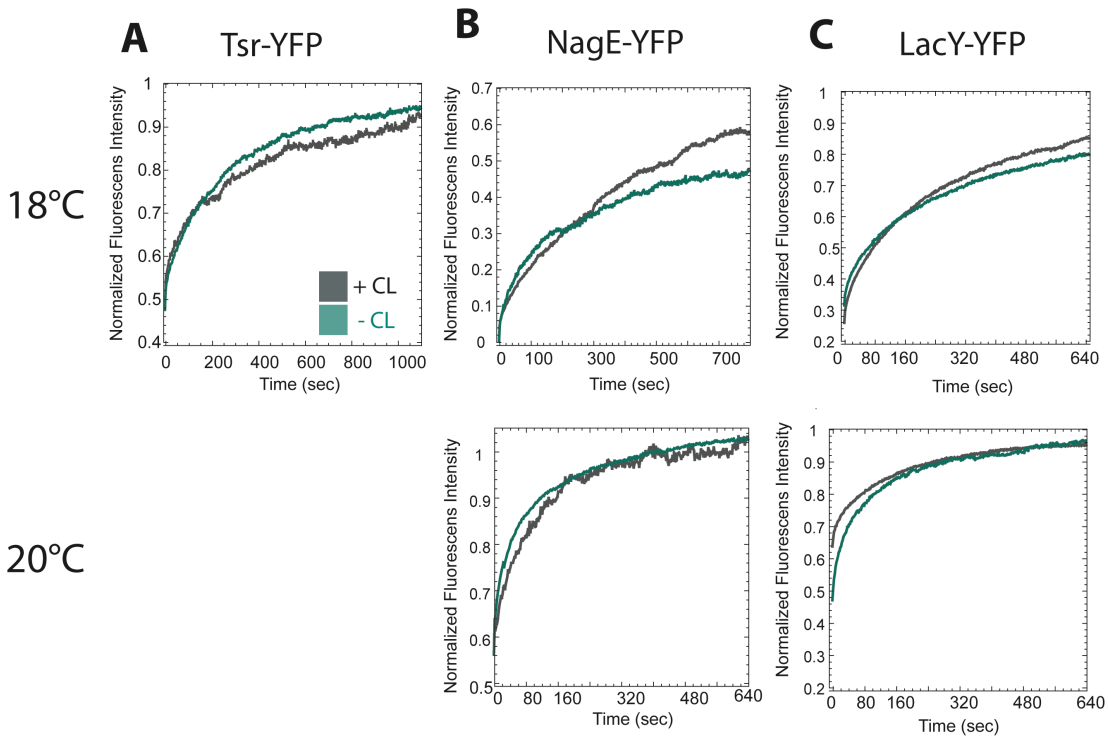

Figure 22. FRAP diffusion experiments with the Tsr receptor, NagE and LacY. Fluorescence recovery curve of the Tsr receptor labelled with YFP in *E. coli WT* (grey) and *E. coli* Δ*clsAybhOymdC* (green) at 18°C experimental temperature (A). Fluorescence recovery curve of NagE (B) and LacY (C) labelled with YFP in *E. coli WT* (grey) and *E. coli* Δ*clsAybhOymdC* (green) at 18°C and 22°C experimental temperature. Curves show averaged fluorescence recovery of minimum 15 different cells out of minimum two independent biological replicates.

4.1.6 Influence of cardiolipin on the motility system of *E. coli*

As already mentioned, soft agar plates are used as assay to examine bacterial growth as well as chemotactic- and motility-dependent effects of for instance mutations, environmental changes and temperature. So far we examined the effect of cardiolipin on the growth of *E. coli* and in more detail for the chemotaxis system by investigating the chemosensing, chemoreceptor clustering as well as the chemoreceptor mobility in the cytoplasmic membrane. Consequently, we continued studying the influence of cardiolipin on the motility system of *E. coli*.

4.1.6.1 Temperature-dependent effect of cardiolipin on flagellar regulation

The already described soft agar experiments (see material and methods, 3.11), performed at different temperatures, revealed that cardiolipin influences the swimming ability of *E. coli*. With increasing temperature from 30°C in four steps to 39°C the diameter of swimming ring for the Tar only *WT* decreases, whereas the swimming ring of the strain lacking cardiolipin increases (Figure 14, B). For the strain with unmodified membrane and expressing Tsr as the only chemoreceptor, the swimming rings become smaller with increasing temperature, and finally at 39°C no motility can be detected. The Tsr-only strain lacking cardiolipin, on the other hand, does still develop clear swimming rings even at high temperature. However, the diameters are decreasing with increasing temperatures (Figure 14, D). With these findings, we assume cardiolipin enhances the motility of *E. coli* more for the Tar receptor than for Tsr receptor. We assume this, as we cannot entirely assign the obtained results from the soft agar plates to the already presented growth or chemotaxis system-dependent results.

For further investigations of motility gene expression, we made use of plasmid-based fluorescent promoter reports (*277*). These low-copy plasmid reporters have a full-length copy of the promoter of interest fused to the green fluorescent protein (GFP). These constructs enable measurements of gene activity in living cells. We used the promoter-reporter for *fliC* (P_{fliC}) representing class 3 motility genes, and the *fliA* promoter-reporter (P_{fliA}) purporting to depict class 2 flagellar genes. We analysed the promoter activity in living cells, sampled from either soft agar plates or liquid cultures at 30°C and 39°C, using a flow-cytometer based analysis. A detailed working protocol is described in material and method, 3.13. For the following experiments, we used Tar as chemoreceptor expressed from plasmid and the indicated promoter-reporter in the receptorless strain with or without cardiolipin. In planktonic culture, the expression of *fliC* at 30°C was higher for the *WT* compared to the cardiolipin lacking strain. At 39°C, the *fliC* expression of the *WT* was off, and the expression of *fliC* in the strain lacking cardiolipin was still slightly turned on (Figure 23, A. We went one step higher in the hierarchy on motility genes in *E. coli* by examining the expression levels of *fliA* as example for

class 2 genes. When grown in liquid medium at 30°C the promoter expression of *fliA* is lowered by half for the strain lacking cardiolipin. With an increase to 39°C growth temperature, the *fliA* expression of the *WT* increases, whereas the *fliA* expression in the *CL*- strain decreases compared to 30°C (Figure 23, B). For examining motility gene expression of cells grown on soft-agar plates, we sampled cells from the outer edge of the precisely formed spreading ring, as these cells have the highest motility in the population. The evaluation of *fliC* expression in cells sampled from soft agar plates showed a marginally higher expression of *fliC* in the *CL*- strain compared to the *WT*. The macroscopic observations of the soft agar plates at 39°C, where the swimming ring for the strain lacking cardiolipin was noticeably more prominent than the *WT* ones, could be confirmed by flow cytometry results. The *fliC* expression at 39°C in the *WT* is off, whereas in the *CL*- strain the expression of flagellin is still turned on (Figure 23, C). When grown on soft agar plates (Figure 23, D) the ratios of *fliA* expression at 30°C correspond to the one in planktonic culture. Interestingly, the *fliA* expression on soft agar plates at 39°C differs from expression in liquid culture. Here the expression level of *fliA* in the cardiolipin lacking strain is comparable to the expression in *WT*, even though the distribution is broader.

At 39°C FliA is turned on and FliC expression is turned off in the *WT*, independent of growth condition. The FliC and FliA expression in the cardiolipin deficient strain is turned off in liquid media and turned on when grown on soft agar plates, corresponding to the formed swimming ring of the mutant. We expect that changes of the membrane composition caused by the deletion of cardiolipin influence the expression of motility genes of *E. coli* at two levels, the FliA independent regulation of FliC and the regulation of FliA.

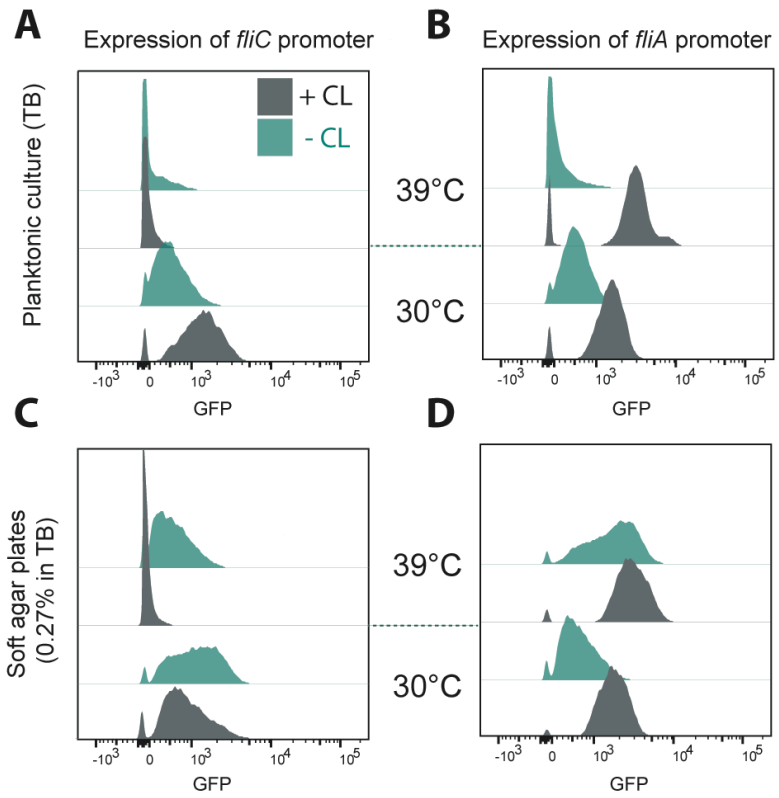

Figure 23. Expression of motility genes *fliC* and *fliA*. Flow cytometry measurements of *fliC* (A) and *fliA* (B) promoter reporters labelled with GFP in *E. coli WT* (grey) and *E. coli* Δ*clsAybhOymdC* (green) sampled planktonic culture grown at 30°C and 39°C. Flow cytometry measurements of *fliC* (C) and *fliA* (D) promoter reporters labelled with GFP in *E. coli WT* (grey) and *E. coli* Δ*clsAybhOymdC* (green) sampled from soft agar plates grown at 30°C and 39°C. Experiments were performed as biological triplicates.

4.1.6.2 FliA expression reverts cardiolipin- and temperature-dependent regulation of the motility system

In planktonic culture, at high temperature (39°C) the expression of Flagellin in *WT* is turned off, whereas *fliA* is still actively expressed. When lacking cardiolipin, the cells switch off the expression of *fliA*. When grown on soft agar plates, the cardiolipin deficient cells have *fliA*, as well as *fliC* expression, turned on, the *WT* cells on the other hand only express *fliA* similar to liquid growth conditions. To further examine the reason for the differences in *fliA* expression and to examine whether we can turn on *fliC* expression in the cardiolipin-lacking cells in liquid culture (as seen on soft agar plates), we examined the expression of *fliA* and *fliC* with overexpression of FliA. Therefore, we expressed *fliA* from a plasmid in the strains growing in liquid culture and the subsequent investigation of *fliC* and *fliA*

expression by making use of the GFP promoter reporters. With additional FliA expression, the *WT*, as well as the cardiolipin lacking strain, show a higher *fliC* promoter expression at both temperatures (Figure 24, A). The expression of *fliC* in the *WT* at 30°C is bimodal, meaning half the population showed high *fliC* expression and the other half showed comparably lower expression, similar result is observed at 39°C. For the cardiolipin-deficient strain we observe the *fliC* expression at 30°C, but furthermore, we detected the expression of *fliC* at 39°C, contrary to the cardiolipin lacking strain without additional FliA expression from Figure 23 A. As expected, with the supplementary expression of FliA, the detected expression of the *fliA* promoter was noticeably increased for the cells grown at 30°C and 39°C (Figure 24, B). For the *WT* at 39°C with additional FliA expression from plasmid, the detected high but widely distributed *fliA* promoter expression is a sign for a caused dysregulation but not further negatively influencing the outcome of the experiments. We could show, that with an expression of FliA, the motility gene expression, as seen for cardiolipin lacking cells growing on soft agar plates, can also be achieved in liquid culture. With this, we expect, that cardiolipin deficiency induces the expression of FliA on half-solid media, which most likely determines the expression of flagellin leading to motile cells at high temperature.

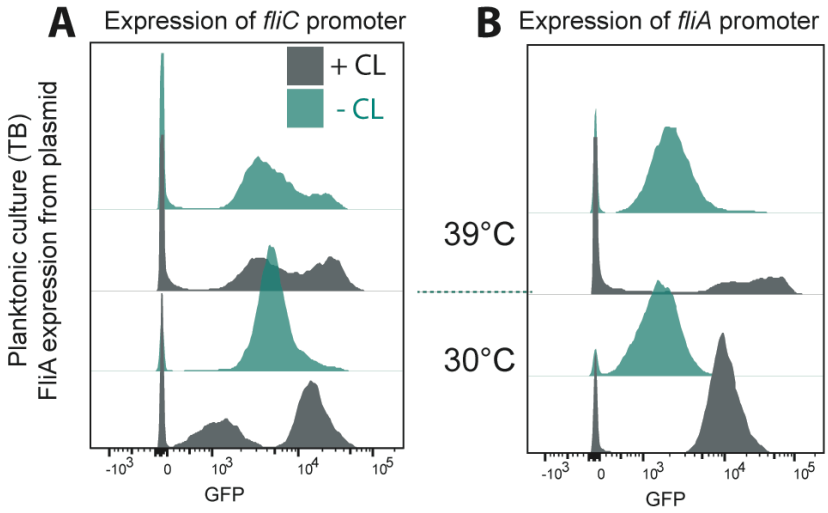

Figure 24. Expression of motility genes *fliC* and *fliA* promoters with additional FliA expression. Flow cytometry measurements of *fliC* (A) and *fliA* (B) promoter reporters labelled with GFP in *E. coli WT* (grey) and *E. coli* Δ*clsAybhOymdC* (green) sampled planktonic culture grown at 30°C and 39°C with additional FliA expression from plasmid. Measurements were performed twice.

4.2 Influence of other membrane alterations on the physiology of *E. coli*

In addition to the effect of cardiolipin depletion in the cytoplasmic membrane on the growth and motility system and chemotaxis system of *E. coli*, we were also interested in the effects of further membrane alterations. We wanted to achieve these alterations by individually raising the level of certain phospholipids (e.g. PE, PG, CL), through overexpression of the respective synthases. Comparable with the publication by Okada *et al*. (*278*) we used phospholipid synthase genes from *B. subtilis* to overexpress them in *E. coli*. With this we wanted to avoid a possible self-regulatory process of *E. coli.* It is possible to overexpress the *E. coli*'s own synthase genes, leading to a higher protein level, however without achieving a difference in phospholipid composition of the membrane (*278*). The two-phospholipid pathways from *E. coli* and *B. subtilis* are highly similar (Supplementary Figure S3) (*279*). There are only minor differences, such as the PssA gene (PE synthesis) of *E. coli* is a type I Pss, whereas the *B. subtilis* PssA synthase is type II Pss (*278, 280*), or the additional existence of the *Bacillus* typical phospholipid LPG, a derivative of PG, synthesised by phosphatidylglycerol lysyltransferase, MprF (*281*).

The genes of interest belonging to the phospholipid pathway of *B. subtilis* (*cdsA, psd, pssA, pgsA, clsA, ywiE, ywjE, mprF*), were cloned into the salicylate inducible vector pKG110. With this we can tightly titrate the expression levels of the foreign phospholipid synthase genes to evaluate the effects of changing membrane alterations. For this project, we chose *E. coli* W3110 rpoS+ as working strain. This strain is a derivative of *E. coli* W3110, with functional *rpoS* (*282*). RpoS is a RNA polymerase sigma factor, constituting the master transcriptional regulator of general stress and stationary phase response (*283, 284*). Most of the following experiments were performed together with the supervised bachelor student, Sara Jakob.

4.2.1 Effect of membrane alterations on the growth of *E. coli*

The fluidity of the cytoplasmic membrane can be influenced not only by membrane alterations, caused overexpression of phospholipid synthases, but also by changing temperatures. High temperatures are known to enhance the fluidity of the cell membrane (*285*), and with this also, the permeability increases. We performed growth experiments to examine the effect of cell membrane alterations in combination with raising temperatures on the growth of *E. coli*. The strains were grown in TB with indicated induction levels (0 µM, 1 µM and 10 µM salicylate) and respective antibiotics, at three different growth temperatures (30°C, 37°C and 42°C). The *E. coli* W3110 rpoS+ strain transformed with the empty pKG110 vector serves as a negative control (*WT*/*WT*-pKG). At 30°C most of the tested strains didn't show any growth issues upon induction of the respective synthases (see Supplementary Figure S4, A). Only the strain expressing PgsA shows growth abnormalities with low and high induction, but not without induction (Figure 25, A). With 1 µM salicylate, the PgsA strain has an elongated lag phase as well as the stationary phase at OD_{600} = 0.35, lower compared to the *WT*-pKG (OD_{600} = 0.45). With higher induction (10 µM salicylate) the strain is unable to grow at 30°C. At 37°C, the optimal growth temperature for *E. coli*, the growth of the PgsA strain is not affected by low induction (1 µM salicylate). With high induction (10 µM salicylate) of PgsA however, the lag phase is elongated but the stationary phase OD_{600} does not differ from the *WT*-pKG (Figure 25, B). Again, the other strains showed no notable differences in growth upon phospholipid synthase induction at this temperature (Supplementary Figure S4, B). At 42°C, only the PgsA expressing strain showed growth deficits with high induction of the PG synthase (Figure 25, C). Here the lag phase is elongated up to seven hours, but the stationary phase level aligns to the *WT*-pKG. As already shown for the lower temperatures, the other strains seem to not be influenced by phospholipid synthase overexpression and the resulting membrane alterations even at high temperature (Supplementary Figure S4, C).

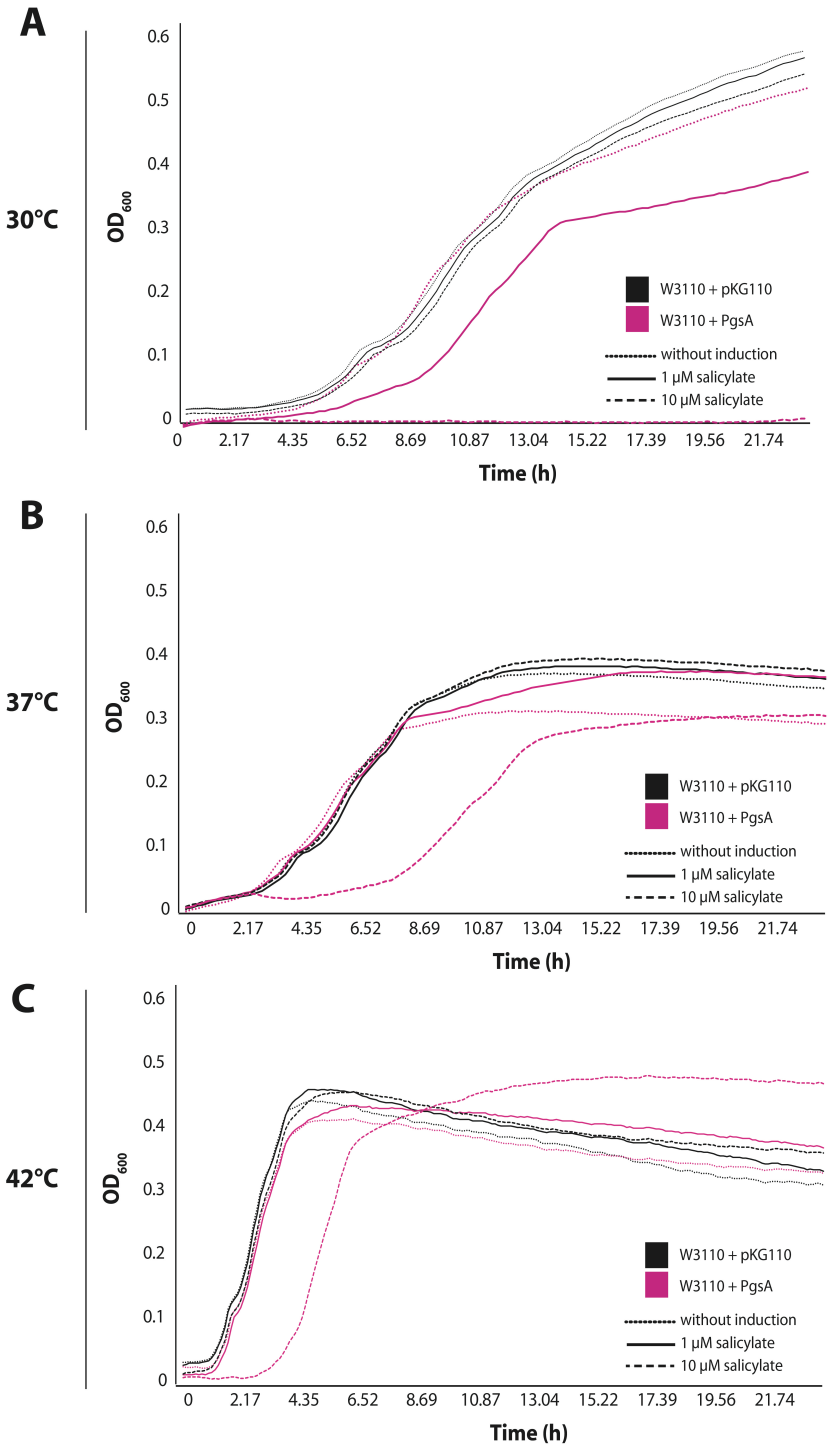

Figure 25. Growth of *E. coli* W3110 *rpos*+ with overexpression of PgsA. Exemplary growth curves of *E. coli* W3110 *rpos*+ with (pink) and without (black) overexpression of PgsA (1 µM salicylate – solid line; 10 µM salicylate – dashed line; without induction – dotted line) at 30°C (A), 37°C (B) and 42°C (C). Growth experiments were repeated as biological triplicates.

4.2.2 Effect of membrane alterations on the *E. coli* behavior on swimming plates

In order to examine how varying membrane compositions can affect bacterial growth, motility and the chemotaxis system, we accomplished soft agar assays (see Material and Methods, 3.11). As membrane fluidity can be influenced by phospholipid composition and by temperature, the experiments were again performed at different growth temperatures (30°C, 34°C, 37°C, 39°C, 40.5°C). The results were evaluated by correlating the diameter of the formed swimming rings towards the *WT*-pKG and additionally by comparing different induction steps (Figure 26). Most drastic effects could be detected upon expression of PgsA. At all tested temperatures, the swimming diameter of the PgsA expressing strain was smaller than the *WT* one. At 30°C the diameter is half the size of the *WT* one, corresponding to the growth experiments (Results, 4.2.1). With rising temperature, the size of swimming rings formed by the PgsA expression strain in comparison to the *WT* decreases (Figure 26). At temperatures from 30°C to 37°C, no other synthases showed noteworthy effects on the behaviour of the cells on soft agar plates. At 39°C and 40.5°C, we could detect a decreased swimming ring for the MprF expression strain. Here, the diameter of the swimming ring is around 30% smaller than the *WT* one and the MprF expressing strain without chemical induction (Figure 26, D, E). Furthermore, at 40.5°C, we could see a striking effect of CdsA overexpression on the behavior on the soft agar plates. However, already the uninduced strain is affected here, what could be caused by a marginally leaking promoter of the plasmid (Figure 26, E).
We expect that overexpression of PgsA impairs the growth of *E. coli*, either by growth inhibition or more likely by deteriorating the cell separation, leading to a smaller swimming rings on soft agar plates.

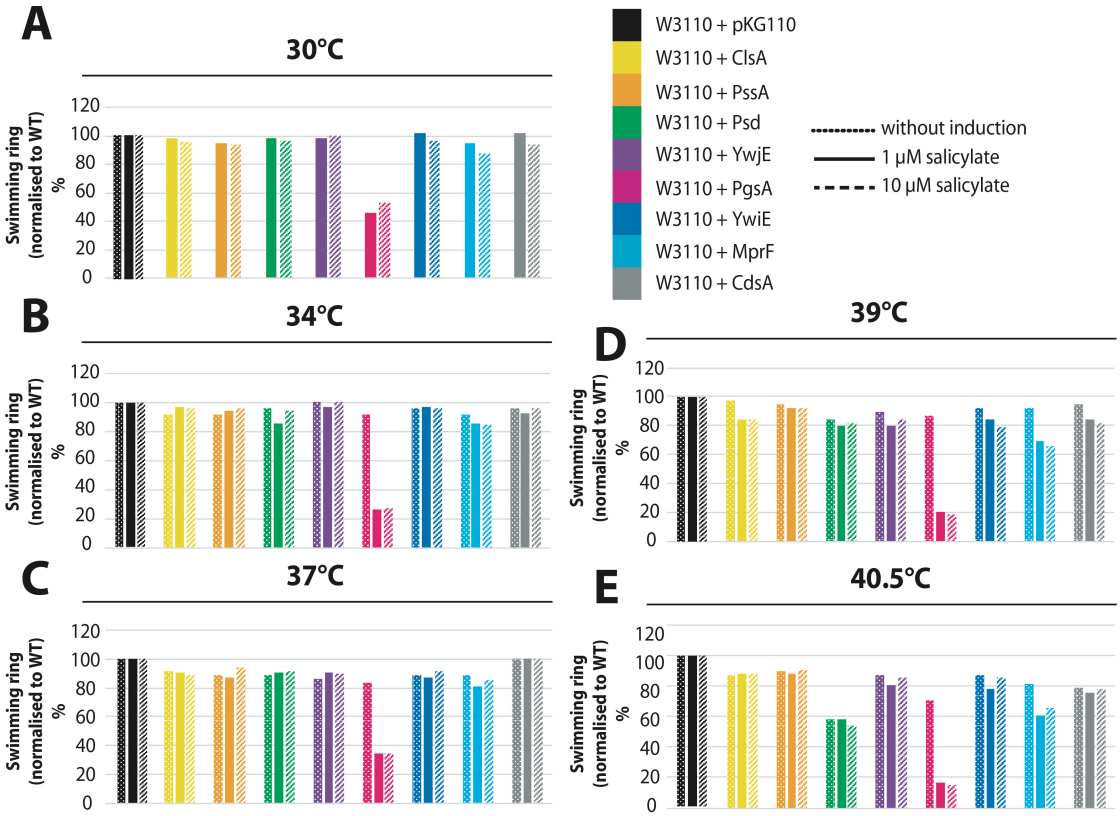

Figure 26. Soft agar assays of *E. coli* W3110 *rpos*+ with overexpression of various phospholipid synthases. Exemplar image of a soft agar plate grown at 37°C with 10 µM salicylate induction of phospholipid synthases indicated by colour (A). Evaluation of soft agar assays at 30°C (A), 34°C (B), 37°C (C), 39°C (D) and 40.5°C (E) without induction (dotted bar), with 10 µM salicylate (filled bar) and with 20 µM salicylate (dashed bar) of *E. coli* W3110 *rpos*+ expressing several phospholipid synthases indicated by colour (B). WT with empty expression vector: black, ClsA: yellow, PssA: orange, Psd: green, YwjE: purple, PgsA: pink, YwiE: blue, MprF: turquois, Cdsa: grey. One biological replicate.

4.2.3 Influence of membrane alterations on the chemoreceptor clustering of *E. coli*

E. coli chemoreceptors are anchored with transmembrane helices in the cytoplasmic membrane; hence we are investigating the effect of membrane alterations on the chemotaxis system, especially the chemoreceptor clustering. We performed cluster analysis of the strains of interest (see material and methods, 3.12.1), using CheY-YFP and CheW-CFP for cluster detection. Results and exemplary microscopic images are shown in Figure 27. For the W3110 *rpoS*+ strain with empty pKG110 plasmid (Figure 27, A), referred to as '*WT*', we detected roughly 1.8 chemoreceptor clusters per cell (Figure 27, C). Only the plasmid-

based overexpression of PgsA showed a difference in cluster numbers, compared to *WT.* The overexpression of PgsA increases the number of chemoreceptor clusters by 3-fold, to 5.4 clusters per cell (Figure 27, C). When evaluating the microscopic images of this strain we noticed that the strain is drastically elongated (Figure 27, B). This finding could explain the increased number of chemoreceptor clusters per cell. It seems that the overexpression of PgsA and the resulting increase of PG within the cytoplasmic membrane leads to an elongation of the cells, probably due to a caused impact on the cell division machinery.

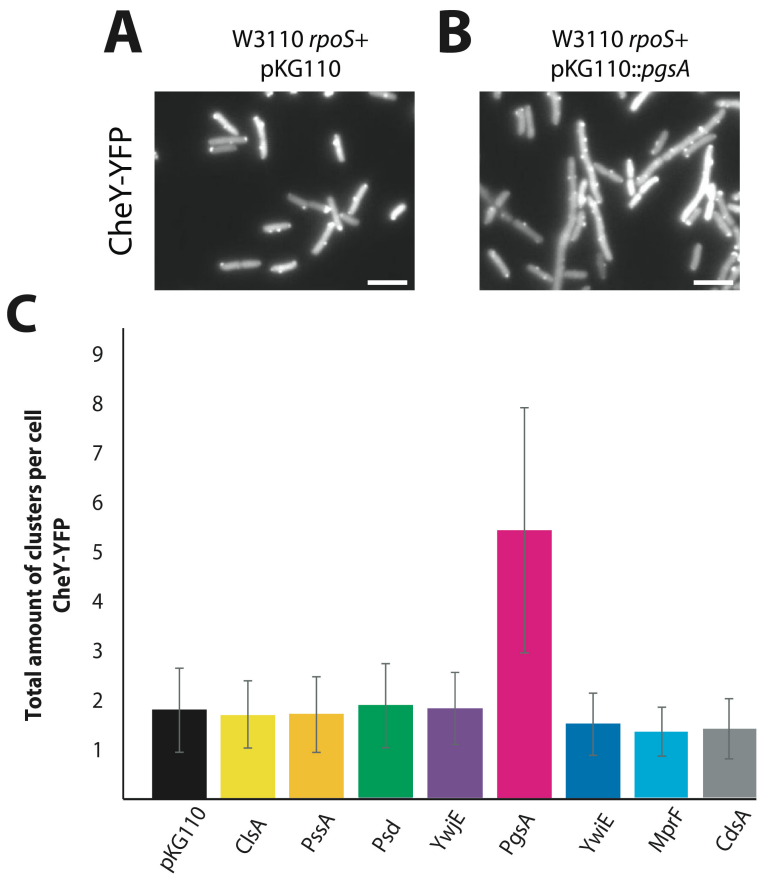

Figure 27. Chemoreceptor clustering in *E. coli* W3110 *rpos+* with overexpression of phospholipid synthases. Fluorescense images of W3110 *rpos+* pKG110 CheY-YFP (A), W3110 *rpos+* pKG110:*pgsA* CheY-YFP (B). Manual analysis of chemoreceptor clusters tagged with CheY-YFP (C) in *E. coli* W3110 *rpos+* expressing several phospholipid synthases indicated by colour. WT with empty expression vector pKG110: black, ClsA: yellow, PssA: orange, Psd: green, YwjE: purple, PgsA: pink, YwiE: blue, MprF: turquois, Cdsa: grey. Error bars indicate the standard error of the mean. Scale bar indicates 2µm.

4.2.4 Membrane alteration affecting the motility system of *E. coli*

Evaluating the promoter activity of a certain gene of interest, can give information like when, how often and how much the gene is being expressed, under certain conditions (*285*). We analysed the activity of motility genes in W3110 *rpoS*+ and how their expression is influenced by membrane alterations. Therefore, we used GFP labelled promoter reporters and analysed the expression with flow cytometry. The experiments were performed as described before (see Material and Methods, 3.13). We focused on the expression of FliC in planktonic culture, on soft agar plates at low and high temperature, and on FliA expression in planktonic culture. *fliC* encodes for flagellin and forms the flagella filament (*286*). The expression of FliC, a representor of Class III motility genes, is controlled by FliA. The results are shown as histograms in Figure 28. We first examined the expression of FliC in our strains overexpressing ClsA, YwiE, YwjE, Psd, PssA, PgsA, MprF and CdsA (marked by colours) in liquid culture at 30°C and 40.5°C (Figure 28, A). Both at low and at high temperatures, the PgsA expression strain was the only one to show a *fliC* expression phenotype that differs distinctly from the *WT*. Expression of PgsA causes a bistable distribution of *fliC* expression. This means the culture is split in two populations with different expression levels of *fliC*. One population has the same expression values as the *WT*, the other population is expressing drastically more *fliC*. At 40.5°C virtually all cells have an increased *fliC* expression. Additionally, to observations of *fliC* expression in liquid culture, we were also interested in the expression of flagellin when the cells are grown on soft agar plates. At 30°C, the *fliC* expression of all tested overexpression strains, including PgsA overexpressing strain, does not vary from the *WT*. This result is surprising, as the swimming ring on soft agar of the PgsA strain is smaller than the *WT* one, which is why generally a lower flagellin expression would be expected (Figure 28, A). When grown on soft agar at 40.5°C (Figure 28, D), the overexpression of PgsA lowers the expression of *fliC*, what matches the drastically smaller swimming ring formed by this strain on soft agar plates. All other strains showed again no difference in *fliC* expression. We continued analysing the effect of membrane alterations on the expression of *fliA*, which is encoding for a minor sigma factor (σ28) and representing class II of the

flagella gene regulation machinery (*287*). Again, we could only detect a change in *fliA* expression with plasmid based expression of PgsA (Figure 28, B). At 30°C, the PgsA overexpression strain shows a bistable expression of *fliA*. With increasing induction of PgsA, the expression of *fliA* drops. *FliA* expression corresponds to the bistable *fliC* expression as described for planktonic culture. The expression of *fliA* at 40.5°C shows no effect of phospholipid synthase expression, contrary to the *fliC* expression at this temperature (Figure 28, A, B).
We expect the effect seen with PgsA overexpression is not exclusively relatable to motility but also affected by the already mentioned defects in cell division, as we detected drastically elongated cells when overexpressing PgsA (see 4.2.3). The temperature-dependent expression of motility genes when expressing PgsA seems to be an additional effect supplementary to the defects caused in cell separation.

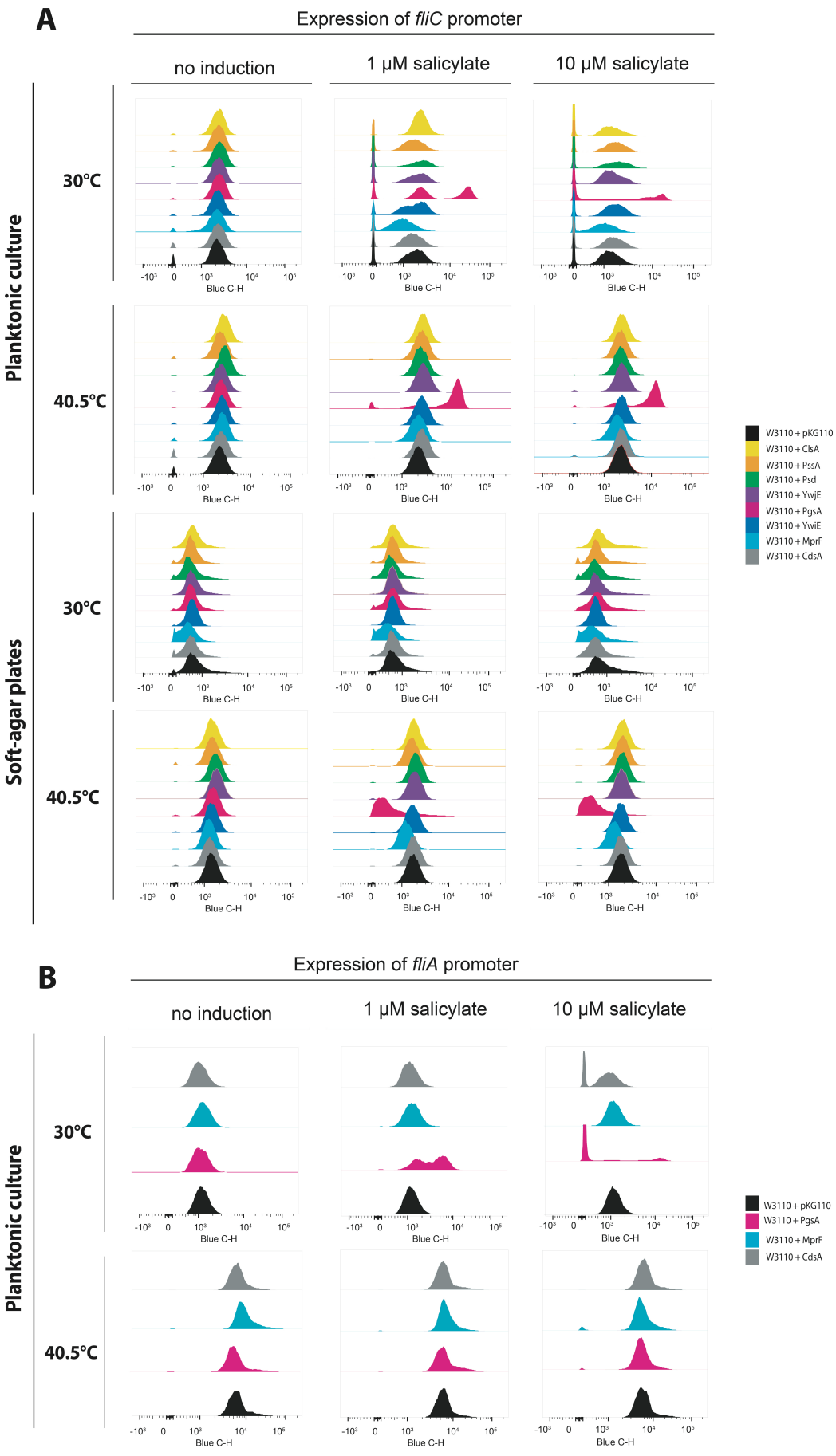
A
Expression of fliC promoter
no induction
1 µM salicylate
10 µM salicylate
Planktonic culture
30°C
40.5°C
Soft-agar plates
30°C
40.5°C
Blue C-H
W3110 + pKG110
W3110 + ClsA
W3110 + PssA
W3110 + Psd
W3110 + YwjE
W3110 + PgsA
W3110 + YwiE
W3110 + MprF
W3110 + CdsA
B
Expression of fliA promoter
no induction
1 µM salicylate
10 µM salicylate
Planktonic culture
30°C
40.5°C
Blue C-H
W3110 + pKG110
W3110 + PgsA
W3110 + MprF
W3110 + CdsA

Figure 28. Expression of motility genes *fliC* and *fliA* in *E. coli* W3110 *rpos+* with overexpression of phospholipid synthases. Exemplary flow cytometry measurements of *fliC* (A) and *fliA* (B) promoter reporters labelled with GFP in *E. coli* W3110 *rpos+* with (10 µM salicylate, 20 µM salicylate) and without additional expression of several phospholipid synthases labelled by colour sampled from liquid culture or soft agar plates at 30°C and 39°C. *WT* with empty expression vector: black, ClsA: yellow, PssA: orange, Psd: green, YwjE: purple, PgsA: pink, YwiE: blue, MprF: turquois, Cdsa: grey. Experiments were performed as biological triplicates.

4.3 Changes in membrane composition on *B. subtilis*

We were not only interested in the effect of membrane alterations in the gram-negative *E. coli*, but also on the impact of membrane alterations on the gram-positive model organism *B. subtilis*. Whereas complete knockouts of most phospholipid synthases would be lethal for *E. coli* and is only possible with the utilisation of e.g. temperature inducible promoters, the knockouts of most phospholipid synthases in *B. subtilis* are feasible. As mentioned earlier (see introduction 1.1.2), the phospholipid pathway of *B. subtilis* is quite similar to the one of *E. coli*. The phospholipid pathways of both organisms are shown in Supplementary Figure S3. CdsA, the phosphatidate cytidylyltransferase, constitutes the pathway begin and is synthesizing CDP-diacylglycerol. Two genes are involved in the synthesis of PE, *pssA* and *psd.* PgsA is responsible for synthesising PG, and *clsA* (*ywnE*), *ywiE* and *ywjE* are involved in cardiolipin synthesis. The additional phospholipid LPG, is synthesised by MprF. The knockouts of the respective genes were achieved by long-flanking homology cloning. With this the genes of interest are disrupted by replacement with a marker cassette integrated into the genome via long flanking homological regions (*288, 289*).

4.3.1 Effect of membrane alterations on the growth and morphology of *B. subtilis*

Bacterial growth, arising through binary fission, is a complex process which involves numerous catabolic and anabolic reactions. Further, the growth is affected by various external impingements e.g. temperature and nutrient supply. To evaluate the effect of phospholipid depletions by synthase knockout, on the growth behaviour of *B. subtilis*, we performed plate reader experiments as described in detail in chapter 3.10.1 The results are shown in Figure 29, A. The *B. subtilis* Δ*pssA* strain shows a slightly slower growth in the lag and exponential phase, reaching the stationary phase at the same level (OD_{600}=0.75) than the *WT*. For the other knockout strains, we could not detect a severe impact of phospholipid synthases on the growth behaviour of *B. subtilis*. The growth phases

(lag, exponential, stationary and death phase) of the knockout strains does not show drastic differences compared to the displayed *WT* curve. The death phase, characterized by a slow decrease in OD, is initiated later for the strains with the respective knockout Δ*pssA*, Δ*mprF,* Δ*ywnEywiE* and Δ*ywnEywjE*. Additionally, to the growth experiments we performed a morphological analysis of the cells via FACS. For the deletion of Psd and ClsA we could detect notably changes in cell morphology and population distribution. For a mid-exponential *WT* culture, grown in TB at 34°C, we could detect roughly 10% of elongated cells (see Figure 29, B). A deletion of Psd causes an increase of elongated cells by 10%. With a knockout of ClsA the elongated cells make half of the population.

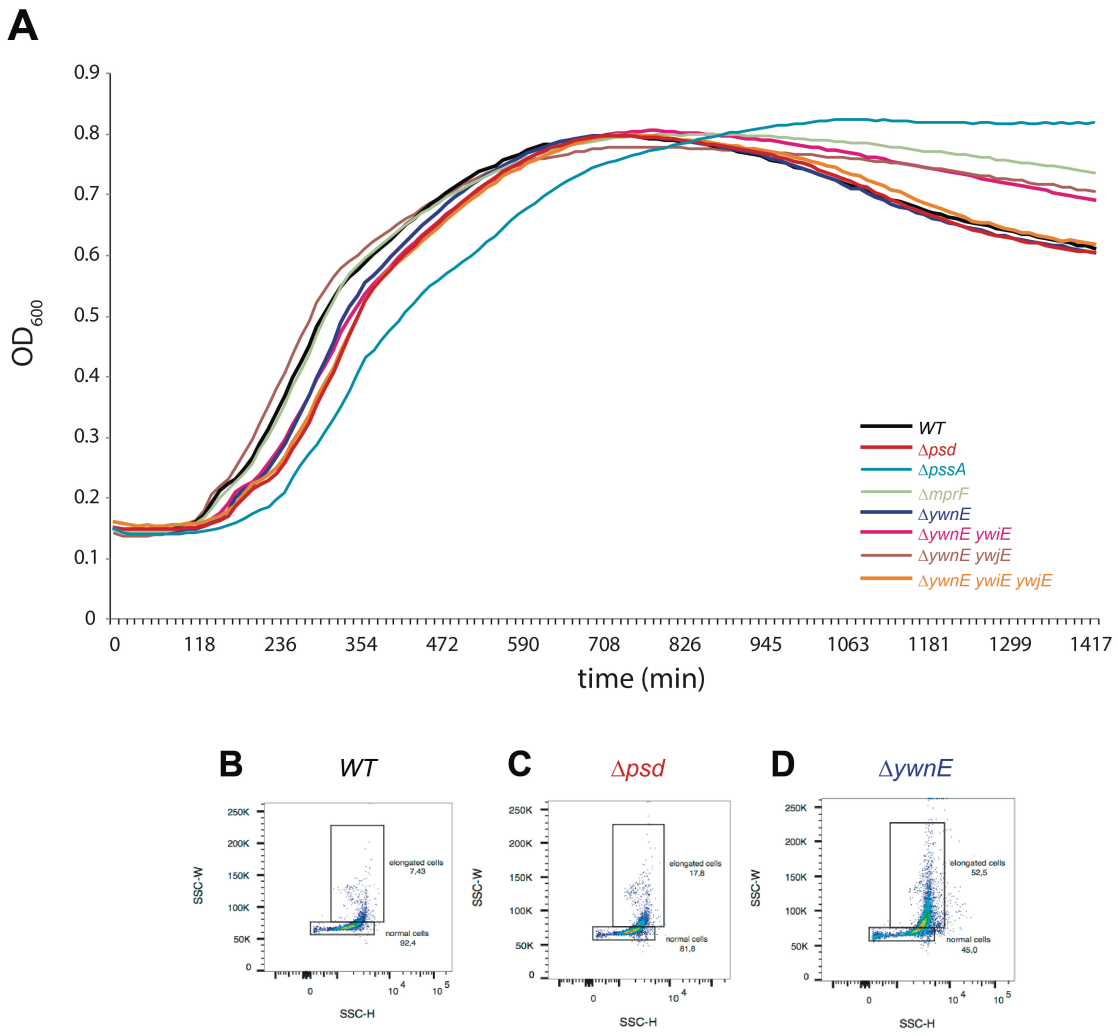

Figure 29. Growth and morphology of *B. subtilis* W168 with membrane alterations. Growth curves of *B. subtilis* W168 with deletions of phospholipid synthases, indicated by colour (*WT*: black, Δ*psd*: red, Δ*pssA*: light blue, Δ*mprF*: green, Δ*ywnE*: dark blue, Δ*ywnEywiE*: pink, Δ*ywnEywjE*: brown, Δ*ywnEywiEywjE*: orange) at 34°C in TB (A). Measurements of cell size of *B. subtilis* W168 (B), *B. subtilis* Δpds (C) and *B. subtilis* ΔywnE (D) by flow cytometry. Experiments were performed in at least duplicates.

4.3.2 Membrane alterations influencing the swimming and swarming ability of *B. subtilis*

In order to address the effect of individual phospholipid synthase deletions on the swimming and swarming ability, we performed soft agar assays (see material and methods, 3.11). Therefore, the respective strains were inoculated from saturated O/N culture on TB plates with 0.3% agar (if not indicated differently) for 20 h at 34°C. As already mentioned, soft agar plates reflect the overall effect on motility, the chemosensing and the effect on growth. The diameters of the swimming rings were measured and related to the unmodified W168. The results are presented in Figure 30, A. A reduction of the swimming diameter for all examined strains could be detected. As expected, the most drastic effect could be seen for the receptorless (ΔMCP) strain. As in this strain all chemoreceptors are knocked out, it is chemotacticaly inactive and can serve as negative control in for example soft agar experiments. The modest difference is detectable for the deletion of ClsA (YwnE), the major cardiolipin synthase. Here the strain reaches almost 70% in diameter compared to the *WT*. With deletion of one or two additional cardiolipin synthases, the swimming ring diameter is decreased to 35-40% compared to the *WT*. The diameters of the other tested knockout strains (W168: *Δpsd*, *ΔpssA, ΔmprF, ΔywnEywiE, ΔywnEywjE*) were reduced by about 60% to 65%. The smaller the detected diameter of swimming ring, the less chemotactic active or motile the cells are expected.

We went on testing selected strains not only on their swimming ability but also on the swarming ability. Therefore, we performed soft agar assays as before, but with different agar concentrations and additionally compared the strains to a strain lacking chemoreceptors as negative control. Plates with an agar concentration lower than 0.5% are called swimming plates, as motile cells are able to swim through the formed agar pores creating the detectable ring of colonisation (*266*). Plates with a higher agar concentration are called swarming plates, as the agar concentration blocks the ability of swimming through the pores, therefore the cells are mostly expected to migrate along the agar surface (*290*). The ring diameters were measured and are displayed in Figure 30, B. As

before, the formed rings of the knockout strains are smaller than the *WT* ones. However, the relative difference between the knockouts and the *WT* varies with agar concentration. The detected rings of the *WT* decrease with increasing agar concentration (0.3-0.6%) and increases again at a concentration of 0.7% agar. The same is true for the evaluated knockout strains. We expect, this can be explained by the most effective agar concentrations for swimming (0.3%) and swarming (0.7%). Strikingly, the deletion of Psd, a synthase catalysing PE from the intermediate phosphatidylserine, shows similar behaviour to the receptorless strain. The fact that the disruption of the PE synthesis has a bigger effect than the deletion of *ywnE* is expected, as PE exists in a higher amount in the cell membrane of *B. subtilis*. By virtue of this fact it is surprising, that the difference between the lack of PE and the lack of CL is comparatively small.

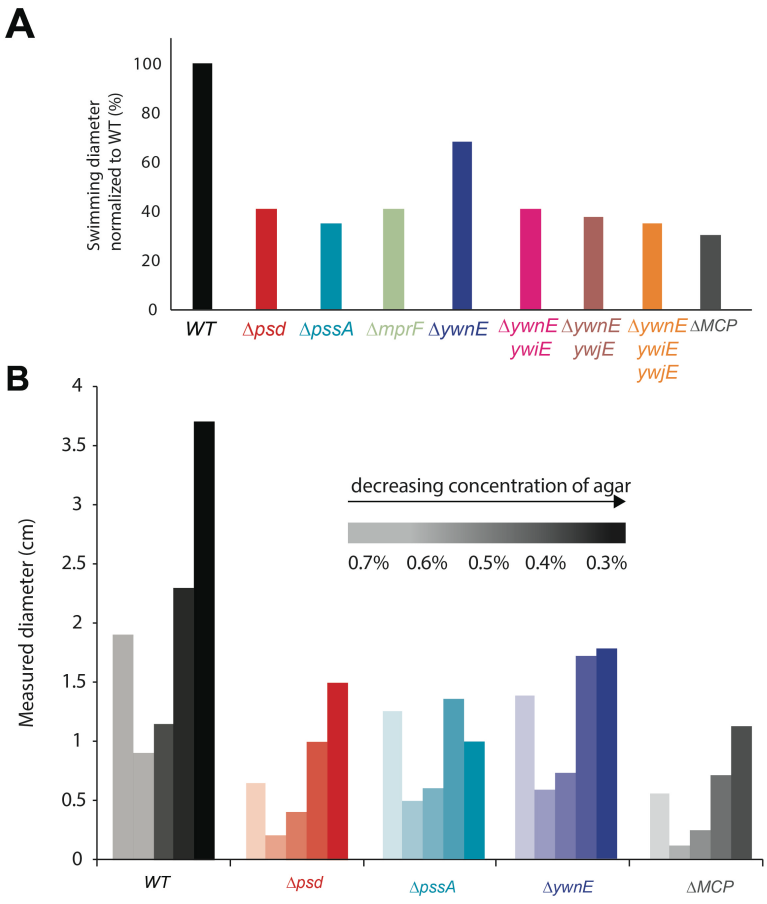

Figure 30. Soft agar assays of *B. subtilis* W168 with membrane alterations. Swimming plates (0.3% agar in TB) of *B. subtilis* W168 with deletions of phospholipid synthases, indicated by colour (*WT*: black, Δ*psd*: red, Δ*pssA*: light blue, Δ*mprF*: green, Δ*ywnE*: dark blue, Δ*ywnEywiE*: pink, Δ*ywnEywjE*: brown, Δ*ywnEywiEywjE*: orange, ΔMCP*: grey*) (A). Swarming plates of *B. subtilis* W168 with indicated agar concentration with knockouts of different phospholipid synthases indicated by colour (*WT*: black, Δ*psd*: red, Δ*pssA*: light blue, Δ*ywnE*: dark blue, ΔMCP: grey) (B). Assays were performed ones.

4.3.3 Effect of membrane alterations on the chemotaxis system of *B. subtilis*

B. subtilis has two soluble chemoreceptors and eight membrane integrated receptors. The fact, that most chemoreceptors of *B. subtilis* are membrane bound, constitutes the reason for our interest in the effect of membrane alteration on the chemotaxis system of the gram-positive microbe. To evaluate the effect of membrane alterations on the chemotaxis system, we made use of fluorescence microscopy to detect chemoreceptor clusters, as well as FRET microscopy to measure the sensitivity towards a certain compound.

4.3.3.1 Chemoreceptor clustering not influenced by membrane alterations

To visualise the chemoreceptor clusters as well as the flagellar motors of *B. subtilis*, we tagged the chemotaxis protein CheY with YFP and the flagellar switch protein FliY with CFP (see material and methods, 3.12.1). With this we wanted to evaluate the effect of membrane alterations on the localization and number of receptor clusters and flagellar motors in *B. subtilis*. Early microscopic results are shown in Figure 31. The *WT* cells show clusters at the poles, as well as along the cell body. In some cases, the loci of CheY and FliY (Figure 31) are located at the same position (red arrows) indicating flagellar motors and receptor clusters, in other cases not (white arrow), what points out receptor clusters. So far our study could not show a detectable difference in case of clustering when evaluating the effects of PE and CL disruptions. Further experiments for evaluation of additional phospholipid synthases as well as more experiments with investigation of other chemotaxis proteins are necessary for further conclusion.

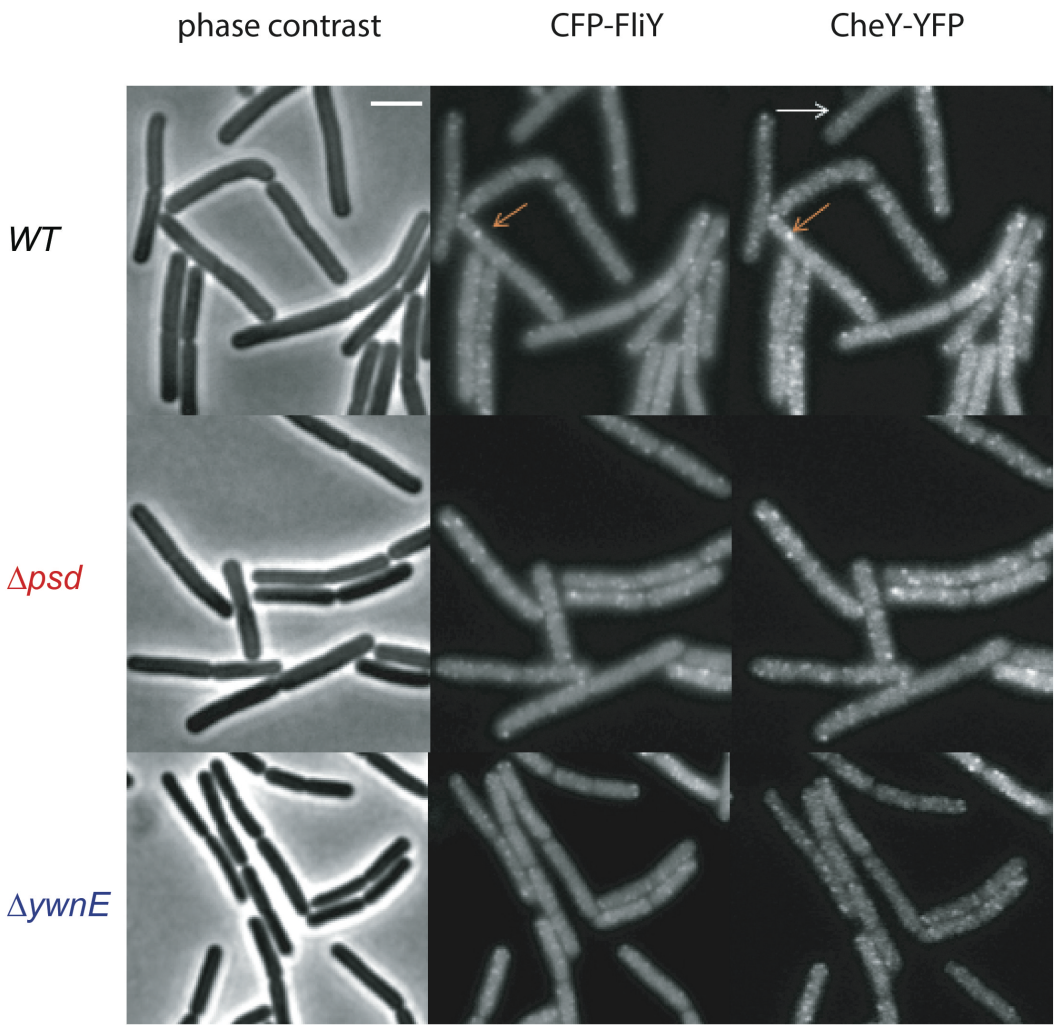

Figure 31. Chemoreceptor clustering and flagella motor localisation in *B. subtilis* W168 with membrane alterations. Exemplary fluorescence images of chemoreceptor clusters labelled with CheY-YFP and flagella motors labelled with CFP-FliY in *B. subtilis* with knockout of Psd and YwnE. Scale bar indicates 2µm.

4.3.3.2 Chemosensing of *B. subtilis* influenced by phospholipid compositions

The just described combination of CheY and FliY tagged with the fluorescence proteins YFP and CFP (Figure 32, A), were also used for preliminary investigations of the chemosensing ability of *B. subtilis* (*291*) using FRET (see material and methods, 3.12.2). We analyzed the response of the *WT* (W168) as positive control, three cardiolipin synthase deletion strains and a PE disruption strain, towards proline, a much-used attractant for *B. subtilis* (*292*). Proline

concentrations from 0.01 µM to 1 mM were used. W168 (Figure 32, D) showed a weak response towards the lowest tested concentration (0.01 µM) and reaches the maximum response amplitude at a concentration of around 30 µM proline. All tested mutants showed a decreased sensitivity towards proline compared to the *WT*. The Psd knockout strain senses proline starting from a concentration of 0.3 µM and reaches the response plateau between 3 µM and 10 µM. Therefore, the amplitudes are smaller than the *WT* ones. The results appear surprising, as in the soft agar plate experiments the Δ*psd* is forming only a slightly larger swimming ring than the chemotactic inactive receptorless strain. The three mutants with various deletions of cardiolipin synthases showed a drastically lower sensitivity towards proline. The tested single knockout of YwnE, and the double knockout strain (Δ*ywnEywiE*) start sensing proline from a concentration of 3 µM on. The plateau is reached already at 30 µM. The amplitudes are drastically reduced with interruption of the cardiolipin pathway. Also, here a different outcome of the FRET experiments for the single knockout of the main cardiolipin synthase compared to the soft-agar experiments need to be discussed. In the FRET experiments the Δ*ywnE* strain seems already drastically influenced by the knockout. The strain is sensing noticeably worse than the *WT* and the Δ*psd* strain, whereas the swimming ring of this strain was the largest of all tested knockout strains, only about 30% reduced compared to the *WT* and almost doubled as large as the formed swimming ring of the Δ*psd* knockout strain.

The complete lack of cardiolipin (Δ*ywnEywiEywjE*) disables *B. subtilis* almost completely from proline sensing. Only at very high ligand concentrations (300 µM and 1 mM) a small response amplitude could be detected. With this, we could show a negative influence of membrane alterations on the chemosensing ability of *B. subtilis*. However, for further confirmation of these preliminary results and for additional investigation of other synthase knockouts more experiments are necessary. So far we could not detect a correlation between the results of the soft-agar plates and the FRET experiment.

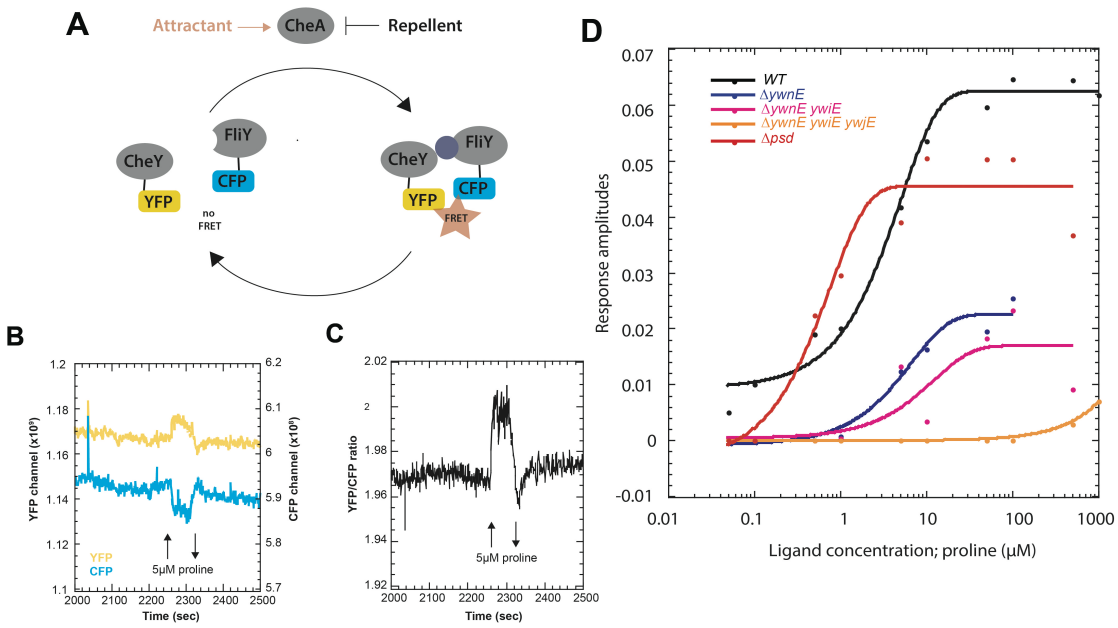

Figure 32. Chemosensing in *B. subtilis* W168 with knockout of several phospholipid synthases. Illustration of the used FRET pair, CheY-YFP and FliY-CFP (A). Exemplary traces of fluorescence intensity of the YFP (yellow) and CFP (cyan) channels (B) for the FRET response observed in (C). Inverse changes in the two channels, characterize specific FRET response. *B. subtilis WT* expressing CheY-YFP and FliY-CFP were stimulated by addition and subsequent removal of 5 μM proline, time points indicated by arrows. Proline (attractant) activates the kinase CheA, leading to an increase in FRET, which is observed as an increase in the YFP/CFP ratio. Conversely, removal of attractants leads to a decrease in the YFP/CFP ratio (C). Response amplitude curves of *B. subtilis 168* (black), *B. subtilis* Δ*psd* (red), *B. subtilis* Δ*ywnE* (dark blue), *B. subtilis* Δ*ywnEywiE* (pink) and *B. subtilis* Δ*ywnEywiEywjE* (orange) for proline sensing measured by FRET (D). Experiments were performed ones.

5 DISCUSSION

The membrane of gram-negative bacteria (e.g. *E. coli*) is characterized by two phospholipid bilayers (inner and outer membrane) separated by a periplasmic space. The inner cytoplasmic membrane of *E. coli* consists mainly of phosphatidylglycerol, phosphatidylethanolamine and cardiolipin and serves as crucial biochemical organelle of the cells (see 1.1.1).

The anionic phospholipid cardiolipin, representing the smallest proportion of the cytoplasmic lipid bilayer, is expected to be mostly found over all domains of life in energy transducing membranes (e.g. mitochondria) (*55, 293*). The large phospholipid is composed of a relatively small hydroxyl head group bound to two long diacylphosphatidyl moieties, what classifies the lipid as 'high curvature lipid'. This structural property induces highly negative curvature in the phospholipid bilayer. Thermodynamic models of the inner membrane organization of bacterial cells indicates that with thermal fluctuations, domains of high-curvature lipids might localize to the cell poles by responding to the curvature of the cell membrane that is not sensed by individual lipid molecules. In parts, this aggregation of cardiolipin is driven by short-range interactions between the lipids. Two constitutive facts are important for the elastic energy of a membrane, the pinning potential and the bending energy. The cell wall is pinning the cytoplasmic membrane, what results in a formation stable finite-sized clusters of high-intrinsic-curvature lipids like cardiolipin. This physical property facilitates the essential formation of cardiolipin membrane domains (*294*), with subsequent targeting to the cell poles. Also, cardiolipin is known for the tendency to disturb the bilayered lamellar phases (*295, 296*).

As the understanding of the physiological role of cardiolipin in bacteria is emerging, various different influences regarding cardiolipin are more and more in the center of interest. Interactions between cardiolipin and aquaporins, the respiratory complex, cytoplasmic DNA replication proteins (DnaA) and cell division proteins (MinD, FtsA, FtsZ) have already been identified (*297*). DnaA activates the initiation of DNA replication in bacteria. The ATP binding of the cytoplasmic DnaA protein is essential for the replication initiation of plasmids carrying the unique chromosomal origin (oriC) of *E. coli*. When ADP is bound to

that site, the DnaA protein is inactive. Cardiolipin is expected to displace the bound nucleotide in the presence of components reconstituting the replication, this fully reactivates the inert of ADP of DnaA (*298*). Certain cell division proteins are thought to interact directly with the membrane phospholipids through specific amphipathic motifs enriched in amino acids with basic sidechains, what confers the preference for anionic lipids (*96, 299*). Additionally, in vitro studies demonstrated a high affinity of these proteins for anionic phospholipids, e.g. cardiolipin (*298, 300*). Besides, cardiolipin is known for its ability to form strong interactions with further membrane proteins. Cardiolipin associates with the SecYEG translocon that mediates the transport or the integration of newly synthesized polypeptides across or into the cytoplasmic membrane (*301*). The lipid stabilises the dimer, creates with this a high binding-affinity for the SecA ATPase and stimulates ATP hydrolysis (*302*). Further the localisation at the poles and the osmosensing of the transporter ProP is dependent on and modulated by cardiolipin (*303*).

Even though cardiolipin is present in most forms of life, the cardiolipin metabolism differs between the species. In mitochondria, the level of cardiolipin remains constant, whereas in bacteria (e.g. *E. coli*) the level changes dependent on the physiological circumstances (*304*). *E. coli* has three cardiolipin synthases: ClsA, a phospholipase D enzyme is catalyzing the transfer of a phosphatidyl moiety between two phosphatidylglycerol molecules (PG) to form cardiolipin (*62, 305*); YbhO acting similarly to ClsA (*64*); YmdC catalyzing the synthesis of cardiolipin from PG and PE (*306*).

This work resulted in several important findings related to interactions between the cytoplasmic membrane and membrane associated proteins, particularly in relation to bacterial chemoreceptors.

5.1 Cardiolipin is dispensable for the general growth of *E. coli*

Each cardiolipin synthase contributes differently to the cardiolipin formation, dependent on the growth phase and growth conditions (*306*). Also the cardiolipin fatty acid composition fluctuates during culture growth and is also dependent on environmental influences (*307*). ClsA, the main cardiolipin synthase is expected

to be the only one active synthase while logarithmic growth phase. With reaching stationary phase the level of cardiolipin increases, due to a up to 10-fold increase in activity of ClsA (*59*). The other two synthases are expected to be only active with reaching stationary growth phase (*306*).

We deleted all three synthases in a chemoreceptorless strain and evaluated the effect of cardiolipin deficiency on the growth behavior of *E. coli*. Irrespective of growth temperature the strain lacking cardiolipin reached a higher OD_{600} in stationary phase compared to the respective *WT* (see 4.1.2.1). This difference could be due to saving of energy and resources due to the prevention of cardiolipin production. The fact that ClsA activity is the highest at early stationary growth phase and the increase in cardiolipin membrane content at this growth phase supports this idea (*59*). Only with drastic elongation of the stationary phase the synthase activity of ClsA drops about half compared to the exponential phase activity (*305*).

Additionally to the stationary-phase growth benefits of the cardiolipin-lacking mutant, we could detect a higher viability of this strain. At the different tested growth temperatures, the count of viable colony-forming-units (CFU) of the cardiolipin deficient strain was higher after 24h and also after 96h of growth (see 4.1.2.4). The CFU counting indicates more or less impact of cardiolipin deletion on the growth and survival of *E. coli* dependent on the evaluated temperature. In general, the longer the cells are exposed to high temperatures (42°C, 96h) the less cells are surviving, this is true for the WT as well as the cardiolipin lacking strain. Whereas at the lower temperatures (30°C and 34°C) the difference in CFU, between the CL- and WT strains is significantly larger than the difference in the growth curves (see Figure 8), at higher temperature the difference in CFU values is smaller than seen in the growth curves. Whereas OD measurements indicate the percent of transmitted light through a sample and cannot distinguish between living and dead cells, the CFU evaluation gives the number of cells able to divide, at indicated time points. Our results display a larger difference in stationary phase survival in dependence of cardiolipin, of minimum doubled the CFUs for the cardiolipin-lacking strain compared to the *WT* at lower temperatures. The difference in measured stationary phase OD of the growth experiments seems smaller. This indicates more cells are able to divide and form colonies on the

plates, which means cells lacking cardiolipin have a higher survival rate especially at lower temperatures (30°C, 34°C).

Comparing the CFU examinations and the growth experiments at 37°C, 39°C and 42°C this ratio of surviving cells is dropping. The CFU values of the cardiolipin deficient strain converge to those of the *WT*. Most likely the absence of cardiolipin is not advantageous for cell proliferation at higher temperatures anymore. The fatty acid composition of cell membrane built-in cardiolipin is changing with addition of salt or sucrose to the growth media by increasing cyclopropane fatty acids (*307*). Assuredly, we could not detect a clear effect of cardiolipin on the growth of *E. coli* in salt or sucrose enriched media (4.1.2.2). Our results suggest a dispensability of cardiolipin for the growth of *E. coli*. Thus, we could examine the effects of cardiolipin on the dynamics and function of chemoreceptors and the motility system without being concerned about indirect effects mediated by growth defects.

However, our findings contradict an early publication by Nishijama *et al.* in 1988, reporting a remarkably faster loss of viability of the ClsA null mutant. This contrasting statement can be explained by the number of synthases knocked out. (*308*). Nishijama *et al.* deleted ClsA as back then only known cardiolipin synthase, whereas we deleted all three currently known cardiolipin synthases. Additionally we propose a dysregulation in case of an incomplete deletion of the three cardiolipin synthases, what further explains the results published by Nishijama *et al.*. We could show that single and double knockouts lead to growth deficits especially in the lag phase. Furthermore, we detected morphological alterations for the single knockout of ClsA and YbhO, resulting in elongated cells and also an additional population with longer cells (see 4.1.2.5). A possible dysregulation is, additionally to the just described findings by Nishijama *et al*., also supported by the publication of Okada *et al.*. The authors expressed phospholipid synthases of *B. subtilis* in *E. coli* resulting in a drastic increase in phopholipid levels, whereas the expression of the *E. coli* counterparts remained gratuitous (*309*). Newer studies were able to modify phospholipid ratios by expressing the *E. coli* own synthases (*310*).

For other bacteria like *Rhodobacter sphaeroides,* cardiolipin is expected to modify cell shape by influencing the peptidoglycan biosynthesis (*311*). For *E. coli*, however we could not detect a change in cell shape after complete inhibition of cardiolipin synthesis (see 4.1.2.6), what agrees with previous publications (*312*).

5.2 Cardiolipin enhances effectiveness of membrane targeting antibiotics

Glycerolipids, cardiolipin and also PG can increase the susceptibility to Polymyxin B. This compound is a cell membrane targeting antimicrobial drug, as early published for the cell wall lacking bacterium *Acholeplasma laidlawii (313).* In general, polymyxins interact with the outer membrane of gram-negative bacteria by interactions with the lipopolysaccahrides (LPS). The polycationic peptide ring displaces the calcium and magnesium bridges stabilizing the LPS and with that it binds to the outer membrane. Polymyxins are taken up by a 'self-promoted uptake' (*314*). It has also been reported that the short fatty acids of glycerolipids do exist in a higher amount in the cell membrane of the Polymyxin B resistant *Acitenobacter baumannii* when compared to Polymyxin B sensitive strains (*315*). Due to the indication that cardiolipin might play a role in the effectiveness of membrane-targeting antimicrobial drugs, we tested two substances (Polymyxin B and Colistin) for the influence on the growth of our cardiolipin deficient strain (see 4.1.2.3). We could show a weak effect of cardiolipin on the effectiveness of the antibiotics dependent on growth medium and temperature. Our data suggests that strains lacking cardiolipin are more resistant towards Polymyxin B and Colistin, especially at higher growth temperatures. Cardiolipin is known to increase membrane fluidity, hence we expect that the elimination of cardiolipin leads to a higher resistance towards membrane-targeting antimicrobial drugs as their effectiveness is also dependent on the fluidity of the target membrane (*285*). This finding matches the just mentioned observations of cardiolipin positively influencing the effectiveness of Polymyxin in other organisms. Nepper *et al.(316)* are proposing that a deletion of all three cardiolipin synthases leads to an increased susceptibility of planktonic *E. coli* cells towards several antimicrobial

drugs including Polymyxin B. With this they are contradicting previous suggestions, and also our findings. However, it is worth noting that under the tested growth conditions of Nepper *et al*, the minimum inhibitory concentration values of Polymyxin B towards the unmodified *WT* (8.7 µg/mL) and the triple-knockout of cardiolipin synthases (4.0 µg/mL) are close with regard to the specified error bars (*316*).

5.3 Temperature-dependent influence of cardiolipin on the chemosensing ability of *E. coli*

E. coli is using the chemotaxis and motility system to move away from non-tolerable and toxic environment towards advantageous conditions. The chemotaxis system allows cells to navigate in gradients of attractants (nutrients) and repellents (toxins). Additionally, the chemotaxis system enables *E. coli* to direct their movement in general environmental gradients e.g. pH and temperature (*317, 318*). The bacterial methyl-accepting trans-membrane chemoreceptors mediate chemotaxis along the gradient of chemical or physical properties. Ligands interact with the external sensing domain of the receptor. Binding of positive ligands (attractants) induces an asymmetric conformational change of the receptor, leading to a small displacement of one of the membrane-spanning helixes (TM2) towards the cytoplasm (*319*). The signal is further transduced by the HAMP domain, playing an important role in signal transmission (*320*). The signal gets further transmitted through the methylation helix bundle and the flexible region of the receptor, towards the protein contact region for interactions with the auto-phosphorylating kinase CheA and CheW. Attractants inhibit the activity of the receptor-associated kinase CheA, whereas repellents stimulate it. CheA subsequently donates the phosphoryl group to the response regulator CheY, controlling the rotation of the flagella motor. CheY-P gets dephosphorylated by the phosphatase CheZ (*321*).

In this study, we focused on the effect of cardiolipin on the chemosensing of *E. coli*'s membrane-anchored major receptors Tar and Tsr (see 4.1.4.2). We could show a temperature-dependent effect of cardiolipin on the chemosensing

properties of the major receptor, Tar. Whereas at 18°C experimental temperature a cardiolipin deficiency seems to decrease the sensing ability of Tar, at 22°C the receptor seems partially more sensitive (4.1.4.2). The artificial cardiolipin deficiency leads to a continuously worsened sensing ability of Tar at the lower tested temperature (18°C), compared to the *WT* strain with unmodified membrane composition. Here, the response amplitudes of Tar in the cardiolipin lacking strain are smaller and also the sensing starts at a higher ligand concentration. At 22°C, cardiolipin deficiency makes Tar more sensitive towards lower concentrations of MeAsp. The cardiolipin-deficient strains starts sensing MeAsp at lower concentrations and also the amplitudes in the area of lower concentrations (0.01 to 2 µM) are larger than the *WT* ones. With increasing attractant concentrations, the response amplitudes of Tar in the WT are larger than in the cardiolipin lacking strain.

The two main chemoreceptors in *E. coli* are not only sensing attractant and repellents but are additionally involved in temperature sensing. Tar and Tsr function as thermosensors through different methylations and the conformational changes (*188, 322*). It was published recently that both receptors mediate thermophilic responses when the cells are adapted to buffer. However with increasing temperature and the resulting increase in methylation level, the response gets weaker (*323*). Additionally, further publications support the importance of the interplay between Tar and Tsr in terms of thermotaxis (*324*). The chemoreceptor Tar is expected to switch from heat seeking to cold seeking in dependency of the methylation grade (*325*). However, in rich media, as we use it in this study, Tar is claimed to be constantly cold seeking. This temperature-dependent behaviour of Tar, the missing interplay partner for an efficient thermotaxis and the alterations of membrane composition by eliminating cardiolipin may all play a role in the different sensing behaviours of Tar in dependency of cardiolipin and temperature. It is possible that the lack of cardiolipin leads to a slight conformational change of the receptors, or varies the chemoreceptor clusters size, leading to an improved sensing especially of lower attractant concentration. This advantage is not detectable anymore at higher ligand concentrations. To explain this phenomenon, and to prove our idea, further investigation is necessary.

Additional to examining the effect of cardiolipin on the attractant sensing, we also had a closer look on the repellent side. Generally, repellents are toxic substances or unfavourable environmental influences that could potentially harm the cells. Examples would be higher concentrations of heavy metal ions like Ni^{2+} or Cu^{2+}, which would form nonspecific complexes in the cell (*318*). Attractant sensing happens through direct ligand binding or indirectly with the help of periplasmic binding proteins. It was suggested that repellent sensing by Tar differs from attractant binding (*326*). Ideas arise that another possibility for sensing repellents is through their effect on membrane fluidity. It was published, though, that the sensing of most repellents is not mediated by their effect on membrane properties (*327*). When observing the repellent sensing of Tar in dependency of cardiolipin, we could detect a slightly worsened sensing of $NiCl_2$ in the absence of cardiolipin. In our preliminary experiments the cardiolipin deficiency leads to smaller response amplitudes of Tar and also the sensing starts at higher repellent concentrations (Figure 16, E). So far, the results suggest that a lack of cardiolipin deteriorates the repellent sensing of Tar. This can also be seen in the pH examinations of Tar sensing (Figure 16, F). pH Values above 7 are sensed by Tar as repellent. Also, here the response amplitudes are smaller in the absence of cardiolipin. This effect on the Tar repellent sensing does not necessarily need to be dependent on the caused change in membrane fluidity with eliminating cardiolipin. It can also be caused by a slight conformational change of the receptors, caused by deletion of the membrane phospholipid, cardiolipin.

Further, we could show that cardiolipin does only influence the sensing ability of the Tar receptor but not of the Tsr receptor. We could not detect differences in sensing various ligand concentrations and response amplitudes of Tsr in dependency of cardiolipin. Further finding regarding chemoreceptor clustering and receptor diffusion supports our suggestion that the effect of cardiolipin is Tar specific.

5.4 Cardiolipin enhances Tar chemoreceptor clustering

Intensive research efforts are focusing on the mechanism of chemoreceptor clustering in *E. coli*. Receptor clusters in *E. coli* are highly organized complex multiprotein structures, consisting of up to five different chemoreceptors and cytoplasmic proteins. Recent findings reported two chemoreceptor trimers of dimers, a CheA dimer and two CheW molecules as smallest functional receptor array (*212*). So far, the complete receptor cluster assembly and its localization mechanism is not entirely explored. Chemoreceptor clusters are expected to form by stochastic self-assembly (*328*). Clustering is expected to be primarily CheA/ CheW-dependent (*329*) but might also be enhanced by interactions between the periplasmic receptor domains (*330*). Additional findings address the possibility of Tar lacking transmembrane domains to form cytoplasmic arrays in presence of CheW and CheA with the help of a molecular crowding agent (*331*). However, polar localization and cluster formation of high-abundance receptors was to some extent observed also in the absence of CheA and CheW (*332*). The positioning of formed chemoreceptor clusters is expected to be dependent on membrane curvature (*333*). Still, the exact mechanism of polar cluster positioning remains partly elusive. Theory arises, that receptor cluster positioning can also be promoted by lipids (*75*), as also the functionality of Tar is proven to be dependent on the lipid environment (*334*).

As cardiolipin is expected to localize at the negatively curved membrane at the poles, we suspected a connection between cardiolipin and the polar localization of chemoreceptor clusters. We focused on the influence of cardiolipin on the clustering of the major chemoreceptors in *E. coli*, Tar and Tsr. Santos *et al*. claim that cardiolipin has no effect on chemoreceptor localization. Additionally, it was stated, that cardiolipin content does not influence the number of polar clusters (*335*). Our finding partly agrees with these statements, as we could not detect a localization difference in dependency of cardiolipin content in the membrane. However, we demonstrated, by comprehensive manual and automated analysis, that with presence of cardiolipin in the cytoplasmic membrane the number of detectable Tar chemoreceptor clusters is twice as high than without cardiolipin. We could show this cardiolipin-dependent ratio of Tar clusters is independent of

growth temperatures and growth phase (see 4.1.4.3). Further, we demonstrated this for cells grown in liquid culture, as well as for chemotactic active cells sampled from the outer swimming ring when grown on soft agar plates (see 4.1.4.3.1). The difference in detectable clusters, can be explained by hydrophobic mismatch, a brought about instability of the clusters or a slower diffusion of single clusters within the membrane due to changes of the membrane composition or a disturbance of cluster assembly by unsuitable membrane composition.

This idea is supported by our examination of varying trans-membrane domain lengths. Whereas elongation of the Tar TM2 domain does not influence the ratio of receptor clusters in terms of cardiolipin content in the membrane, we showed that a reduction of the Tar TM2 domain by one and two amino acid residues reverses the cardiolipin-dependent effect on Tar clustering (see 4.1.4.3.2). A recent study reports the capability of the Tar trans-membrane domains of forming cluster-like structures (*208*). We could show that the formation of these cluster-like structures of trans-membrane helices is also influenced by the presence of cardiolipin in the membrane (see 4.1.4.3.2). In the absence of cardiolipin fewer cluster-like structures are formed, irrespective of the trans-membrane helix length modification. The unmodified trans-membrane helix construct did not form any cluster-like structures. This finding is also mentioned in the original publication (*208*). The shortening of the Tar TM2 helix reverses the cardiolipin-dependent effect on the receptor clustering, whereas this cannot be observed for the TM only constructs. The full-length Tar constructs with modified trans-membrane helix can also be influenced by e.g. structural changes of the whole receptor, whereas the TM only constructs lack all receptor parts besides the transmembrane helices. This can be an explanation for the different influence of cardiolipin on these constructs.

We claim the cardiolipin-dependent effect on chemoreceptor clustering is Tar specific, since we could not detect significant differences of Tsr clustering (see 4.1.4.3.1). Generally, it must be mentioned that cardiolipin might not reduce the number of clusters or cluster-like structures but definitely the number of detectable clusters. We cannot rule out the possibility of cardiolipin influencing

only the size of the receptor clusters, making them impossible to detect by our method, but not the cluster formation itself. Cardiolipin might influence either the stability of the Tar chemoreceptor clusters, or the diffusion of single membrane-integrated Tar receptors joining the existing receptor clusters.

5.5 Cardiolipin enhances chemoreceptor diffusion

One explanation for the just discussed influence of cardiolipin on the clustering of Tar could be the receptor diffusion within the membrane. Therefore, we were interested in the membrane diffusion behaviour of chemoreceptors in dependence of cardiolipin. Accordingly, we decided to perform FRAP (Fluorescence Recovery After Photobleaching) experiments to examine the diffusion of the major chemoreceptors in *E. coli* (see 4.1.5). Generally, chemoreceptors can diffuse either as part of a receptor cluster or individually. The diffusion of receptors associated in a cluster can be due to diffusion of the entire cluster or the movement of a single receptor within the cluster. We made use of different versions of Tar (short, long, modified TM2) tagged with YFP, as well as Tsr-YFP and two more random membrane proteins as working constructs. The full-length version of the chemoreceptor Tar is capable of forming clusters and is diffusing through the membrane as trimer of dimers with 12 transmembrane helices (*336*). It is known, that protein diffusion in the membrane is much slower compared of a cytoplasmic protein. For the full-length version of Tar only a partial recovery in FRAP experiments is expected, as the cluster associated receptors remain immobile on the time scale of our experiment (*337*). The truncated version of Tar, Tar^{1-319}-YFP, is not capable of forming cluster-like structure and diffuses through the membrane as dimer with four transmembrane helices (*237*). We could show an interesting biophysical effect of temperature and cardiolipin-dependent Tar receptor mobility within the inner membrane. At 18°C, the full-length Tar-YFP construct as well as the truncated version shows a significantly slower recovery in the cardiolipin-deficient strain. This cardiolipin-dependent difference in recovery could not be detected at much lower (8°C) or higher (22°C, 30°C) temperatures (4.1.5.1). A temperature-dependent effect of lateral protein diffusion is also known for mammalian cells. Temperatures below 20°C seem to

increase the protein diffusion rates there (*338*). For our case, we wanted to examine the peak of lowered diffusion caused by the lack of cardiolipin. Therefore, we performed FRAP experiments at tighter temperature steps around 18°C. We could show that cardiolipin deficiency leads to a slower recovery of Tar also at 16°C and 17°C. Surprisingly at 19°C the effect is indiscernible. Due to these findings, we expect a tight temperature scope where cardiolipin influences the membrane diffusion of Tar. It was shown that an increase in temperature changes the diffusion of transmembrane proteins in dependency on the number and size of their transmembrane domains (*339*). However, the cardiolipin-dependent decrease and increase in receptor mobility with increasing temperature is most likely based on several interplaying mechanisms. The receptor diffusion itself can be influenced by temperature as well as by membrane composition and its fluidity. Also, the exact positioning of the transmembrane domains of Tar can be influenced by the surrounding phospholipids as well as by temperature. Additionally, the membrane fluidity is affected by temperature. We could prove that the temperature-dependent effect of cardiolipin deficiency on the diffusion of Tar can be partly explained by membrane fluidity (see 4.1.5.2).

As cardiolipin is known to increase membrane fluidity, a depletion leads to a decreased fluidity (*72*). This effect can be reversed by treating the cells with benzyl alcohol (BzA) which increases the fluidity by decreasing the lipid order in dose-dependent manner (*274*). Our work confirmed this hypothesis, the membrane fluidity increased and enabled Tar to diffuse again independently of cardiolipin and temperature effects. We suggest, that cardiolipin shortage leads to a temperature-dependent immobilisation of the Tar receptor within the membrane. As we could not detect a cardiolipin-dependent effect on the recovery of the Tsr receptor and other membrane proteins, we can exclude a general influence of cardiolipin on membrane protein diffusion. It seems the effect is rather Tar-specific. Further we investigated the correlation between cardiolipin and temperature influencing the receptor diffusion and its transmembrane domains (see 4.1.5.3). Diffusion of the transmembrane modified Tar-YFP constructs remained unchanged in the *WT*. In the cardiolipin lacking strain however, an elongation of the Tar TM2 domain by two residues, restores the mobility of the receptor at 18°C. An elongation by two and three residues of the

TM2 domain of Tar prevents the receptor from sensing MeAsp as attractant. The elongated receptors gives a repellent response upon binding of MeAsp (*238*). The three amino acids elongated receptor version shows a temperature-dependent upshift or reversion in terms of cardiolipin-dependent influence on the receptor diffusion. At 22°C, the three residues elongated version of Tar shows the same cardiolipin-dependent effect on diffusion as the non-modified receptor version at 18°C. However, at 18°C the diffusion of the Tar-TM(+3) construct is only slightly slower in the cardiolipin deficient strain. The importance and correlation of the temperature range from 16°C to 18°C and cardiolipin in terms of membrane fluidity are still unsettled.

The so far only known possible connection is shown as thermographs of differential scanning calorimetry. Here three peaks for synthetic TMCL (tetramyristol cardiolipin) when performing a cooling scan started from high temperature to 0°C can be detected. These peaks are at roughly 41°C, 28°C and around 18°C (*340*). The phase change of a cardiolipin containing membrane at 18°C, might correlate with our findings. We suppose cardiolipin, as bulky phospholipid, plays a role as perhaps even Tar specific fluidity buffer comparable with cholesterol in eukaryotic membranes. Cholesterol is disturbing the membrane order especially at lower temperatures to keep the membrane fluid. At higher temperatures cholesterol prevents the membrane from being totally fluid (*341*). Considering our results, we suspect Tar organising a shell-like lipid composition surrounding its transmembrane domains. This shell might hinder the receptor from continuous diffusion within the membrane. Lacking cardiolipin the diffusion of Tar impairs in a temperature-dependent manner. The effect can be reversed by an increase of membrane fluidity (see BzA) or an extension of the hydrophobic mismatch by elongation of the membrane helices. The connection between the cardiolipin-mediated temperature-dependent enhancement of receptor mobility and the cardiolipin-dependent enhancement of receptor clustering remains to be verified.

5.6 Cardiolipin affects the motility system of *E. coli*

For evaluating the effect of cardiolipin on the motility system in more detail, we made use of soft agar plates. These soft-agar assays can provide information regarding the growth and chemosensing ability of tested strains, but also about their motility system. We performed our chemoreceptor-specific experiments in temperature range from 30°C to 39°C (see 4.1.3). For the two main chemoreceptors in *E. coli*, Tar and Tsr, we could identify a negative effect of cardiolipin on the swimming ability at higher temperatures. The cardiolipin knockout strains are forming larger swimming rings compared to the belonging *WT* independent of temperature. At 30°C however, the difference seems minor. Especially for expressing Tar as only receptor we could detect an expanding diameter of the swimming rings with rising temperatures for the cardiolipin deficient strain. Consistent with the results of our soft agar assays, we could detect expression of FliC (flagellin) in the cardiolipin lacking strain at 39°C, compared to no expression of FliC for the *WT*. The *fliA* promoter of both strains is still turned on under these conditions (see 4.1.6.1). One can speculate, even though unlikely, cardiolipin behaves as fluidity buffer (see 5.5), therefore we would expect only minor changes for the *WT* at temperatures between 30°C and 39°C, as cardiolipin keeps the membrane in a similar fluidity state. Contrary, the cardiolipin deficient strain lacks its fluidity buffer, so we expect changes in the membrane fluidity at higher temperatures.

Nepper *et al*. stated recently contradicting results of a positive influence of cardiolipin on the swimming and swarming behaviour of *E. coli* MG1655 in terms of Rcs phosphorelay and biofilm research (*316*). The authors suggest a molecular connection between biofilm formation in *E. coli* and the ratio of membrane phospholipids. They claim that the absence of cardiolipin reduces the biofilm formation by *E. coli*. However, these findings seem contradicting, as a reduction of biofilm formation would lead to an increase in swimming behaviour, what is exactly what we see in our soft agar plates. A lack of cardiolipin increases the diameter of the formed swimming rings of *E. coli*. Further Nepper *at al.* demonstrated that the lack of cardiolipin impairs the protein translocation across the cytoplasmic membrane. Due to that finding, they propose, that the depletion

of the anionic phospholipid cardiolipin activates the Rcs signalling system (regulation of the colonic acid synthesis) through the outer membrane protein RcsF. This leads to a reduction in biofilm growth and initial biofilm attachment as well as this system represses the production of flagella. The authors report a smaller diameter of swarming and swimming rings with absence of cardiolipin. They performed the swarming plates with inoculating 3µL of saturated *E. coli* culture onto 0.6% Eiken agar LB plates with additional 0.5% glucose (w/v) and the swimming plates were inoculated similarly in 0.3% agar in M9 minimal medium. Both plate types of Nepper *et al*. were grown for 24h at 30°C. Their results were confirmed by immunostaining of FliC, and subsequent counting of flagella. For the *WT*, more flagellar were detected, compared to the cardiolipin lacking strain ((*316*), figure 6). Our soft agar assays were performed in TB medium with 0.27% agar for maximum six hours at various temperatures. We could especially detect a cardiolipin-dependent effect at higher temperatures, whereas 30°C doesn't reveal a cardiolipin effect on the swimming ability. A growth for 24h at our setup would result in completely overlapping swimming rings already at 30°C, were the slowest of all growth speeds for the tested temperatures is expected. Apart from our findings, and the statements of Nepper *et al*., so far only a defect in synthesis of PG, one of the major phospholipids in the cytoplasmic membrane, is reported to exhibit deficiencies in flagella synthesis (*342, 343*). The comparability of these to a certain extent contradicting results remains elusive, as the experimental setups differ in growth conditions (e.g. media, incubation time) and also in utilization of different strain backgrounds. Our working strain (VS367) is a chemoreceptor-less derivative of RP437 (*344*), a strain often used for chemotaxis and also motility related studies. It is documented for our experimental conditions, that the strain MG1655 forms larger swimming rings on semi-solid agar than RP437 or also W3110 (*345*). Additionally MG1655 is better in surface colonization and biofilm formation (*346*). Without additional expression of minimum one chemoreceptor, the background strain VS367 is non-chemotactic. The expression of Tar as only chemoreceptor can restore the swarming as well as the swimming ability of *E. coli* almost completely (*347*). With using the approach of a receptorless and additional expression of single chemoreceptors, we could examine the influence of cardiolipin in detail on

single chemoreceptors, whereas investigations with MG1655 would give a more general view.

5.7 Effect of further membrane alterations in *E. coli* achieved by overexpression of phospholipid synthases

Additionally, to the effect of cardiolipin synthase deletions on several systems of *E. coli*, we were also interested in the effect of other membrane alterations. As mentioned earlier, the overexpression of *E. coli*'s own phospholipid synthases leads to an increase in protein, but does not necessarily increase the level of phospholipid (*309*). We suspect a so far unknown regulatory process here. The results we gained with single deletion of cardiolipin synthases (see 4.1.2.5), supporting this hypothesis. To overcome a possible dysregulation by phospholipid synthase overexpression we decided to use the synthases of *B. subtilis*. Okada et al. published the efficient overexpression of *B. subtilis* synthases in *E. coli*, leading to an increase of desired phospholipid (*309*). However, overexpression of PgsARs from *R. sphaeroides* in *E. coli* did not have drastic effects on the membrane composition of the cells, what serves as basis for the proof of an active regulation of this PG synthase in *E. coli* (*348*). The effect of PgsA absence is discussed. Mileykovskaya *et al*. reports a PgsA null mutation to have less effect on the growth behaviour, as the cells show relatively normal cell division (*349*). Others report a *pgsA*30::kan lpp-2 mutation in *E. coli* W3110 leads to cell lysis upon temperature upshift from 30°C to 42°C, and an impaired growth in minimal and low osmolarity media (*48*). Further a reported growth arrest of a PgsA mutant is thought to be dependent on the role of anionic phospholipids in advancing DnaA reactivation (*350*). So far, little is known about the effect of PgsA overexpression on *E. coli*. We focused on the effect of membrane alterations on growth, the chemotaxis and motility system at various temperatures.

We could show a drastic effect of overexpressing PgsA (PG synthase) on the growth behaviour of *E. coli*. At lower temperature, the lag phase is extended and the cells reach stationary phase at a lower OD_{600} level, independent of synthase

induction levels. With increasing temperature (37°C and 42°C), the high overexpression of PgsA leads to drastic elongation of lag phase, up to 7h when compared to the negative control comprising only the empty expression vector (see 4.2.1). Additional to the effect on growth, we could also show a drastic effect of PG overproduction on the swimming behaviour of *E. coli*. Upon PgsA overexpression the swimming rings formed on soft agar plates are drastically downsized (see 4.2.2). Swimming plates combine the impact of growth, chemotaxis and motility (*267*). The impact of PgsA overexpression on the swimming behaviour seems too strong to be explained only by the growth effect. Therefore, we were additionally focusing on the PgsA effect on the chemotaxis system by observing the amount of detectable chemoreceptor clusters. When imaging the PgsA overexpression strain we noticed drastically elongated W3110 cells, and a thereby resulting high number of chemoreceptor clusters (4.3.3). We expect increasing quantities of PG to cause difficulties in cell separation. This can explain the elongated lag phases in the growth experiments and does not contradict the normal growth behaviour (at higher temperature) after exiting lag phase. The growth experiments were performed by OD measurement. Optical density is defined as logarithm of the ratio of the intensity of light falling upon the sample and the transmitted intensity. It does not differentiate between cell lengths. Exemplary, this can mean that the OD of two smaller cells can respond to the OD of one larger cell. As on soft agar plates the cells have to navigate through agar pores, the cell size can be a hindrance. Drastically elongated cells will get stuck in the agar mesh. This explains the smaller swimming rings of the PgsA overexpression strain, detected with our soft agar assay. Nevertheless, we investigated the effect of phospholipid synthase overexpression on the regulation of motility with the help of promoter reporters (see 4.2.5). The overexpression of PgsA leads to a bistable distribution of *fliC* expression independent of temperature. The expression of *fliC* in this strain, grown on soft agar plates, differs. At 30°C *fliC* expression is higher compared to the *WT*, whereas at 42°C the fliC expression is drastically lower than in the *WT*. PgsA overexpression reduces the spreading of *E. coli* cells on soft agar, what might cause the increasing expression of *fliC* as an artefact. To explain the exact context of the elongated cells, the poorly swimming behaviour on soft agar plates and the

temperature-dependent regulation of the motility genes further investigation are necessary. We expect the elongated cells upon PgsA overexpression, are caused by the co-localisation of MinD and PG (*351*). MinD is an ATP requiring septum-site determining protein. The Min proteins facilitate the mid-cell formation of the FtsZ ring. MinD works together with MinC as cell division inhibitors, by blocking the formation of polar Z-ring septum (*352, 353*). Results of Mileykovskaya *et al.* suggest, that MinD prefers negatively charge phospholipids (e.g. PG) and due to that the selection of the cell division site might be influenced by the membrane phospholipid composition (*300*). The observed elongated cells might be caused by the malfunction of FtsZ ring positioning, what prevents the cells from separation, due to an increase of PG in the cytoplasmic membrane.

5.8 Membrane alteration in *B. subtilis*

Escherichia coli served us as gram-negative model bacteria. However, we were further interested in the effect of membrane alterations in bacteria with a gram-positive cell envelope. We decided for one of the best-studied gram-positive organisms as working strain, *B. subtilis*. Similar to our approach in *E. coli*, we examined the effect of various membrane alterations on the growth, chemotaxis and motility system of *B. subtilis*. It is known that *Bacillus* alters its membrane composition in dependency on growth condition (*354*). We could show that membrane alterations caused by synthase knockouts do not affect drastically the growth of *B. subtilis* (see 4.3.1). This confirms the statement of Salzberg *et al*., reporting a high tolerance level for membrane alterations of *B. subtilis*. Even drastic alterations in phospholipid head group composition does not lead to extreme growth proficiency (*87*). The only slight abnormality, we could detect in our experiments, is delayed death phase for some knockout strains. In general, the cell deaths in this phase can be caused by several injurious conditions e.g. lack in nutrient supply or an increase in toxic metabolic products. A delayed death phase can be an indication for a higher resistance against the conditions of the late stationary phase. The knockout of PssA, MprF and the double knockouts of YwnEYwiE and YwnEYwjE elongated the late stationary phase. The knockout of PssA slightly elongated the lag phase of *B. subtilis* growth but also significantly

elongated the late stationary phase. Even after 24h we could not detect the death phase for this knockout strain. We propose, that there is no distinct correlation between membrane alterations and the general growth behavior of *B. subtilis*, however certain membrane alterations do influence the cell morphology of *B. subtilis*. Knockouts of different phospholipid synthases effected subpopulations with elongated cells for up to half of the population (see 4.3.1). For more precise insight into the connection of membrane alterations and morphology further research is necessary.

An early study proposed that a transient alteration of the membrane potential can induce changes of the swimming behavior (*355*). We can confirm this statement with our results gained by performing swimming plate assays. All strains possessing a synthase knockout do form smaller swimming ring on 0.3% soft agar (see 4.3.2). The knockout of Psd, a phosphatidylserine carboxylase, impairs swarming motility on soft agar plates. The behavior on these half-solid plates combines growth ability and a functional chemotaxis and motility system. To further investigate the reason of smaller rings detected in the soft agar assays, we performed microscopic analyses of chemoreceptor and flagella motor localization. Our preliminary results gave no clue for a correlation between membrane composition and chemoreceptor clustering (see 4.3.3.1). When investigating the effect of membrane alteration in *B. subtilis* on its chemosensing, we could show a more clear influence. The knockout of Psd, as well as of the single and double cardiolipin synthase knockouts drastically reduce the sensing of proline. The complete elimination of cardiolipin, by the knockout of all three cardiolipin synthases impairs proline sensing almost completely (see 4.3.3.2). Previous statements of cardiolipin domains localizing to the septal and polar regions of the *B. subtilis* cell (*74*) linking cardiolipin to polar protein targeting, cell division and as mode of action for membrane targeting antimicrobial drugs, got disproved (*356*). The authors state that *B. subtilis* has no cardiolipin-specific microdomains. The influence of cardiolipin on proline sensing in *B. subtilis* thus remains so far elusive and needs further investigation.

6 SUPPLEMENTARY

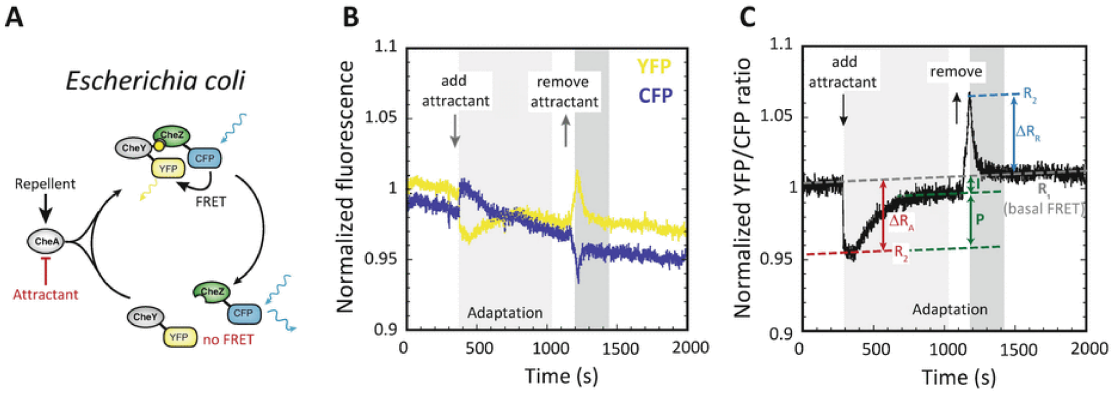

Figure S1. FRET-based analysis of *E. coli* chemotaxis pathway responses. Attractant addition or removal changes the CheA activity, with this the interaction between CheY and CheZ. As a result, the energy transfer (FRET) between CheZ-CFP (donor) and CheY-YFP) acceptor drops (A). Time traces of the normalized fluorescence intensity in the YFP (yellow) and CFP (cyan) channels as FRET response (B). Normalized YFP/CFP ratio showing the addition and subsequent removal of attractant to cells attached in the flow chamber resulting in a decrease in the YFP/CFP ratio due to the reduced numbers of CheY-P-CheZ complexes. Vice versa, removal of attractants or addition of repellents leads to an increase in the YFP/CFP ratio (C). Reprinted from Paulick *et al.*, 2018, (*291*).

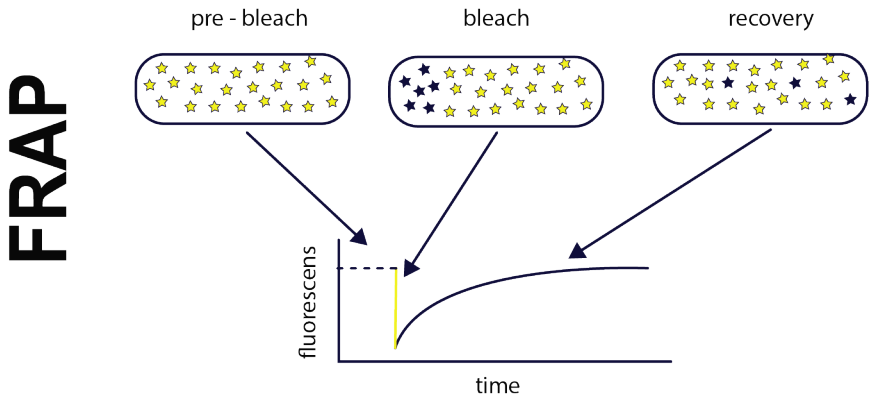

Figure S2. Schematic illustration of Fluorescence Recovery after Photobleaching (FRAP) of a fluorescently tagged protein of interest.

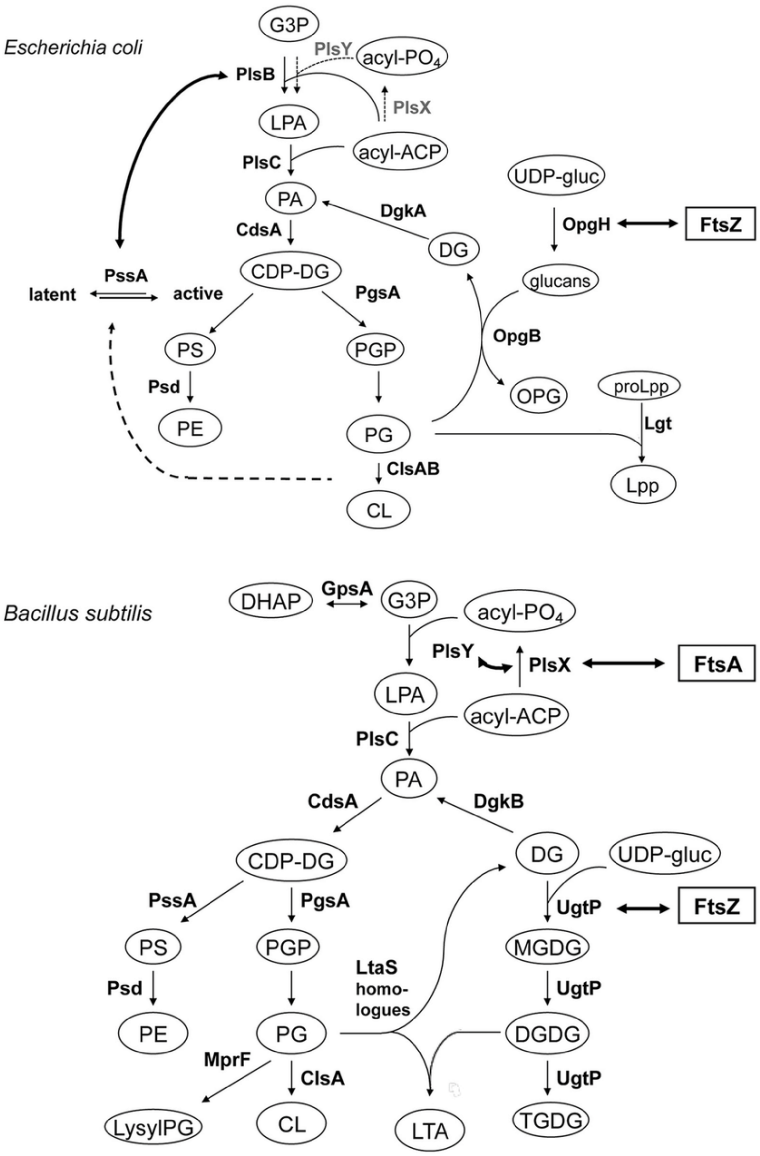

Figure S3. Lipid biosynthetic pathways of *E. coli* and *B. subtilis* and the interactions of phospholipid synthases and proteins involved in cell division. Reprinted from Matsumoto et al., 2015, (*279*).

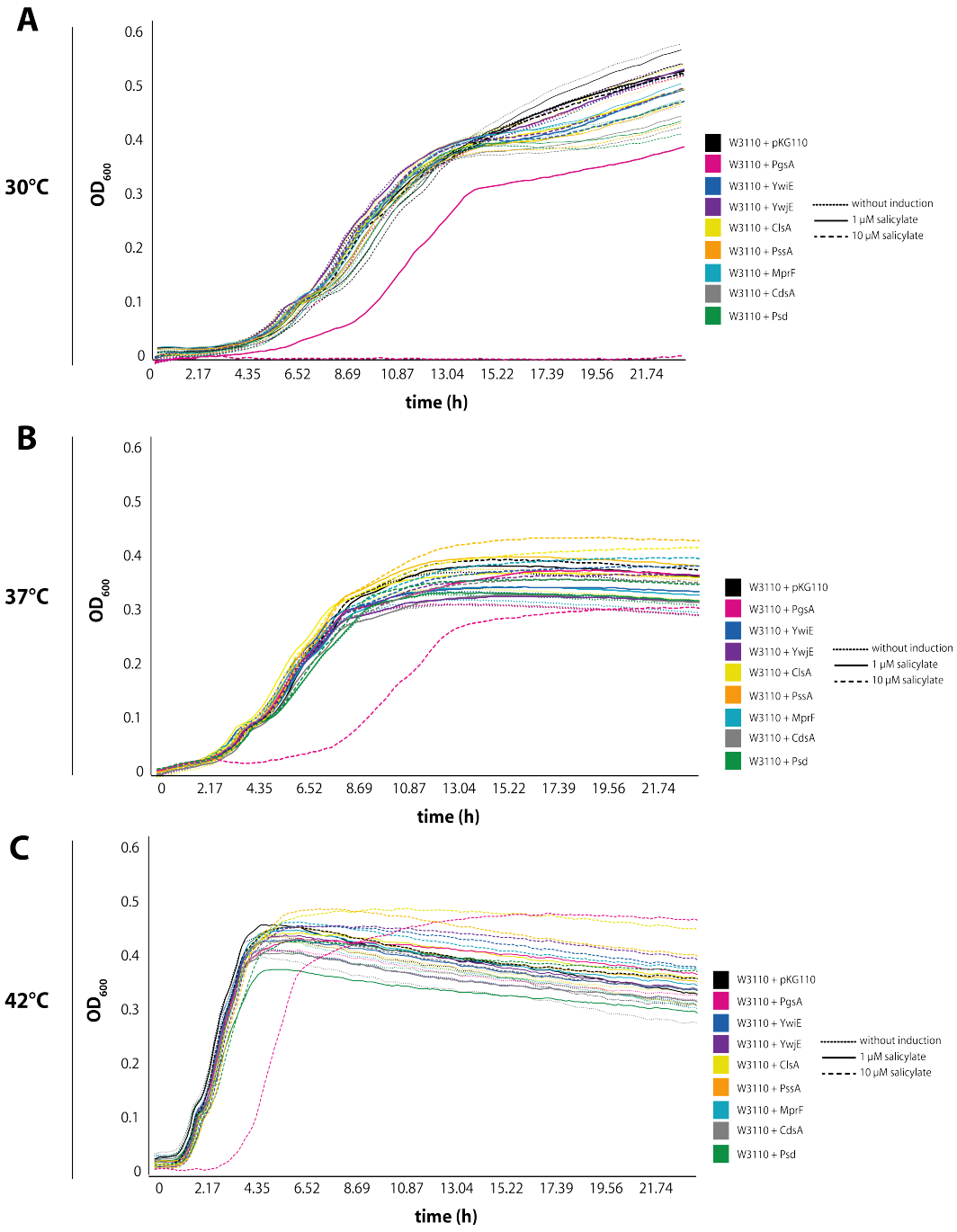

Figure S4. Growth of *E. coli W3110 rpoS+* with overexpression of several phospholipid synthases. Growth curves of *E. coli W3110 rpoS+* with overexpression of several phospholipid synthases (WT with empty expression vector: black, ClsA: yellow, PssA: orange, Psd: green, YwjE: purple, PgsA: pink, YwiE: blue, MprF: turquois, CdsA: grey) at 30°C (A), 37°C (B) and 42°C (C).

7 BIBLIOGRAPHY

1. H. Gram, Method of distinguishing between two major classes of bacteria. *Friedländer's Journal Fortschritte der Medizin*, (1884).
2. T. J. Silhavy, D. Kahne, S. Walker, The bacterial cell envelope. *Cold Spring Harbor perspectives in biology* **2**, a000414 (2010).
3. F. C. Neuhaus, J. Baddiley, A continuum of anionic charge: structures and functions of D-alanyl-teichoic acids in gram-positive bacteria. *Microbiol. Mol. Biol. Rev.* **67**, 686-723 (2003).
4. J. R. Scott, T. C. Barnett, Surface proteins of gram-positive bacteria and how they get there. *Annu. Rev. Microbiol.* **60**, 397-423 (2006).
5. A. M. Glauert, M. J. Thornley, The topography of the bacterial cell wall. *Annual review of microbiology* **23**, 159-198 (1969).
6. Y. Kamio, H. Nikaido, Outer membrane of Salmonella typhimurium: accessibility of phospholipid head groups to phospholipase c and cyanogen bromide activated dextran in the external medium. *Biochemistry* **15**, 2561-2570 (1976).
7. C. R. Raetz, C. Whitfield, Lipopolysaccharide endotoxins. *Annual review of biochemistry* **71**, 635-700 (2002).
8. K. Sankaran, H. C. Wu, Lipid modification of bacterial prolipoprotein. Transfer of diacylglyceryl moiety from phosphatidylglycerol. *Journal of Biological Chemistry* **269**, 19701-19706 (1994).
9. H. Miyadai, K. Tanaka-Masuda, S.-i. Matsuyama, H. Tokuda, Effects of lipoprotein overproduction on the induction of DegP (HtrA) involved in quality control in the Escherichia coli periplasm. *Journal of Biological Chemistry* **279**, 39807-39813 (2004).
10. S. Cowan *et al.*, Crystal structures explain functional properties of two E. coli porins. *Nature* **358**, 727-733 (1992).
11. S. E. Rollauer, M. A. Sooreshjani, N. Noinaj, S. K. Buchanan, Outer membrane protein biogenesis in Gram-negative bacteria. *Philosophical Transactions of the Royal Society B: Biological Sciences* **370**, 20150023 (2015).
12. V. Braun, Covalent lipoprotein from the outer membrane of Escherichia coli. *Biochimica et Biophysica Acta (BBA)-Reviews on Biomembranes* **415**, 335-377 (1975).
13. C. W. Mullineaux, A. Nenninger, N. Ray, C. Robinson, Diffusion of green fluorescent protein in three cell environments in Escherichia coli. *Journal of bacteriology* **188**, 3442-3448 (2006).
14. F. Duong, J. Eichler, A. Price, M. R. Leonard, W. Wickner, Biogenesis of the gram-negative bacterial envelope. *Cell* **91**, 567-573 (1997).
15. C. Raetz, W. Dowhan, Biosynthesis and function of phospholipids in Escherichia coli. *Journal of Biological Chemistry* **265**, 1235-1238 (1990).
16. R. E. Dalbey, P. Wang, A. Kuhn, Assembly of bacterial inner membrane proteins. *Annual review of biochemistry* **80**, 161-187 (2011).
17. W. Vollmer, D. Blanot, M. A. De Pedro, Peptidoglycan structure and architecture. *FEMS microbiology reviews* **32**, 149-167 (2008).

18. J. E. Cronan Jr, E. P. Gelmann, Physical properties of membrane lipids: biological relevance and regulation. *Bacteriological reviews* **39**, 232 (1975).
19. D. Clark *et al.*, Regulation of phospholipid biosynthesis in Escherichia coli. Cloning of the structural gene for the biosynthetic sn-glycerol-3-phosphate dehydrogenase. *Journal of Biological Chemistry* **255**, 714-717 (1980).
20. Y. Hara *et al.*, Involvement of PlsX and the acyl-phosphate dependent sn-glycerol-3-phosphate acyltransferase PlsY in the initial stage of glycerolipid synthesis in Bacillus subtilis. *Genes & genetic systems* **83**, 433-442 (2008).
21. R. J. Heath, H. Goldfine, C. O. Rock, A gene (plsD) from Clostridium butyricum that functionally substitutes for the sn-glycerol-3-phosphate acyltransferase gene (plsB) of Escherichia coli. *Journal of bacteriology* **179**, 7257-7263 (1997).
22. J. Coleman, Characterization of Escherichia coli cells deficient in 1-acyl-sn-glycerol-3-phosphate acyltransferase activity. *Journal of Biological Chemistry* **265**, 17215-17221 (1990).
23. W. Dowhan, CDP-diacylglycerol synthase of microorganisms. *Biochimica et Biophysica Acta (BBA)-Lipids and Lipid Metabolism* **1348**, 157-165 (1997).
24. J. E. Cronan, Bacterial membrane lipids: where do we stand? *Annual review of microbiology* **57**, 203-224 (2003).
25. D. Cavard, C. Rampini, E. Barbu, J. Polonovski, [Phospholipase activity and other modifications in metabolism of the phospholipids consequent to the action of the colicins on E. coli]. *Bulletin de la Societe de chimie biologique* **50**, 1455-1471 (1968).
26. M. C. Simmler, M. E. Barbu, [Modification of the phospholipid composition of E. coli cells during their transformation into spheroplasts]. *Annales de l'Institut Pasteur* **119**, 289-301 (1970).
27. J. Starka, J. Moravova, Phospholipids and cellular division of Escherichia coli. *Journal of general microbiology* **60**, 251-257 (1970).
28. R. H. Peterson, C. S. Buller, Phospholipid metabolism in T4 bacteriophage infected Escherichia coli K-12 (lambda). *Journal of virology* **3**, 463-468 (1969).
29. J. E. Cronan, P. R. Vagelos, Metabolism and function of the membrane phospholipids of Escherichia coli. *Biochimica et biophysica acta* **265**, 25-60 (1972).
30. P. Burn, Talking point Amphitropic proteins: a new class of membrane proteins. *Trends in biochemical sciences* **13**, 79-83 (1988).
31. A. DeChavigny, P. N. Heacock, W. Dowhan, Sequence and inactivation of the pss gene of Escherichia coli. Phosphatidylethanolamine may not be essential for cell viability. *Journal of Biological Chemistry* **266**, 5323-5332 (1991).
32. N. Wellner, T. A. Diep, C. Janfelt, H. S. Hansen, N-acylation of phosphatidylethanolamine and its biological functions in mammals. *Biochimica et biophysica acta* **1831**, 652-662 (2013).
33. M. Mishkind, Phosphatidylethanolamine – in a pinch. *Trends in Cell Biology* **10**, 368 (2000).

34. R. J. Kelly Karen, Phospholipid Biosynthesis. *The AOCS Lipid Library*, (2011).
35. M. Bogdanov, P. N. Heacock, W. Dowhan, A polytopic membrane protein displays a reversible topology dependent on membrane lipid composition. *The EMBO journal* **21**, 2107-2116 (2002).
36. X. Wang, M. Bogdanov, W. Dowhan, Topology of polytopic membrane protein subdomains is dictated by membrane phospholipid composition. *The EMBO journal* **21**, 5673-5681 (2002).
37. M. Bogdanov, J. Sun, H. R. Kaback, W. Dowhan, A phospholipid acts as a chaperone in assembly of a membrane transport protein. *Journal of Biological Chemistry* **271**, 11615-11618 (1996).
38. M. Bogdanov, W. Dowhan, Phosphatidylethanolamine is required for in vivo function of the membrane-associated lactose permease of Escherichia coli. *Journal of Biological Chemistry* **270**, 732-739 (1995).
39. M. Bogdanov, W. Dowhan, Phospholipid‐assisted protein folding: phosphatidylethanolamine is required at a late step of the conformational maturation of the polytopic membrane protein lactose permease. *The EMBO journal* **17**, 5255-5264 (1998).
40. A. Ohta, I. Shibuya, Membrane phospholipid synthesis and phenotypic correlation of an Escherichia coli pss mutant. *Journal of bacteriology* **132**, 434-443 (1977).
41. N. I. Mikhaleva *et al.*, Depletion of phosphatidylethanolamine affects secretion of Escherichia coli alkaline phosphatase and its transcriptional expression. *FEBS letters* **493**, 85-90 (2001).
42. E. Mileykovskaya, W. Dowhan, The Cpx two-component signal transduction pathway is activated in Escherichia coli mutant strains lacking phosphatidylethanolamine. *Journal of bacteriology* **179**, 1029-1034 (1997).
43. E. Kitamura, Y. Nakayama, H. Matsuzaki, K. Matsumoto, I. Shibuya, Acidic-phospholipid deficiency represses the flagellar master operon through a novel regulatory region in Escherichia coli. *Bioscience, biotechnology, and biochemistry* **58**, 2305-2307 (1994).
44. C. Rathmann, A. S. Schlösser, J. Schiller, M. Bogdanov, T. Brüser, Tat transport in Escherichia coli requires zwitterionic phosphatidylethanolamine but no specific negatively charged phospholipid. *FEBS letters* **591**, 2848-2858 (2017).
45. C. Yu, M. Li, Y. Sun, X. Wang, Y. Chen, Phosphatidylethanolamine Deficiency Impairs Escherichia coli Adhesion by Downregulating Lipopolysaccharide Synthesis, Which is Reversible by High Galactose/Lactose Cultivation. *Cell communication & adhesion* **23**, 1-10 (2017).
46. Y. H. Lu, Z. Guan, J. Zhao, C. R. Raetz, Three phosphatidylglycerol-phosphate phosphatases in the inner membrane of Escherichia coli. *The Journal of biological chemistry* **286**, 5506-5518 (2011).
47. C. Li, B. K. Tan, J. Zhao, Z. Guan, In Vivo and in Vitro Synthesis of Phosphatidylglycerol by an Escherichia coli Cardiolipin Synthase. *The Journal of biological chemistry* **291**, 25144-25153 (2016).
48. S. Kikuchi, I. Shibuya, K. Matsumoto, Viability of an Escherichia coli pgsA null mutant lacking detectable phosphatidylglycerol and cardiolipin. *Journal of bacteriology* **182**, 371-376 (2000).

49. M. Suzuki, H. Hara, K. Matsumoto, Envelope disorder of Escherichia coli cells lacking phosphatidylglycerol. *Journal of bacteriology* **184**, 5418-5425 (2002).
50. K. Matsumoto, Dispensable nature of phosphatidylglycerol in Escherichia coli: dual roles of anionic phospholipids. *Molecular microbiology* **39**, 1427-1433 (2001).
51. W. Zheng, Z. Li, K. Skarstad, E. Crooke, Mutations in DnaA protein suppress the growth arrest of acidic phospholipid‐deficient Escherichia coli cells. *The EMBO journal* **20**, 1164-1172 (2001).
52. P. N. Heacock, W. Dowhan, Alteration of the phospholipid composition of Escherichia coli through genetic manipulation. *Journal of Biological Chemistry* **264**, 14972-14977 (1989).
53. T. De Vrije, R. De Swart, W. Dowhan, J. Tommassen, B. De Kruijff, Phosphatidylglycerol is involved in protein translocation across Escherichia coli inner membranes. *Nature* **334**, 173-175 (1988).
54. R. Kusters, W. Dowhan, B. De Kruijff, Negatively charged phospholipids restore prePhoE translocation across phosphatidylglycerol-depleted Escherichia coli inner membranes. *Journal of Biological Chemistry* **266**, 8659-8662 (1991).
55. E. Mileykovskaya, M. Zhang, W. Dowhan, Cardiolipin in energy transducing membranes. *Biochemistry (Moscow)* **70**, 154-158 (2005).
56. F. L. Hoch, Cardiolipins and biomembrane function. *Biochimica et biophysica acta* **1113**, 71-133 (1992).
57. J. Lecocq, C. E. Ballou, ON THE STRUCTURE OF CARDIOLIPIN. *Biochemistry* **3**, 976-980 (1964).
58. B. K. Tan *et al.*, Discovery of a cardiolipin synthase utilizing phosphatidylethanolamine and phosphatidylglycerol as substrates. *Proceedings of the National Academy of Sciences of the United States of America* **109**, 16504-16509 (2012).
59. S. Hiraoka, H. Matsuzaki, I. Shibuya, Active increase in cardiolipin synthesis in the stationary growth phase and its physiological significance in Escherichia coli. *FEBS letters* **336**, 221-224 (1993).
60. T. Romantsov, Z. Guan, J. M. Wood, Cardiolipin and the osmotic stress responses of bacteria. *Biochimica et biophysica acta* **1788**, 2092-2100 (2009).
61. M. Schlame, Thematic Review Series: Glycerolipids. Cardiolipin synthesis for the assembly of bacterial and mitochondrial membranes. *Journal of lipid research* **49**, 1607-1620 (2008).
62. C. B. Hirschberg, E. P. Kennedy, Mechanism of the enzymatic synthesis of cardiolipin in Escherichia coli. *Proceedings of the National Academy of Sciences* **69**, 648-651 (1972).
63. S. Hiraoka, K. Nukui, N. Uetake, A. Ohta, I. Shibuya, Amplification and substantial purification of cardiolipin synthase of Escherichia coli. *Journal of biochemistry* **110**, 443-449 (1991).
64. D. Guo, B. E. Tropp, A second Escherichia coli protein with CL synthase activity. *Biochimica et biophysica acta* **1483**, 263-274 (2000).
65. G. Pluschke, Y. Hirota, P. Overath, Function of phospholipids in Escherichia coli. Characterization of a mutant deficient in cardiolipin synthesis. *The Journal of biological chemistry* **253**, 5048-5055 (1978).

66. B. K. Tan *et al.*, Discovery of a cardiolipin synthase utilizing phosphatidylethanolamine and phosphatidylglycerol as substrates. *Proceedings of the National Academy of Sciences* **109**, 16504-16509 (2012).
67. R. N. Lewis, R. N. McElhaney, The physicochemical properties of cardiolipin bilayers and cardiolipin-containing lipid membranes. *Biochimica et biophysica acta* **1788**, 2069-2079 (2009).
68. M. Schlame, M. Ren, Y. Xu, M. L. Greenberg, I. Haller, Molecular symmetry in mitochondrial cardiolipins. *Chemistry and physics of lipids* **138**, 38-49 (2005).
69. E. Mileykovskaya, W. Dowhan, Cardiolipin membrane domains in prokaryotes and eukaryotes. *Biochimica et Biophysica Acta (BBA)-Biomembranes* **1788**, 2084-2091 (2009).
70. G. L. Powell, S.-W. Hui, Tetraoleoylpyrophosphatidic acid: a four acyl-chain lipid which forms a hexagonal II phase with high curvature. *Biophysical journal* **70**, 1402-1406 (1996).
71. R. Rand, S. Sengupta, Cardiolipin forms hexagonal structures with divalent cations. *Biochimica et Biophysica Acta (BBA)-Biomembranes* **255**, 484-492 (1972).
72. J. D. Unsay, K. Cosentino, Y. Subburaj, A. J. Garcia-Saez, Cardiolipin effects on membrane structure and dynamics. *Langmuir : the ACS journal of surfaces and colloids* **29**, 15878-15887 (2013).
73. V. W. Rowlett *et al.*, Impact of Membrane Phospholipid Alterations in Escherichia coli on Cellular Function and Bacterial Stress Adaptation. *Journal of bacteriology* **199**, (2017).
74. F. Kawai *et al.*, Cardiolipin domains in Bacillus subtilis marburg membranes. *Journal of bacteriology* **186**, 1475-1483 (2004).
75. E. Mileykovskaya, W. Dowhan, Visualization of phospholipid domains in Escherichia coli by using the cardiolipin-specific fluorescent dye 10-N-nonyl acridine orange. *Journal of bacteriology* **182**, 1172-1175 (2000).
76. C. M. Koppelman, T. Den Blaauwen, M. C. Duursma, R. M. Heeren, N. Nanninga, Escherichia coli minicell membranes are enriched in cardiolipin. *Journal of bacteriology* **183**, 6144-6147 (2001).
77. L. D. Renner, D. B. Weibel, Cardiolipin microdomains localize to negatively curved regions of Escherichia coli membranes. *Proceedings of the National Academy of Sciences* **108**, 6264-6269 (2011).
78. E. Mileykovskaya *et al.*, Cardiolipin binds nonyl acridine orange by aggregating the dye at exposed hydrophobic domains on bilayer surfaces. *FEBS letters* **507**, 187-190 (2001).
79. P. M. Oliver *et al.*, Localization of anionic phospholipids in Escherichia coli cells. *Journal of bacteriology* **196**, 3386-3398 (2014).
80. M. C. Pangborn, A simplified preparation of cardiolipin, with a note on purification of lecithin for serologic use. *The Journal of biological chemistry* **161**, 71-82 (1945).
81. C. Mereschkowsky, Uber natur und ursprung der chromatophoren im pflanzenreiche. *Biologisches Centralblatt* **25**, 293-604 (1905).
82. J. Dudek, Role of cardiolipin in mitochondrial signaling pathways. *Frontiers in cell and developmental biology* **5**, 90 (2017).

83. J. van Beilen *et al.*, RodZ and PgsA play intertwined roles in membrane homeostasis of Bacillus subtilis and resistance to weak organic acid stress. *Frontiers in microbiology* **7**, 1633 (2016).
84. A. Nishibori, J. Kusaka, H. Hara, M. Umeda, K. Matsumoto, Phosphatidylethanolamine domains and localization of phospholipid synthases in Bacillus subtilis membranes. *Journal of bacteriology* **187**, 2163-2174 (2005).
85. A. Reder, D. Höper, U. Gerth, M. Hecker, Contributions of individual σB-dependent general stress genes to oxidative stress resistance of Bacillus subtilis. *Journal of bacteriology* **194**, 3601-3610 (2012).
86. C. S. Lopez, A. F. Alice, H. Heras, E. A. Rivas, C. Sanchez-Rivas, Role of anionic phospholipids in the adaptation of Bacillus subtilis to high salinity. *Microbiology* **152**, 605-616 (2006).
87. L. I. Salzberg, J. D. Helmann, Phenotypic and transcriptomic characterization of Bacillus subtilis mutants with grossly altered membrane composition. *Journal of bacteriology* **190**, 7797-7807 (2008).
88. P. Jorasch, F. P. Wolter, U. Zähringer, E. Heinz, A UDP glucosyltransferase from Bacillus subtilis successively transfers up to four glucose residues to 1, 2‐diacylglycerol: expression of ypfP in Escherichia coli and structural analysis of its reaction products. *Molecular microbiology* **29**, 419-430 (1998).
89. L. E. Cybulski, G. Del Solar, P. O. Craig, M. Espinosa, D. De Mendoza, Bacillus subtilis DesR functions as a phosphorylation-activated switch to control membrane lipid fluidity. *Journal of Biological Chemistry* **279**, 39340-39347 (2004).
90. G. E. Schujman, L. Paoletti, A. D. Grossman, D. de Mendoza, FapR, a bacterial transcription factor involved in global regulation of membrane lipid biosynthesis. *Developmental cell* **4**, 663-672 (2003).
91. C. S. López, H. Heras, S. M. Ruzal, C. Sánchez-Rivas, E. A. Rivas, Variations of the envelope composition of Bacillus subtilis during growth in hyperosmotic medium. *Current microbiology* **36**, 55-61 (1998).
92. D. Minnikin, H. Abdolrahimzadeh, Effect of pH on the proportions of polar lipids, in chemostat cultures of Bacillus subtilis. *Journal of bacteriology* **120**, 999-1003 (1974).
93. I. Barák, K. Muchová, A. J. Wilkinson, P. J. O'Toole, N. Pavlendová, Lipid spirals in Bacillus subtilis and their role in cell division. *Molecular microbiology* **68**, 1315-1327 (2008).
94. Y. Wu, F. L. Yeh, F. Mao, E. R. Chapman, Biophysical characterization of styryl dye-membrane interactions. *Biophysical journal* **97**, 101-109 (2009).
95. I. Fishov, C. L. Woldringh, Visualization of membrane domains in Escherichia coli. *Molecular microbiology* **32**, 1166-1172 (1999).
96. E. Mileykovskaya, W. Dowhan, Role of membrane lipids in bacterial division-site selection. *Current opinion in microbiology* **8**, 135-142 (2005).
97. J. Gidden, J. Denson, R. Liyanage, D. M. Ivey, J. O. Lay Jr, Lipid compositions in Escherichia coli and Bacillus subtilis during growth as determined by MALDI-TOF and TOF/TOF mass spectrometry. *International journal of mass spectrometry* **283**, 178-184 (2009).

98. J. L. Ramos *et al.*, Responses of Gram-negative bacteria to certain environmental stressors. *Current opinion in microbiology* **4**, 166-171 (2001).
99. B. D. Needham, M. S. Trent, Fortifying the barrier: the impact of lipid A remodelling on bacterial pathogenesis. *Nature Reviews Microbiology* **11**, 467-481 (2013).
100. J. Cronan Jr, R. Gennis, S. Maloy, Cytoplasmic membrane. *Escherichia coli and Salmonella typhimurium: cellular and molecular biology. American Society for Microbiology, Washington, DC*, 31-55 (1987).
101. R. N. McElhaney, in *Current topics in membranes and transport*. (Elsevier, 1982), vol. 17, pp. 317-380.
102. S. Morein, A.-S. Andersson, L. Rilfors, G. Lindblom, Wild-type Escherichia coli cells regulate the membrane lipid composition in a window between gel and non-lamellar structures. *Journal of Biological Chemistry* **271**, 6801-6809 (1996).
103. J. R. Hazel, Thermal adaptation in biological membranes: is homeoviscous adaptation the explanation? *Annual review of physiology* **57**, 19-42 (1995).
104. A. R. Cossins, *Temperature adaptation of biological membranes*. (Portland Press, 1994).
105. A. Krogh, B. Larsson, G. Von Heijne, E. L. Sonnhammer, Predicting transmembrane protein topology with a hidden Markov model: application to complete genomes. *Journal of molecular biology* **305**, 567-580 (2001).
106. G. von Heijne, Recent advances in the understanding of membrane protein assembly and structure. *Quarterly reviews of biophysics* **32**, 285-307 (1999).
107. J. W. De Gier, J. Luirink, Biogenesis of inner membrane proteins in Escherichia coli. *Molecular microbiology* **40**, 314-322 (2001).
108. R. J. Keenan, D. M. Freymann, R. M. Stroud, P. Walter, The signal recognition particle. *Annual review of biochemistry* **70**, 755-775 (2001).
109. R. S. Ullers *et al.*, Sequence-specific interactions of nascent Escherichia coli polypeptides with trigger factor and signal recognition particle. *Journal of Biological Chemistry* **281**, 13999-14005 (2006).
110. D. Schibich *et al.*, Global profiling of SRP interaction with nascent polypeptides. *Nature* **536**, 219-223 (2016).
111. J. D. Miller, H. D. Bernstein, P. Walter, Interaction of E. coli Ffh/4.5 S ribonucleoprotein and FtsY mimics that of mammalian signal recognition particle and its receptor. *Nature* **367**, 657-659 (1994).
112. Y. Zhou, T. Ueda, M. Müller, Signal recognition particle and SecA cooperate during export of secretory proteins with highly hydrophobic signal sequences. *PloS one* **9**, (2014).
113. X. Zhang, R. Rashid, K. Wang, S.-o. Shan, Sequential checkpoints govern substrate selection during cotranslational protein targeting. *Science (New York, N.Y.)* **328**, 757-760 (2010).
114. A. G. Lee, How lipids and proteins interact in a membrane: a molecular approach. *Molecular BioSystems* **1**, 203-212 (2005).
115. M. Ø. Jensen, O. G. Mouritsen, Lipids do influence protein function—the hydrophobic matching hypothesis revisited. *Biochimica et Biophysica Acta (BBA)-Biomembranes* **1666**, 205-226 (2004).

116. H. R. Kaback *et al.*, The lactose permease meets Frankenstein. *Journal of Experimental Biology* **196**, 183-195 (1994).
117. R. E. Dalbey, Leader peptidase. *Molecular microbiology* **5**, 2855-2860 (1991).
118. B. D. Rao, S. Shrivastava, A. Chattopadhyay, in *Membrane Organization and Dynamics*. (Springer, 2017), pp. 375-387.
119. M. R. de Planque, J. A. Killian*, Protein–lipid interactions studied with designed transmembrane peptides: role of hydrophobic matching and interfacial anchoring. *Molecular membrane biology* **20**, 271-284 (2003).
120. M. Venturoli, B. Smit, M. M. Sperotto, Simulation studies of protein-induced bilayer deformations, and lipid-induced protein tilting, on a mesoscopic model for lipid bilayers with embedded proteins. *Biophysical journal* **88**, 1778-1798 (2005).
121. J. Ren, S. Lew, J. Wang, E. London, Control of the transmembrane orientation and interhelical interactions within membranes by hydrophobic helix length. *Biochemistry* **38**, 5905-5912 (1999).
122. S. Mall, R. Broadbridge, R. P. Sharma, J. M. East, A. G. Lee, Self-association of model transmembrane α-helices is modulated by lipid structure. *Biochemistry* **40**, 12379-12386 (2001).
123. S. Özdirekcan, D. T. Rijkers, R. M. Liskamp, J. A. Killian, Influence of flanking residues on tilt and rotation angles of transmembrane peptides in lipid bilayers. A solid-state 2H NMR study. *Biochemistry* **44**, 1004-1012 (2005).
124. E. Strandberg *et al.*, Tilt angles of transmembrane model peptides in oriented and non-oriented lipid bilayers as determined by 2H solid-state NMR. *Biophysical journal* **86**, 3709-3721 (2004).
125. J. A. Killian, T. K. Nyholm, Peptides in lipid bilayers: the power of simple models. *Current opinion in structural biology* **16**, 473-479 (2006).
126. K. F. Jarrell, M. J. McBride, The surprisingly diverse ways that prokaryotes move. *Nature Reviews Microbiology* **6**, 466-476 (2008).
127. M. Silverman, M. Simon, Flagellar rotation and the mechanism of bacterial motility. *Nature* **249**, 73-74 (1974).
128. H. C. Berg, The rotary motor of bacterial flagella. *Annual review of biochemistry* **72**, (2003).
129. S. A. Lloyd, H. Tang, X. Wang, S. Billings, D. F. Blair, Torque generation in the flagellar motor of Escherichia coli: evidence of a direct role for FliG but not for FliM or FliN. *Journal of bacteriology* **178**, 223-231 (1996).
130. N. R. Francis, G. E. Sosinsky, D. Thomas, D. J. DeRosier, Isolation, characterization and structure of bacterial flagellar motors containing the switch complex. *Journal of molecular biology* **235**, 1261-1270 (1994).
131. N. R. Francis, V. M. Irikura, S. Yamaguchi, D. J. DeRosier, R. M. Macnab, Localization of the Salmonella typhimurium flagellar switch protein FliG to the cytoplasmic M-ring face of the basal body. *Proceedings of the National Academy of Sciences* **89**, 6304-6308 (1992).
132. M. A. Mathews, H. L. Tang, D. F. Blair, Domain Analysis of the FliM Protein ofEscherichia coli. *Journal of bacteriology* **180**, 5580-5590 (1998).
133. A. Bren, M. Eisenbach. (Elsevier, 1998).
134. K. Paul, D. F. Blair, Organization of FliN subunits in the flagellar motor of Escherichia coli. *Journal of bacteriology* **188**, 2502-2511 (2006).

135. R. M. Macnab, Genetics and biogenesis of bacterial flagella. *Annual review of genetics* **26**, 131-158 (1992).
136. R. M. Macnab, Bacterial flagella rotating in bundles: a study in helical geometry. *Proceedings of the National Academy of Sciences* **74**, 221-225 (1977).
137. L. Turner, A. S. Stern, H. C. Berg, Growth of flagellar filaments of Escherichia coli is independent of filament length. *Journal of bacteriology* **194**, 2437-2442 (2012).
138. I. A. Hajam, P. A. Dar, I. Shahnawaz, J. C. Jaume, J. H. Lee, Bacterial flagellin—a potent immunomodulatory agent. *Experimental & molecular medicine* **49**, e373-e373 (2017).
139. M. Homma, H. Fujita, S. Yamaguchi, T. Iino, Excretion of unassembled flagellin by Salmonella typhimurium mutants deficient in hook-associated proteins. *Journal of bacteriology* **159**, 1056-1059 (1984).
140. T. Ikeda, M. Homma, T. Iino, S. Asakura, R. Kamiya, Localization and stoichiometry of hook-associated proteins within Salmonella typhimurium flagella. *Journal of bacteriology* **169**, 1168-1173 (1987).
141. G. S. Chilcott, K. T. Hughes, Coupling of Flagellar Gene Expression to Flagellar Assembly in Salmonella enterica Serovar Typhimurium andEscherichia coli. *Microbiol. Mol. Biol. Rev.* **64**, 694-708 (2000).
142. F. F. Chevance, K. T. Hughes, Coordinating assembly of a bacterial macromolecular machine. *Nature Reviews Microbiology* **6**, 455-465 (2008).
143. O. A. Soutourina, P. N. Bertin, Regulation cascade of flagellar expression in Gram-negative bacteria. *FEMS microbiology reviews* **27**, 505-523 (2003).
144. S. Shin, C. Park, Modulation of flagellar expression in Escherichia coli by acetyl phosphate and the osmoregulator OmpR. *Journal of bacteriology* **177**, 4696-4702 (1995).
145. O. A. Soutourina *et al.*, Regulation of bacterial motility in response to low pH in Escherichia coli: the role of H-NS protein. *Microbiology* **148**, 1543-1551 (2002).
146. W. Shi, C. Li, C. Louise, J. Adler, Mechanism of adverse conditions causing lack of flagella in Escherichia coli. *Journal of bacteriology* **175**, 2236-2240 (1993).
147. N. De Lay, S. Gottesman, A complex network of small non‐coding RNAs regulate motility in E scherichia coli. *Molecular microbiology* **86**, 524-538 (2012).
148. O. Soutourina *et al.*, Multiple control of flagellum biosynthesis in Escherichia coli: role of H-NS protein and the cyclic AMP-catabolite activator protein complex in transcription of the flhDC master operon. *Journal of bacteriology* **181**, 7500-7508 (1999).
149. K. Kutsukake, Y. Ohya, T. Iino, Transcriptional analysis of the flagellar regulon of Salmonella typhimurium. *Journal of bacteriology* **172**, 741-747 (1990).
150. X. Liu, P. Matsumura, The FlhD/FlhC complex, a transcriptional activator of the Escherichia coli flagellar class II operons. *Journal of bacteriology* **176**, 7345-7351 (1994).
151. Y. Komeda, Transcriptional control of flagellar genes in Escherichia coli K-12. *Journal of bacteriology* **168**, 1315-1318 (1986).

152. G. W. Daughdrill, M. S. Chadsey, J. E. Karlinsey, K. T. Hughes, F. W. Dahlquist, The C-terminal half of the anti-sigma factor, FlgM, becomes structured when bound to its target, σ 28. *Nature structural biology* **4**, 285-291 (1997).
153. D. M. Fitzgerald, R. P. Bonocora, J. T. Wade, Comprehensive mapping of the Escherichia coli flagellar regulatory network. *PLoS genetics* **10**, (2014).
154. K. Hollands, D. J. Lee, G. S. Lloyd, S. J. Busby, Activation of σ 28 - dependent transcription in Escherichia coli by the cyclic AMP receptor protein requires an unusual promoter organization. *Molecular microbiology* **75**, 1098-1111 (2010).
155. T. K. Kundu, S. Kusano, A. Ishihama, Promoter selectivity of Escherichia coli RNA polymerase sigmaF holoenzyme involved in transcription of flagellar and chemotaxis genes. *Journal of bacteriology* **179**, 4264-4269 (1997).
156. K. Zhao, M. Liu, R. R. Burgess, Adaptation in bacterial flagellar and motility systems: from regulon members to 'foraging'-like behavior in E. coli. *Nucleic acids research* **35**, 4441-4452 (2007).
157. M. Ko, C. Park, Two novel flagellar components and H-NS are involved in the motor function of Escherichia coli. *Journal of molecular biology* **303**, 371-382 (2000).
158. X. Liu, P. Matsumura, Differential regulation of multiple overlapping promoters in flagellar class II operons in Escherichia coli. *Molecular microbiology* **21**, 613-620 (1996).
159. S. Kalir, U. Alon, Using a quantitative blueprint to reprogram the dynamics of the flagella gene network. *Cell* **117**, 713-720 (2004).
160. J. Adler, Chemoreceptors in bacteria. *Science (New York, N.Y.)* **166**, 1588-1597 (1969).
161. G. H. Wadhams, J. P. Armitage, Making sense of it all: bacterial chemotaxis. *Nature reviews. Molecular cell biology* **5**, 1024-1037 (2004).
162. R. M. Harshey, Bacterial motility on a surface: many ways to a common goal. *Annual Reviews in Microbiology* **57**, 249-273 (2003).
163. M. D. Manson, P. Tedesco, H. C. Berg, F. M. Harold, C. Van der Drift, A protonmotive force drives bacterial flagella. *Proceedings of the National Academy of Sciences* **74**, 3060-3064 (1977).
164. H. C. Berg, D. A. Brown, Chemotaxis in Escherichia coli analysed by three-dimensional tracking. *Nature* **239**, 500-504 (1972).
165. L. Turner, W. S. Ryu, H. C. Berg, Real-time imaging of fluorescent flagellar filaments. *Journal of bacteriology* **182**, 2793-2801 (2000).
166. V. Sourjik, H. C. Berg, Functional interactions between receptors in bacterial chemotaxis. *Nature* **428**, 437-441 (2004).
167. N. Vladimirov, V. Sourjik, Chemotaxis: how bacteria use memory. *Biological chemistry* **390**, 1097-1104 (2009).
168. M. J. Tindall, E. A. Gaffney, P. K. Maini, J. P. Armitage, Theoretical insights into bacterial chemotaxis. *Wiley Interdisciplinary Reviews: Systems Biology and Medicine* **4**, 247-259 (2012).
169. H. Levine, W.-J. Rappel, The physics of eukaryotic chemotaxis. *Physics today* **66**, (2013).

170. S. H. Kim, G. G. Prive, J. Yeh, W. G. Scott, M. V. Milburn, A model for transmembrane signaling in a bacterial chemotaxis receptor. *Cold Spring Harbor symposia on quantitative biology* **57**, 17-24 (1992).
171. J. S. Parkinson, G. L. Hazelbauer, J. J. Falke, Signaling and sensory adaptation in Escherichia coli chemoreceptors: 2015 update. *Trends Microbiol* **23**, 257-266 (2015).
172. V. Sourjik, Receptor clustering and signal processing in E. coli chemotaxis. *Trends Microbiol* **12**, 569-576 (2004).
173. J. E. Segall, M. D. Manson, H. C. Berg, Signal processing times in bacterial chemotaxis. *Nature* **296**, 855-857 (1982).
174. N. Barkai, S. Leibler, Robustness in simple biochemical networks. *Nature* **387**, 913-917 (1997).
175. D. N. Amin, G. L. Hazelbauer, The chemoreceptor dimer is the unit of conformational coupling and transmembrane signaling. *Journal of bacteriology* **192**, 1193-1200 (2010).
176. U. Alon, M. G. Surette, N. Barkai, S. Leibler, Robustness in bacterial chemotaxis. *Nature* **397**, 168-171 (1999).
177. V. Sourjik, H. C. Berg, Receptor sensitivity in bacterial chemotaxis. *Proceedings of the National Academy of Sciences* **99**, 123-127 (2002).
178. H. C. Berg, P. Tedesco, Transient response to chemotactic stimuli in Escherichia coli. *Proceedings of the National Academy of Sciences* **72**, 3235-3239 (1975).
179. S. Neumann, C. H. Hansen, N. S. Wingreen, V. Sourjik, Differences in signalling by directly and indirectly binding ligands in bacterial chemotaxis. *The EMBO journal* **29**, 3484-3495 (2010).
180. V. Sourjik, Receptor clustering and signal processing in E. coli chemotaxis. *Trends in Microbiology* **12**, 569-576 (2004).
181. V. Sourjik, A. Vaknin, T. S. Shimizu, H. C. Berg, In vivo measurement by FRET of pathway activity in bacterial chemotaxis. *Methods in enzymology* **423**, 365-391 (2007).
182. Y. Zhang *et al.*, Model of maltose-binding protein/chemoreceptor complex supports intrasubunit signaling mechanism. *Proceedings of the National Academy of Sciences* **96**, 939-944 (1999).
183. Y. Yang *et al.*, Relation between chemotaxis and consumption of amino acids in bacteria. *Molecular microbiology* **96**, 1272-1282 (2015).
184. W. Abouhamad, M. Manson, M. Gibson, C. Higgins, Peptide transport and chemotaxis in Escherichia coli and Salmonella typhimurium: characterization of the dipeptide permease (Dpp) and the dipeptide‐binding protein. *Molecular microbiology* **5**, 1035-1047 (1991).
185. H. Kondoh, C. B. Ball, J. Adler, Identification of a methyl-accepting chemotaxis protein for the ribose and galactose chemoreceptors of Escherichia coli. *Proceedings of the National Academy of Sciences* **76**, 260-264 (1979).
186. H. Salman, A. Libchaber, A concentration-dependent switch in the bacterial response to temperature. *Nature cell biology* **9**, 1098-1100 (2007).
187. T. Nara, L. Lee, Y. Imae, Thermosensing ability of Trg and Tap chemoreceptors in Escherichia coli. *Journal of bacteriology* **173**, 1120-1124 (1991).

188. T. Mizuno, Y. Imae, Conditional inversion of the thermoresponse in Escherichia coli. *Journal of bacteriology* **159**, 360-367 (1984).
189. A. Repik *et al.*, PAS domain residues involved in signal transduction by the Aer redox sensor of Escherichia coli. *Molecular microbiology* **36**, 806-816 (2000).
190. B. L. Taylor, I. B. Zhulin, M. S. Johnson, Aerotaxis and other energy-sensing behavior in bacteria. *Annual Reviews in Microbiology* **53**, 103-128 (1999).
191. S. I. Bibikov, A. C. Miller, K. K. Gosink, J. S. Parkinson, Methylation-independent aerotaxis mediated by the Escherichia coli Aer protein. *Journal of bacteriology* **186**, 3730-3737 (2004).
192. C. A. Adase, R. R. Draheim, G. Rueda, R. Desai, M. D. Manson, Residues at the cytoplasmic end of transmembrane helix 2 determine the signal output of the Tar Ec chemoreceptor. *Biochemistry* **52**, 2729-2738 (2013).
193. P. Ames, Q. Zhou, J. S. Parkinson, HAMP domain structural determinants for signalling and sensory adaptation in Tsr, the E scherichia coli serine chemoreceptor. *Molecular microbiology* **91**, 875-886 (2014).
194. P. Ames, Q. Zhou, J. S. Parkinson, Mutational analysis of the connector segment in the HAMP domain of Tsr, the Escherichia coli serine chemoreceptor. *Journal of bacteriology* **190**, 6676-6685 (2008).
195. P. Mowery, J. B. Ostler, J. S. Parkinson, Different signaling roles of two conserved residues in the cytoplasmic hairpin tip of Tsr, the Escherichia coli serine chemoreceptor. *Journal of bacteriology* **190**, 8065-8074 (2008).
196. R. R. Draheim, A. F. Bormans, R.-Z. Lai, M. D. Manson, Tuning a bacterial chemoreceptor with protein− membrane interactions. *Biochemistry* **45**, 14655-14664 (2006).
197. S. Bi, V. Sourjik, Stimulus sensing and signal processing in bacterial chemotaxis. *Current opinion in microbiology* **45**, 22-29 (2018).
198. J. E. Gestwicki, L. E. Strong, L. L. Kiessling, Tuning chemotactic responses with synthetic multivalent ligands. *Chemistry & biology* **7**, 583-591 (2000).
199. J. S. Parkinson, P. Ames, C. A. Studdert, Collaborative signaling by bacterial chemoreceptors. *Current opinion in microbiology* **8**, 116-121 (2005).
200. P. Ames, C. A. Studdert, R. H. Reiser, J. S. Parkinson, Collaborative signaling by mixed chemoreceptor teams in Escherichia coli. *Proceedings of the National Academy of Sciences* **99**, 7060-7065 (2002).
201. K. K. Kim, H. Yokota, S. H. Kim, Four-helical-bundle structure of the cytoplasmic domain of a serine chemotaxis receptor. *Nature* **400**, 787-792 (1999).
202. M. Li, G. L. Hazelbauer, Core unit of chemotaxis signaling complexes. *Proceedings of the National Academy of Sciences* **108**, 9390-9395 (2011).
203. M. Koler, E. Peretz, C. Aditya, T. S. Shimizu, A. Vaknin, Long-term positioning and polar preference of chemoreceptor clusters in E. coli. *Nature communications* **9**, 1-10 (2018).

204. P. Zhang, C. M. Khursigara, L. M. Hartnell, S. Subramaniam, Direct visualization of Escherichia coli chemotaxis receptor arrays using cryo-electron microscopy. *Proceedings of the National Academy of Sciences* **104**, 3777-3781 (2007).
205. J. Skidmore *et al.*, Polar Clustering of the Chemoreceptor Complex inEscherichia coli Occurs in the Absence of Complete CheA Function. *Journal of bacteriology* **182**, 967-973 (2000).
206. V. Sourjik, H. C. Berg, Localization of components of the chemotaxis machinery of Escherichia coli using fluorescent protein fusions. *Molecular microbiology* **37**, 740-751 (2000).
207. C. A. Haselwandter, N. S. Wingreen, The role of membrane-mediated interactions in the assembly and architecture of chemoreceptor lattices. *PLoS computational biology* **10**, (2014).
208. A. M. Pollard, V. Sourjik, Transmembrane region of bacterial chemoreceptor is capable of promoting protein clustering. *Journal of Biological Chemistry* **293**, 2149-2158 (2018).
209. S. R. Lybarger, U. Nair, A. A. Lilly, G. L. Hazelbauer, J. R. Maddock, Clustering requires modified methyl‐accepting sites in low‐abundance but not high‐abundance chemoreceptors of Escherichia coli. *Molecular microbiology* **56**, 1078-1086 (2005).
210. S. Lybarger, J. Maddock, Differences in the polar clustering of the high- and low-abundance chemoreceptors of Escherichia coli. *Proceedings of the National Academy of Sciences* **97**, 8057-8062 (2000).
211. S. Bi, A. M. Pollard, Y. Yang, F. Jin, V. Sourjik, Engineering hybrid chemotaxis receptors in bacteria. *ACS synthetic biology* **5**, 989-1001 (2016).
212. G. E. Piñas, V. Frank, A. Vaknin, J. S. Parkinson, The source of high signal cooperativity in bacterial chemosensory arrays. *Proceedings of the National Academy of Sciences* **113**, 3335-3340 (2016).
213. J. R. Maddock, L. Shapiro, Polar location of the chemoreceptor complex in the Escherichia coli cell. *Science (New York, N.Y.)* **259**, 1717-1723 (1993).
214. G. L. Hazelbauer, J. J. Falke, J. S. Parkinson, Bacterial chemoreceptors: high-performance signaling in networked arrays. *Trends in biochemical sciences* **33**, 9-19 (2008).
215. D. Shiomi, M. Yoshimoto, M. Homma, I. Kawagishi, Helical distribution of the bacterial chemoreceptor via colocalization with the Sec protein translocation machinery. *Molecular microbiology* **60**, 894-906 (2006).
216. J. A. Gegner, D. R. Graham, A. F. Roth, F. W. Dahlquist, Assembly of an MCP receptor, CheW, and kinase CheA complex in the bacterial chemotaxis signal transduction pathway. *Cell* **70**, 975-982 (1992).
217. G. Li, R. M. Weis, Covalent modification regulates ligand binding to receptor complexes in the chemosensory system of Escherichia coli. *Cell* **100**, 357-365 (2000).
218. S. Schulmeister *et al.*, Protein exchange dynamics at chemoreceptor clusters in Escherichia coli. *Proceedings of the National Academy of Sciences of the United States of America* **105**, 6403-6408 (2008).
219. W. Draper, J. Liphardt, Origins of chemoreceptor curvature sorting in Escherichia coli. *Nature communications* **8**, 14838 (2017).

220. K. A. Borkovich, N. Kaplan, J. F. Hess, M. I. Simon, Transmembrane signal transduction in bacterial chemotaxis involves ligand-dependent activation of phosphate group transfer. *Proceedings of the National Academy of Sciences* **86**, 1208-1212 (1989).
221. L. F. Garrity, G. W. Ordal, Activation of the CheA kinase by asparagine in Bacillus subtilis chemotaxis. *Microbiology* **143**, 2945-2951 (1997).
222. P. Cluzel, M. Surette, S. Leibler, An ultrasensitive bacterial motor revealed by monitoring signaling proteins in single cells. *Science (New York, N.Y.)* **287**, 1652-1655 (2000).
223. D. S. Bischoff, R. B. Bourret, M. L. Kirsch, G. W. Ordal, Purification and characterization of Bacillus subtilis CheY. *Biochemistry* **32**, 9256-9261 (1993).
224. M. A. Zimmer, J. Tiu, M. A. Collins, G. W. Ordal, Selective methylation changes on the Bacillus subtilis chemotaxis receptor McpB promote adaptation. *Journal of biological chemistry* **275**, 24264-24272 (2000).
225. M. M. L. Rosario, J. R. Kirby, D. A. Bochar, G. W. Ordal, Chemotactic methylation and behavior in Bacillus subtilis: role of two unique proteins, CheC and CheD. *Biochemistry* **34**, 3823-3831 (1995).
226. C. J. Kristich, G. W. Ordal, Bacillus subtilis CheD is a chemoreceptor modification enzyme required for chemotaxis. *Journal of biological chemistry* **277**, 25356-25362 (2002).
227. E. Karatan, M. M. Saulmon, M. W. Bunn, G. W. Ordal, Phosphorylation of the response regulator CheV is required for adaptation to attractants during Bacillus subtilischemotaxis. *Journal of Biological Chemistry* **276**, 43618-43626 (2001).
228. E. Ward *et al.*, Organization of the flagellar switch complex of Bacillus subtilis. *Journal of bacteriology* **201**, e00626-00618 (2019).
229. C. V. Rao, J. R. Kirby, A. P. Arkin, Design and diversity in bacterial chemotaxis: a comparative study in Escherichia coli and Bacillus subtilis. *PLoS biology* **2**, (2004).
230. M. A. Zimmer *et al.*, The role of heterologous receptors in McpB‐mediated signalling in Bacillus subtilis chemotaxis. *Molecular microbiology* **45**, 555-568 (2002).
231. P. Tohidifar, M. J. Plutz, G. W. Ordal, C. V. Rao, The mechanism of bidirectional pH taxis in Bacillus subtilis. *Journal of bacteriology* **202**, (2020).
232. G. D. Glekas *et al.*, The Bacillus subtilis chemoreceptor McpC senses multiple ligands using two discrete mechanisms. *Journal of Biological Chemistry* **287**, 39412-39418 (2012).
233. S. Hou *et al.*, Myoglobin-like aerotaxis transducers in Archaea and Bacteria. *Nature* **403**, 540 (2000).
234. P. P. Cherepanov, W. Wackernagel, Gene disruption in Escherichia coli: TcR and KmR cassettes with the option of Flp-catalyzed excision of the antibiotic-resistance determinant. *Gene* **158**, 9-14 (1995).
235. A. Zaslaver *et al.*, A comprehensive library of fluorescent transcriptional reporters for Escherichia coli. *Nature methods* **3**, 623 (2006).
236. D. Kentner, S. Thiem, M. Hildenbeutel, V. Sourjik, Determinants of chemoreceptor cluster formation in Escherichia coli. *Molecular microbiology* **61**, 407-417 (2006).

237. M. Kumar, M. S. Mommer, V. Sourjik, Mobility of cytoplasmic, membrane, and DNA-binding proteins in Escherichia coli. *Biophysical journal* **98**, 552-559 (2010).
238. S. Bi, F. Jin, V. Sourjik, Inverted signaling by bacterial chemotaxis receptors. *Nature communications* **9**, 1-13 (2018).
239. T. Baba *et al.*, Construction of Escherichia coli K‐12 in‐frame, single‐gene knockout mutants: the Keio collection. *Molecular systems biology* **2**, (2006).
240. L. C. Thomason, N. Costantino, D. L. Court, E. coli genome manipulation by P1 transduction. *Current protocols in molecular biology* **79**, 1.17. 11-11.17. 18 (2007).
241. A. Paintdakhi *et al.*, Oufti: an integrated software package for high-accuracy, high-throughput quantitative microscopy analysis. *Molecular microbiology* **99**, 767-777 (2016).
242. O. Sliusarenko, J. Heinritz, T. Emonet, C. Jacobs-Wagner, High-throughput, subpixel precision analysis of bacterial morphogenesis and intracellular spatio-temporal dynamics. *Molecular microbiology* **80**, 612-627 (2011).
243. M. Version. (Natick, MA: The MathWorks, Inc, 2014).
244. P. R. Selvin, The renaissance of fluorescence resonance energy transfer. *Nature Structural & Molecular Biology* **7**, 730 (2000).
245. B. Herman, in *Methods in cell biology*. (Elsevier, 1989), vol. 30, pp. 219-243.
246. J. Schindelin *et al.*, Fiji: an open-source platform for biological-image analysis. *Nature methods* **9**, 676 (2012).
247. J. M. Wood, Osmosensing by bacteria: signals and membrane-based sensors. *Microbiol. Mol. Biol. Rev.* **63**, 230-262 (1999).
248. T. Romantsov *et al.*, Cardiolipin promotes polar localization of osmosensory transporter ProP in Escherichia coli. *Molecular microbiology* **64**, 1455-1465 (2007).
249. S. V. MacMillan *et al.*, The ion coupling and organic substrate specificities of osmoregulatory transporter ProP in Escherichia coli. *Biochimica et Biophysica Acta (BBA)-Biomembranes* **1420**, 30-44 (1999).
250. F. Lang, Mechanisms and significance of cell volume regulation. *Journal of the American college of nutrition* **26**, 613S-623S (2007).
251. S. D. McNeil, M. L. Nuccio, A. D. Hanson, Betaines and related osmoprotectants. Targets for metabolic engineering of stress resistance. *Plant Physiology* **120**, 945-949 (1999).
252. L. N. Csonka, Physiological and genetic responses of bacteria to osmotic stress. *Microbiology and Molecular Biology Reviews* **53**, 121-147 (1989).
253. R. W. Jones, R. Storey, in *The physiology and biochemistry of drought resistance in plants*. (Academic Press Sydney, 1981), pp. 171-204.
254. A. Pollard, R. W. Jones, Enzyme activities in concentrated solutions of glycinebetaine and other solutes. *Planta* **144**, 291-298 (1979).
255. W. G. Roth, M. P. Leckie, D. N. Dietzler, Restoration of colony-forming activity in osmotically stressed Escherichia coli by betaine. *Appl. Environ. Microbiol.* **54**, 3142-3146 (1988).
256. B. Perroud, D. Le Rudulier, Glycine betaine transport in Escherichia coli: osmotic modulation. *Journal of bacteriology* **161**, 393-401 (1985).

257. D. Landman, C. Georgescu, D. A. Martin, J. Quale, Polymyxins revisited. *Clinical microbiology reviews* **21**, 449-465 (2008).
258. T. Velkov, K. D. Roberts, R. L. Nation, P. E. Thompson, J. Li, Pharmacology of polymyxins: new insights into an 'old'class of antibiotics. *Future microbiology* **8**, 711-724 (2013).
259. T. Preobrazhenskaia, E. Korepanova, I. Vladimirov, Comparative effect of polymyxin B on lipid bilayer membranes with different lipid composition. *Biofizika* **39**, 1021-1024 (1994).
260. A. Kwa, S. K. Kasiakou, V. H. Tam, M. E. Falagas, Polymyxin B: similarities to and differences from colistin (polymyxin E). *Expert review of anti-infective therapy* **5**, 811-821 (2007).
261. M. E. Evans, D. J. Feola, R. P. Rapp, Polymyxin B sulfate and colistin: old antibiotics for emerging multiresistant gram-negative bacteria. *Annals of Pharmacotherapy* **33**, 960-967 (1999).
262. E. Goldman, L. H. Green, *Practical handbook of microbiology*. (CRC press, 2015).
263. K. D. Young, Bacterial morphology: why have different shapes? *Current opinion in microbiology* **10**, 596-600 (2007).
264. P. Nonejuie, M. Burkart, K. Pogliano, J. Pogliano, Bacterial cytological profiling rapidly identifies the cellular pathways targeted by antibacterial molecules. *Proceedings of the National Academy of Sciences* **110**, 16169-16174 (2013).
265. N. Grandgenett, Kaleidagraph. *Mathematics and Computer Education* **38**, 341 (2004).
266. J. Adler, Chemotaxis in bacteria. *Science (New York, N.Y.)* **153**, 708-716 (1966).
267. O. A. Croze, G. P. Ferguson, M. E. Cates, W. C. Poon, Migration of chemotactic bacteria in soft agar: role of gel concentration. *Biophysical journal* **101**, 525-534 (2011).
268. R. Mesibov, G. W. Ordal, J. Adler, The range of attractant concentrations for bacterial chemotaxis and the threshold and size of response over this range: Weber law and related phenomena. *The Journal of general physiology* **62**, 203-223 (1973).
269. V. Sourjik, H. C. Berg, Localization of components of the chemotaxis machinery of Escherichia coli using fluorescent protein fusions. *Molecular microbiology* **37**, 740-751 (2000).
270. R. G. Endres, Polar chemoreceptor clustering by coupled trimers of dimers. *Biophysical journal* **96**, 453-463 (2009).
271. B. Herman, Fluorescence microscopy. *Current protocols in immunology* **Chapter 21**, Unit 21.22 (2002).
272. J. Pogliano, K. Pogliano, D. S. Weiss, R. Losick, J. Beckwith, Inactivation of FtsI inhibits constriction of the FtsZ cytokinetic ring and delays the assembly of FtsZ rings at potential division sites. *Proceedings of the National Academy of Sciences* **94**, 559-564 (1997).
273. D. Shiomi, H. Niki, A mutation in the promoter region of zipA, a component of the divisome, suppresses the shape defect of RodZ‐deficient cells. *MicrobiologyOpen* **2**, 798-810 (2013).
274. G. Friedlander, C. Le Grimellec, M.-C. Giocondi, C. Amiel, Benzyl alcohol increases membrane fluidity and modulates cyclic AMP synthesis in

intact renal epithelial cells. *Biochimica et Biophysica Acta (BBA)-Biomembranes* **903**, 341-348 (1987).
275. I. West, Lactose transport coupled to proton movements in Escherichia coli. *Biochemical and biophysical research communications* **41**, 655-661 (1970).
276. R. White, The role of the phosphoenolpyruvate phosphotransferase system in the transport of N-acetyl-D-glucosamine by Escherichia coli. *Biochemical Journal* **118**, 89-92 (1970).
277. J. Lissemore, J. Jankowski, C. Thomas, D. Mascotti, P. DeHaseth, Green fluorescent protein as a quantitative reporter of relative promoter activity in E. coli. *Biotechniques* **28**, 82-89 (2000).
278. M. Okada, H. Matsuzaki, I. Shibuya, K. Matsumoto, Cloning, sequencing, and expression in Escherichia coli of the Bacillus subtilis gene for phosphatidylserine synthase. *Journal of bacteriology* **176**, 7456-7461 (1994).
279. K. Matsumoto, H. Hara, I. Fishov, E. Mileykovskaya, V. Norris, The membrane: transertion as an organizing principle in membrane heterogeneity. *Frontiers in microbiology* **6**, 572 (2015).
280. K. Matsumoto, Phosphatidylserine synthase from bacteria. *Biochimica et Biophysica Acta (BBA)-Lipids and Lipid Metabolism* **1348**, 214-227 (1997).
281. S. Samant, F.-F. Hsu, A. A. Neyfakh, H. Lee, The Bacillus anthracis protein MprF is required for synthesis of lysylphosphatidylglycerols and for resistance to cationic antimicrobial peptides. *Journal of bacteriology* **191**, 1311-1319 (2009).
282. D. O. Serra, A. M. Richter, G. Klauck, F. Mika, R. Hengge, Microanatomy at cellular resolution and spatial order of physiological differentiation in a bacterial biofilm. *mBio* **4**, e00103-00113 (2013).
283. K. Tanaka, Y. Takayanagi, N. Fujita, A. Ishihama, H. Takahashi, Heterogeneity of the principal sigma factor in Escherichia coli: the rpoS gene product, sigma 38, is a second principal sigma factor of RNA polymerase in stationary-phase Escherichia coli. *Proceedings of the National Academy of Sciences* **90**, 3511-3515 (1993).
284. H. Weber, T. Polen, J. Heuveling, V. F. Wendisch, R. Hengge, Genome-wide analysis of the general stress response network in Escherichia coli: σS-dependent genes, promoters, and sigma factor selectivity. *Journal of bacteriology* **187**, 1591-1603 (2005).
285. P. J. Quinn, in *Symp Soc Exp Biol*. (1988), vol. 42, pp. 237-258.
286. G. Schoenhals, C. Whitfield, Comparative analysis of flagellin sequences from Escherichia coli strains possessing serologically distinct flagellar filaments with a shared complex surface pattern. *Journal of bacteriology* **175**, 5395-5402 (1993).
287. X. Liu, P. Matsumura, An alternative sigma factor controls transcription of flagellar class-III operons in Escherichia coli: gene sequence, overproduction, purification and characterization. *Gene* **164**, 81-84 (1995).
288. A. Wach, PCR‐synthesis of marker cassettes with long flanking homology regions for gene disruptions in S. cerevisiae. *Yeast* **12**, 259-265 (1996).

289. J. Wendland, PCR-based methods facilitate targeted gene manipulations and cloning procedures. *Current genetics* **44**, 115-123 (2003).
290. D. B. Kearns, R. Losick, Swarming motility in undomesticated Bacillus subtilis. *Molecular microbiology* **49**, 581-590 (2003).
291. A. Paulick, V. Sourjik, in *Bacterial Chemosensing*. (Springer, 2018), pp. 107-126.
292. C. J. Kristich, G. W. Ordal, Analysis of chimeric chemoreceptors in Bacillus subtilis reveals a role for CheD in the function of the McpC HAMP domain. *Journal of bacteriology* **186**, 5950-5955 (2004).
293. W. Dowhan, Molecular basis for membrane phospholipid diversity: why are there so many lipids? *Annual review of biochemistry* **66**, 199-232 (1997).
294. , (!!! INVALID CITATION !!! (3-6)).
295. G. Carranza *et al.*, Cardiolipin plays an essential role in the formation of intracellular membranes in Escherichia coli. *Biochimica et Biophysica Acta (BBA)-Biomembranes* **1859**, 1124-1132 (2017).
296. A. Ortiz, J. A. Killian, A. J. Verkleij, J. Wilschut, Membrane fusion and the lamellar-to-inverted-hexagonal phase transition in cardiolipin vesicle systems induced by divalent cations. *Biophysical journal* **77**, 2003-2014 (1999).
297. , (!!! INVALID CITATION !!! (9-12)).
298. K. Sekimizu, A. Kornberg, Cardiolipin activation of dnaA protein, the initiation protein of replication in Escherichia coli. *Journal of Biological Chemistry* **263**, 7131-7135 (1988).
299. W. Dowhan, E. Mileykovskaya, M. Bogdanov, Diversity and versatility of lipid–protein interactions revealed by molecular genetic approaches. *Biochimica et Biophysica Acta (BBA)-Biomembranes* **1666**, 19-39 (2004).
300. E. Mileykovskaya *et al.*, Effects of phospholipid composition on MinD-membrane interactions in vitro and in vivo. *Journal of Biological Chemistry* **278**, 22193-22198 (2003).
301. C. Breyton, W. Haase, T. A. Rapoport, W. Kühlbrandt, I. Collinson, Three-dimensional structure of the bacterial protein-translocation complex SecYEG. *Nature* **418**, 662-665 (2002).
302. , (!!! INVALID CITATION !!! (17)).
303. , (!!! INVALID CITATION !!! (6, 18)).
304. I. Shibuya, Metabolic regulation and biological functions of phospholipids in Escherichia coli. *Progress in lipid research* **31**, 245-299 (1992).
305. E. Tunaitis, J. E. Cronan Jr, Characterization of the cardiolipin synthetase activity of Escherichia coli envelopes. *Archives of biochemistry and biophysics* **155**, 420-427 (1973).
306. , (!!! INVALID CITATION !!! (23)).
307. J. T. McGarrity, J. B. Armstrong, The effect of temperature and other growth conditions on the fatty acid composition of Escherichia coli. *Canadian journal of microbiology* **27**, 835-840 (1981).
308. S. Nishijima *et al.*, Disruption of the Escherichia coli cls gene responsible for cardiolipin synthesis. *Journal of bacteriology* **170**, 775-780 (1988).
309. , (!!! INVALID CITATION !!! (27)).
310. A. Jeucken, J. B. Helms, J. F. Brouwers, Cardiolipin synthases of Escherichia coli have phospholipid class specific phospholipase D activity dependent on endogenous and foreign phospholipids. *Biochimica*

et Biophysica Acta (BBA)-Molecular and Cell Biology of Lipids **1863**, 1345-1353 (2018).
311. T.-Y. Lin, W. S. Gross, G. K. Auer, D. B. Weibel, Cardiolipin Alters Rhodobacter sphaeroides Cell Shape by Affecting Peptidoglycan Precursor Biosynthesis. *mBio* **10**, e02401-02418 (2019).
312. , (!!! INVALID CITATION !!! (23, 30)).
313. M. Teuber, J. Bader, Action of polymyxin B on bacterial membranes: phosphatidylglycerol-and cardiolipin-induced susceptibility to polymyxin B in Acholeplasma laidlawii B. *Antimicrobial agents and chemotherapy* **9**, 26-35 (1976).
314. A. P. Zavascki, L. Z. Goldani, J. Li, R. L. Nation, Polymyxin B for the treatment of multidrug-resistant pathogens: a critical review. *Journal of antimicrobial chemotherapy* **60**, 1206-1215 (2007).
315. P. Lopalco, J. Stahl, C. Annese, B. Averhoff, A. Corcelli, Identification of unique cardiolipin and monolysocardiolipin species in Acinetobacter baumannii. *Scientific reports* **7**, 1-12 (2017).
316. J. F. Nepper, Y. C. Lin, D. B. Weibel, Rcs phosphorelay activation in cardiolipin-deficient Escherichia coli reduces biofilm formation. *Journal of bacteriology* **201**, e00804-00818 (2019).
317. K. Maeda, Y. Imae, J.-I. Shioi, F. Oosawa, Effect of temperature on motility and chemotaxis of Escherichia coli. *Journal of bacteriology* **127**, 1039-1046 (1976).
318. W.-W. Tso, J. Adler, Negative chemotaxis in Escherichia coli. *Journal of bacteriology* **118**, 560-576 (1974).
319. , (!!! INVALID CITATION !!! (38)).
320. J. S. Parkinson, Signaling mechanisms of HAMP domains in chemoreceptors and sensor kinases. *Annual review of microbiology* **64**, 101-122 (2010).
321. J. J. Falke, R. B. Bass, S. L. Butler, S. A. Chervitz, M. A. Danielson, The two-component signaling pathway of bacterial chemotaxis: a molecular view of signal transduction by receptors, kinases, and adaptation enzymes. *Annual review of cell and developmental biology* **13**, 457-512 (1997).
322. L. Lee, T. Mizuno, Y. Imae, Thermosensing properties of Escherichia coli tsr mutants defective in serine chemoreception. *Journal of bacteriology* **170**, 4769-4774 (1988).
323. A. Paulick *et al.*, Mechanism of bidirectional thermotaxis in Escherichia coli. *Elife* **6**, e26607 (2017).
324. A. Yoney, H. Salman, Precision and variability in bacterial temperature sensing. *Biophysical journal* **108**, 2427-2436 (2015).
325. S. i. Nishiyama, T. Umemura, T. Nara, M. Homma, I. Kawagishi, Conversion of a bacterial warm sensor to a cold sensor by methylation of a single residue in the presence of an attractant. *Molecular microbiology* **32**, 357-365 (1999).
326. A. Krikos, M. P. Conley, A. Boyd, H. C. Berg, M. I. Simon, Chimeric chemosensory transducers of Escherichia coli. *Proceedings of the National Academy of Sciences* **82**, 1326-1330 (1985).
327. M. Eisenbach, C. Constantinou, H. Aloni, M. Shinitzky, Repellents for Escherichia coli operate neither by changing membrane fluidity nor by

being sensed by periplasmic receptors during chemotaxis. *Journal of bacteriology* **172**, 5218-5224 (1990).
328. , (!!! INVALID CITATION !!! (49)).
329. , (!!! INVALID CITATION !!! (50, 51)).
330. S.-H. Kim, W. Wang, K. K. Kim, Dynamic and clustering model of bacterial chemotaxis receptors: structural basis for signaling and high sensitivity. *Proceedings of the National Academy of Sciences* **99**, 11611-11615 (2002).
331. A. Briegel *et al.*, Structure of bacterial cytoplasmic chemoreceptor arrays and implications for chemotactic signaling. *Elife* **3**, e02151 (2014).
332. , (!!! INVALID CITATION !!! (54)).
333. , (!!! INVALID CITATION !!! (55-57)).
334. D. N. Amin, G. L. Hazelbauer, Influence of membrane lipid composition on a transmembrane bacterial chemoreceptor. *Journal of biological Chemistry* **287**, 41697-41705 (2012).
335. T. M. Santos, T. Y. Lin, M. Rajendran, S. M. Anderson, D. B. Weibel, Polar localization of Escherichia coli chemoreceptors requires an intact Tol-Pal complex. *Molecular microbiology* **92**, 985-1004 (2014).
336. , (!!! INVALID CITATION !!! (61, 62)).
337. , (!!! INVALID CITATION !!! (63)).
338. M. Edidin, V. A. Petit, in *Ciba Foundation Symposium*. (1977), pp. 155-174.
339. D. Lucena, M. Mauri, F. Schmidt, B. Eckhardt, P. L. Graumann, Microdomain formation is a general property of bacterial membrane proteins and induces heterogeneity of diffusion patterns. *BMC biology* **16**, 1-17 (2018).
340. R. N. Lewis, D. Zweytick, G. Pabst, K. Lohner, R. N. McElhaney, Calorimetric, X-ray diffraction, and spectroscopic studies of the thermotropic phase behavior and organization of tetramyristoyl cardiolipin membranes. *Biophysical journal* **92**, 3166-3177 (2007).
341. S.-T. Yang, A. J. Kreutzberger, J. Lee, V. Kiessling, L. K. Tamm, The role of cholesterol in membrane fusion. *Chemistry and physics of lipids* **199**, 136-143 (2016).
342. J. Uchiyama *et al.*, Involvement of σS accumulation in repression of the flhDC operon in acidic phospholipid-deficient mutants of Escherichia coli. *Microbiology* **156**, 1650-1660 (2010).
343. A. Tomura, T. Ishikawa, Y. Sagara, T. Miki, K. Sekimizu, Requirement of phosphatidylglycerol for flagellation of Escherichia coli. *FEBS letters* **329**, 287-290 (1993).
344. J. S. Parkinson, Complementation analysis and deletion mapping of Escherichia coli mutants defective in chemotaxis. *Journal of bacteriology* **135**, 45-53 (1978).
345. S. Schulmeister, K. Grosse, V. Sourjik, Effects of receptor modification and temperature on dynamics of sensory complexes in Escherichia coli chemotaxis. *BMC microbiology* **11**, 1-10 (2011).
346. E. Tamar, M. Koler, A. Vaknin, The role of motility and chemotaxis in the bacterial colonization of protected surfaces. *Scientific reports* **6**, 1-11 (2016).

347. M. Burkart, A. Toguchi, R. M. Harshey, The chemotaxis system, but not chemotaxis, is essential for swarming motility in Escherichia coli. *Proceedings of the National Academy of Sciences* **95**, 2568-2573 (1998).
348. S. C. Dryden, W. Dowhan, Isolation and expression of the Rhodobacter sphaeroides gene (pgsA) encoding phosphatidylglycerophosphate synthase. *Journal of bacteriology* **178**, 1030-1038 (1996).
349. E. Mileykovskaya *et al.*, Phosphatidic acid and N-acylphosphatidylethanolamine form membrane domains in Escherichia coli mutant lacking cardiolipin and phosphatidylglycerol. *Journal of Biological Chemistry* **284**, 2990-3000 (2009).
350. W. Xia, W. Dowhan, In vivo evidence for the involvement of anionic phospholipids in initiation of DNA replication in Escherichia coli. *Proceedings of the National Academy of Sciences* **92**, 783-787 (1995).
351. I. Barák, K. Muchová, The role of lipid domains in bacterial cell processes. *International journal of molecular sciences* **14**, 4050-4065 (2013).
352. P. De Boer, R. Crossley, A. Hand, L. Rothfield, The MinD protein is a membrane ATPase required for the correct placement of the Escherichia coli division site. *The EMBO journal* **10**, 4371-4380 (1991).
353. G. Li, K. D. Young, Isolation and identification of new inner membrane‐associated proteins that localize to cell poles in Escherichia coli. *Molecular microbiology* **84**, 276-295 (2012).
354. D. Minnikin, H. Abdolrahimzadeh, J. Baddiley, Variation of polar lipid composition of Bacillus subtilis (Marburg) with different growth conditions. *FEBS letters* **27**, 16-18 (1972).
355. J. B. Miller, D. Koshland, Sensory electrophysiology of bacteria: relationship of the membrane potential to motility and chemotaxis in Bacillus subtilis. *Proceedings of the National Academy of Sciences* **74**, 4752-4756 (1977).
356. A.-R. Pogmore, K. H. Seistrup, H. Strahl, The Gram-positive model organism Bacillus subtilis does not form detectable cardiolipin-specific lipid domains. *bioRxiv*, 190306 (2017).